AD-A031 063 TEXAS INSTRUMENTS INC DALLAS CENTRAL RESEARCH LABS F/G 20/1
ACOUSTIC ADAPTIVE TRANSVERSAL FILTER.(U)
SEP 76 R M HAYS DAAB07-75-C-1309
UNCLASSIFIED TI-08-76-50 ECOM-75-C-1309-F NL

1 OF 2
AD
A031063

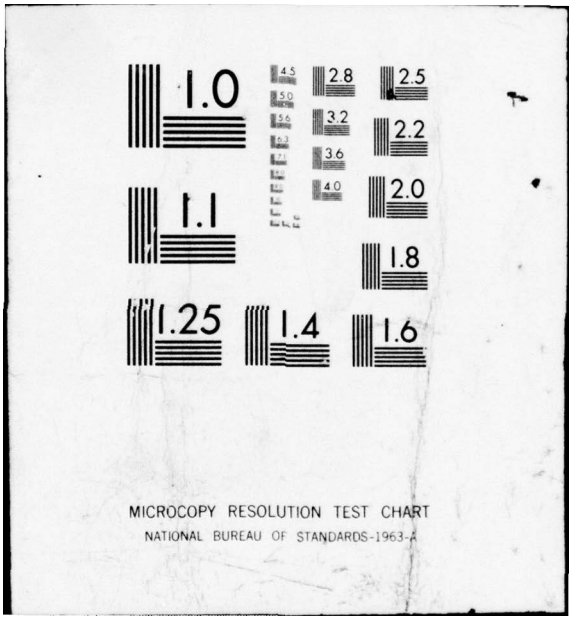
1.0
1.1
1.25
1.4
1.6
1.8
2.0
2.2
2.5
2.8
3.2
3.6
4.0
4.5
5.0
5.6
MICROCOPY RESOLUTION TEST CHART
NATIONAL BUREAU OF STANDARDS-1963-A

REPORTS CONTROL SYMBOL
OSD-1366

Research and Development Technical Report

Report ECOM-75-C-1309-F

12

ACOUSTIC ADAPTIVE TRANSVERSAL FILTER

R. M. Hays
Texas Instruments Incorporated
Central Research Laboratories
13500 North Central Expressway
Dallas, Texas 75222

September 1976

Final Technical Report for Period 24 January 1975 - 1 May 1976

Approved for public release; distribution unlimited.

ECOM

US ARMY ELECTRONICS COMMAND FORT MONMOUTH, NEW JERSEY 07703

UNCLASSIFIED

SECURITY CLASSIFICATION OF THIS PAGE (When Data Entered)

REPORT DOCUMENTATION PAGE

READ INSTRUCTIONS BEFORE COMPLETING FORM

1. REPORT NUMBER: ECOM-75-C-1309-F	2. GOVT ACCESSION NO.
3. RECIPIENT'S CATALOG NUMBER	
4. TITLE (and Subtitle): Acoustic Adaptive Transversal Filter,	5. TYPE OF REPORT & PERIOD COVERED: Final Technical Report, 24 Jan 75 — 1 May 76
6. PERFORMING ORG. REPORT NUMBER: TI-08-76-50	
7. AUTHOR(s): R. M. Hays	8. CONTRACT OR GRANT NUMBER(s): DAAB07-75-C-1309
9. PERFORMING ORGANIZATION NAME AND ADDRESS: Texas Instruments Incorporated, Central Research Laboratories, 13500 North Central Expressway, Dallas, Texas 75222	10. PROGRAM ELEMENT, PROJECT, TASK AREA & WORK UNIT NUMBERS: Project No. 1S7-62705-AH94-A2-05
11. CONTROLLING OFFICE NAME AND ADDRESS: U. S. Army Electronics Command, Attn: AMSEL-TL-MM, Fort Monmouth, New Jersey 07703	12. REPORT DATE: Sept 1976
	13. NUMBER OF PAGES: 159 (167 p.)
14. MONITORING AGENCY NAME & ADDRESS (if different from Controlling Office): DA-1-S-76270S-AH-94 (17) 1-S-76270S-AH-94-A-2	15. SECURITY CLASS. (of this report): Unclassified
	15a. DECLASSIFICATION/DOWNGRADING SCHEDULE

16. DISTRIBUTION STATEMENT (of this Report)

Approved for public release; distribution unlimited.

17. DISTRIBUTION STATEMENT (of the abstract entered in Block 20, if different from Report)

18. SUPPLEMENTARY NOTES

19. KEY WORDS (Continue on reverse side if necessary and identify by block number)

Adaptable Bandpass/Bandstop	Adaptive Filters
Ultrasonic	Matched Filtering
Surface Acoustic Waves	Chirp Transform
Signal Processing	Spread Spectrum
Prewhitening	Programmable Filter

20. ABSTRACT (Continue on reverse side if necessary and identify by block number)

The availability of spectral information in real-time clearly permits many important new signal processing applications. Although understanding the basic operating principles of the Transform Adaptable Processing System is more complex than is the case for a conventional programmable filter, its physical implementation is considerably simpler, since it consists of a small number of SAW chirp filters, mixers and amplifiers, and a timing generator. The capability of providing accurate transform information in real-time has been demonstrated, and prototype results for continuously variable bandpass/bandstop

DD FORM 1 JAN 73 1473 EDITION OF 1 NOV 65 IS OBSOLETE 403 833

UNCLASSIFIED

SECURITY CLASSIFICATION OF THIS PAGE (When Data Entered)

filtering, versatile programmable matched filtering, and prewhitening for suppression of narrowband interference evidence the power of the transform processing approach to many signal processing problems. This report has described this approach in detail and demonstrated its feasibility with extensive experimental results of the prototype Transform Adaptable Processing System.

TABLE OF CONTENTS

LIST OF ILLUSTRATIONS

(Continued)

LIST OF ILLUSTRATIONS

(Continued)

LIST OF ILLUSTRATIONS

(Continued)

LIST OF ILLUSTRATIONS

(Continued)

LIST OF TABLES

SECTION I

INTRODUCTION

This program has developed and demonstrated an acoustic adaptive transversal filter based on a novel transform processing technique.[1-3] An adaptive transversal filter is one whose impulse response can be programmed to be virtually any function that is desired, limited only by the bandwidth and time duration of the filter. The classic approach for realizing such a filter is a programmable Kallman filter,[4] which consists of a tapped delay line with variable amplitude and phase control at each tap. The transform approach adopted for this development has capabilities that go far beyond those of previous programmable filters, however, and simultaneously circumvent serious fabrication difficulties that accompany the various conventional tapped-delay line methods of achieving variable response.

Variable response is required for many applications of SAW devices, including tunable bandpass/bandstop filtering, programmable matched filters in spread-spectrum communications or radar pulse compression, and frequency synthesis. Although SAW devices have been very successful in realizing high-performance, fixed-tuned filters[5-11] for many comparable applications, the use of SAW devices in applications requiring programmable, or variable, responses has awaited further development to remove the fixed-tuned limitation associated with SAW achievements. The first steps toward removal of this limitation have been demonstrated with the selectable filter[12-14] and biphase programmable PSK correlators.[15] The selectable filter provides discrete tuning through the selection of any of a large number of variable center frequency or variable bandwidth bandpass filter responses that are achieved with a modest number of SAW devices and switches. Biphase programmable PSK correlators are achieved with tapped delay lines and switches, but, for codes longer than 100 chips, present similar, but simpler, fabrication problems than the more general adaptive transversal filter. The prototype developed under this contract completely removes this fixed-tuned limitation, permitting continuously tuned, programmable filtering with flexibility that has not been possible before.

Furthermore, the transform processing approach not only fulfills the existing needs for variable response filters,[1, 16-18] but also permits many important new signal processing functions such as prewhitening for spread-spectrum systems.[1-3]

The principal building block for this acoustic adaptive transversal filter is the chirp transform.[19] The chirp transform orders the frequency components of an input signal serially in time; that is, the output time response is proportional to the Fourier transform (or frequency spectrum) of the input time signal. Surface wave linear FM devices can be used to perform the chirp transform and thereby convert successive intervals of a time-varying input signal into their respective transforms. The configuration of SAW chirp filters required to perform this transform and the basis of operation are described both mathematically and heuristically through each step of the transform process in Section III of this report. The experimental results of the prototype shown in that section demonstrate the accuracy with which the spectral information is delivered in real-time and suggest many spectrum analysis applications such as those in radar Doppler processing or seismic data processing in conjunction with time compression and in EW or spread-spectrum systems.

More important, these surface wave components, which can be viewed as a continuous signal version of a discrete chirp-Z transform discussed by Alsup,[20,21] can be assembled into a Transform Adaptable Processor System (TAPS) to provide unique signal processing functions due to the accessibility of the input signal spectrum and the ease with which it can be modified to produce a variety of programmable filter responses. The first of these to be described and demonstrated in Section IV of this report is the continuously variable bandpass/bandstop filter developed under this contract: the acoustic adaptive transversal filter (Figure 1). This is achieved

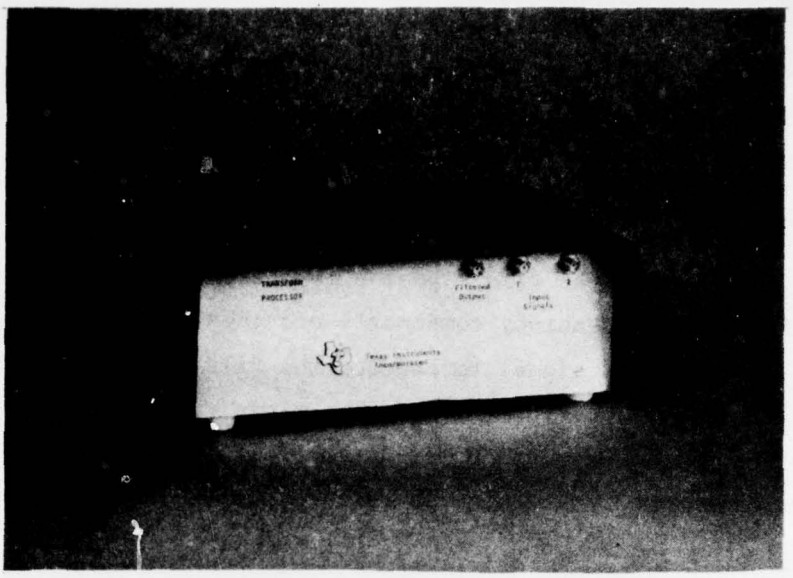

(a)

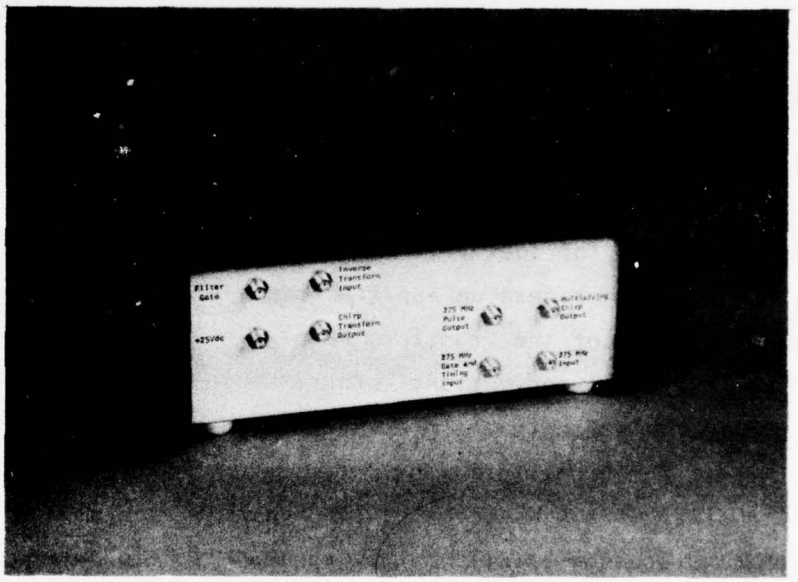

(b)

Figure 1 Transform Adaptable Processing System (TAPS) Prototype. (a) Front view; (b) back view.

by simply modulating the time signal after performing the transform to pass or remove the desired frequency components and then performing the inverse transform of the modulated signal to produce the filtered time domain signal. The inverse transform is performed through a minor variation in the surface wave filter arrangement, permitting reconstruction of the original signal as shown with simulations and the prototype results.

The flexibility and superiority of this implementation of the adaptive filter becomes clearer with the demonstration of the TAPS system for programmable matched filtering and prewhitening. This approach offers much greater versatility than other programmable approaches since it can process a larger class of signals, encompassing both PSK and FM signals within the same system. Of greater importance, perhaps, is the facility to suppress narrow-band interference that could otherwise destroy spread-spectrum system processing. This is achieved with simple clipping or bandstop filtering of the interference from the total spectrum made available by the chirp transform approach. These TAPS configurations are described and prototype results presented in Section V.

The availability of spectral information in real time clearly permits many important new signal processing applications. Although understanding the basic operating principles of the Transform Adaptable Processing System is more complex than is the case for a conventional programmable filter, its physical implementation is considerably simpler, since it consists of a small number of SAW chirp filters, mixers and amplifiers, and a timing generator. This contrasts with the fabrication difficulties associated with the conventional switched, tapped delay line approach discussed briefly in the next section. The capability of providing accurate transform information in real time has been demonstrated, and prototype results for continuously variable bandpass/bandstop filtering, versatile programmable matched filtering, and prewhitening for suppression of narrowband interference

evidence the power of the transform processing approach to many signal processing problems. This report describes this approach in detail and demonstrates its feasibility with extensive experimental results using the prototype Transform Adaptable Processing System.

SECTION II

TECHNICAL APPROACH FOR THE ACOUSTIC ADAPTIVE FILTER

There are two distinctly different technological approaches to the realization of surface wave filter subsystems for adaptive filter applications in the frequency domain or for programmable correlation in the time domain. One approach requires a surface wave, tapped delay line transversal filter with provision for the control of the amplitude and phase of each tap. This method is a modern implementation of the adaptive filter concept introduced 34 years ago by Kallmann.[4] The various techniques that are currently being developed for programmable tapped delay lines are summarized below with a short discussion of their relative advantages and disadvantages.

The major alternative to the tapped delay line approach is the Transform Adaptable Processor System (TAPS), which is superior both in terms of performance as an adaptive filter and in its potential for expansion to meet a wide range of future military signal processing requirements with simple, reliable components.

It should be noted that the selectable bandpass filter[12-14] developed at Texas Instruments under ECOM Contract No. DAAB07-73-C-0094 provides discretely tunable bandpass-bandstop channels and has much potential for EW receiver and fast-hop synthesizer applications. Although this subsystem offers better performance, it does not provide the continuously variable control that can be achieved with an adaptive filter. It should also be noted that the nonlinear acoustic convolvers[22-26] can be used for many applications in time domain correlation in direct competition with the programmable tapped delay lines. However, the time compression associated with these devices makes them unsuitable for adaptive filter needs.

A. Programmable Tapped Delay Lines

The accessibility of surface waves to tapping has made them natural candidates for programmable tapped delay lines.[27] Three techniques will be briefly

discussed: individual taps with external switches and control circuitry, integration of switches with MOSFET surface wave detectors, and monolithic devices using epitaxial layers of aluminum nitride and silicon, both on sapphire. The conceptual simplicity of these techniques is offset by the mechanical and electrical complexity of interconnecting and switching the many taps required to meet the technical objectives of this program.

Perhaps the most direct technique for obtaining a programmable transversal filter is to construct a surface wave delay line with separate taps and external switching and control circuitry. Many possible configurations for the tap control[28-30] are under development for programmable matched filter applications. As compared to other surface wave tapped delay lines, this technique has two primary advantages for achieving amplitude and phase control. First, the acoustic delay line medium and the electronic switching can be chosen and optimized independently. For example, the delay line might be chosen for low temperature coefficient, while the switching might be chosen for power considerations. The second advantage of the diode switched technique is that it makes maximum use of existing SAW and electronic technologies.

There are several drawbacks to this approach if more than a few taps are required. First, and probably most serious, a very large number of rf interconnections must be made in a very small space, which leads to severe fabrication difficulty and reliability problems in a completed unit. This problem might be overcome by application of high reliability beam lead techniques. A second problem area is that the switching diodes have a reverse bias capacitance that is typically significant compared to the capacitance of a single delay line tap. This results in a poor on/off ratio for the switch, which can cause distortion of the desired filter characteristic. A final problem is the close proximity of the various SWD delay line taps, which makes it difficult to eliminate electrical crosstalk between taps.

A desire to integrate surface wave filter functions with standard MOS circuitry led to the unique concept for surface wave detection on silicon by means of the piezoresistance effect in the inversion layer of a metal oxide silicon field effect transistor. This technique was first demonstrated by Claiborne, et al.,[31] and is particularly well suited to programmable filters, since a static control shift register can be integrated onto the same silicon chip with the acoustic delay line. The basic building blocks for such a device consist of (a) a sputtered ZnO overlay transducer for generating the acoustic surface waves on the silicon substrate, (b) the programmable MOSFET detectors to provide taps on the SWD delay line, and (c) a static serial MOS shift register for controlling the various delay line taps. More complex circuitry is required to achieve analog amplitude and phase control.

The advantages of a MOSFET approach are: (a) the surface wave detectors and the binary control register are completely monolithic, thus eliminating the interconnection problem; (b) with the exception of the ZnO input transducer, the entire device uses standard, well-established MOS processes; (c) since piezoresistance detection is linearly proportional to dc current flow, the delay line taps have excellent on/off ratio and good amplitude control; (d) the control leads are dc rather than rf, eliminating crosstalk; and (e) piezoresistive detection does not extract energy from the acoustic beam, thus minimizing distortion.

This technique also has several disadvantages. Piezoresistance is a weak effect that leads to moderate power consumption. Also, silicon has a 30 ppm surface wave temperature sensitivity, which is undesirable. Finally, MOSFET detectors require multiple levels of oxides, diffusions, and metallizations; this forces the acoustic wave to travel in a multilayer medium with many discontinuities.

Monolithic filters have been developed using AℓN on sapphire and silicon on sapphire.[32,33] Epitaxial layers of piezoelectric AℓN and semiconducting silicon are grown on adjacent areas of a common sapphire substrate. Then a tapped SWD delay line is constructed on the AℓN, and electronic switching is constructed in the silicon to yield a programmable line. The AℓN on sapphire is particularly useful for high frequency, high data rate correlators due to its large (6.1×10^5 cm/sec) acoustic velocity. However, this high velocity makes it less suitable for long time delays. The primary advantages of this technology are: (a) it is compatible with completely integrating the control register, the switches and the delay line; (b) the aluminum nitride on sapphire has a moderately strong surface wave coupling coefficient; and (c) silicon on sapphire has a sizable technology base and is particularly well suited for high performance rf switching.

There are three disadvantages of the AℓN/Si on sapphire technique. First, it is an entirely new materials and process technology with unproven production reliability. Also, if yield is a problem for the large-size silicon MOSFET chips, it is probably worse for this much newer technology. Finally, the AℓN on sapphire has a moderate temperature sensitivity (40 ppm/°C) for acoustic surface wave propagation.

B. Transform Adaptable Processing System

The Transform Adaptable Processing System (TAPS) is a revolutionary development that eliminates the need for the large number of independently controlled and closely spaced taps while still realizing the same function that the taps perform. The system can be easily programmed to perform identically any function of the classic adaptive filter while avoiding the corresponding implementation problems. In this section a brief explanation is given of the internal operation of TAPS, which departs radically from the classic Kallman approach. A more detailed and rigorous explanation of TAPS operation is given in Section IV.

The transform adaptive processor operates by dividing an input signal into short blocks, sequentially processing each block, and summing the individual processed output signal packets to obtain a continuous processed output stream. Each time block of the input signal is processed by using SAW chirp filters in a configuration known as the chirp-Z transform. The adaptive filter consists of three processing stages including two chirp transform stages, as shown in Figure 2. The input signal block S(t) is applied to the input of the chirp-Z transform unit. This performs an analog Fourier transform operation on the signal, thereby resolving the frequency components in time. The output signal F(t) from the first transformer is the spectrum of the applied input such that magnitude and phase of this signal at different time positions correspond to the magnitude and phase of the Fourier transform of the input signal at different frequency points. In this system the starting portion of F(t) corresponds to the low frequency end of the system bandwidth, the end portion of F(t) corresponds to the high frequency end of the system bandwidth, and frequencies inside the band are spread linearly in time between these extremes.

Thus, the input signal is transformed from the time domain to the frequency domain. The adaptive filtering is effected on this transformed signal by simply multiplying each frequency component by its appropriate amplitude and phase weighting coefficient using an ordinary rf mixer. A special case of this general technique is the subject adaptive filter for continuously variable bandpass or bandstop filtering. In this domain, bandpass filtering consists of simple on-off (or pulse) modulation, since all the frequency components of the input signal are separated in time. The bandpass selection is accomplished with a modulator such as a double-balanced mixer, and, by varying the modulation function G(t), the portion of the input spectrum (or switch) that passes through the filter can be selected.

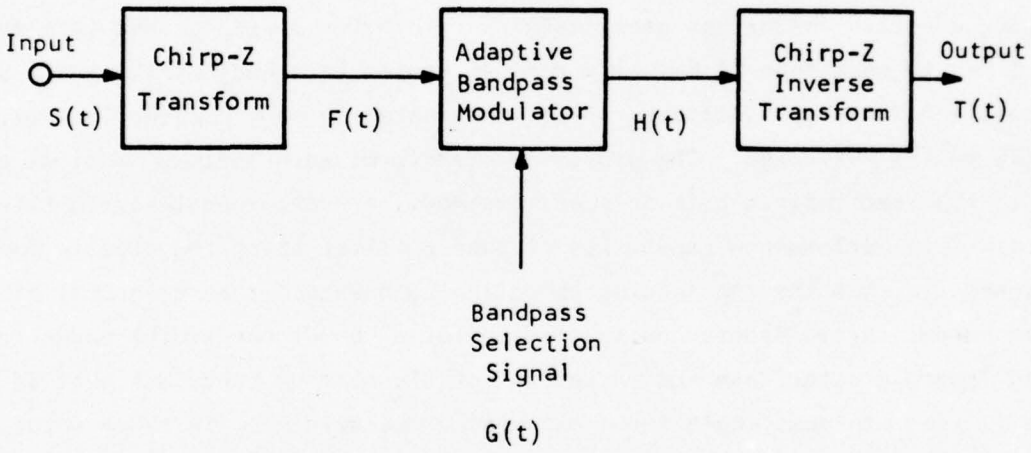

Figure 2 Block Diagram of the Acoustic Adaptive Transversal Filter Using the Transform Adaptable Processing System (TAPS)

In the final stage, the remaining spectral components H(t) that were selected by the modulator are transformed back to the time domain by an inverse chirp-Z transform. The resultant output signal T(t) is a filtered version of the input. The modulation function G(t) is the transfer function (or frequency response) of the bandpass filter. This is described in more detail including the continuous operation methods, in Section IV, but one can see that while this technique operates in a radically different manner from the classic programmable Kallmann filter approach, it provides the identical filter function.

The Transform Adaptable Processing System to demonstrate feasibility of the acoustic adaptive filter has been designed to provide variable bandwidth from less than 1 MHz to more than 50 MHz at a nominal center frequency of 150 MHz. Both bandpass and bandstop functions can be implemented in many combinations within the 125 to 175 MHz range. The processor transforms each successive block of time in 1.9 μsec intervals in a repetitive mode, as described later in this report. Full performance capability of such a filter using the classic approach would require that the tap spacing be nominally one-half the reciprocal of the filter bandwidth (10 nanosecond separation for a 50 MHz bandwidth) and a total tapped length greater than the reciprocal of the minimum bandwidth that is desired (1 μsec minimum length for 1 MHz minimum bandwidth). In other words, to achieve this level of performance in an equivalent performance Kallmann filter, more than 100 programmable taps would be needed.

In addition to this clear performance advantage of TAPS over the Kallman filter approach, there are several other important advantages of TAPS. First, this approach uses standard SAW technology and automatically benefits from SAW technology advances. The competing techniques use specialized technologies that have limited use elsewhere. A second advantage is that in addition to adaptive

filtering, TAPS provides the frequency spectrum of the input signal. This spectral information is needed in many systems applications of an adaptive filter. For example, when an adaptive filter is used to cancel unwanted interference in a wideband communications system due to other transmitters, the frequency spectrum of the interfering signals must first be measured so that the proper programming information for the adaptive filter can be calculated. TAPS provides this spectrum information with no additional hardware, whereas additional hardware and processing time would be needed to obtain this vital information with a programmable Kallman filter. Thus, TAPS not only provides all the filter functions of a classic adaptive filter, but it also has the additional capability of providing the spectral information needed in many systems that use adaptive filters. A third advantage of the transform technique is that the basic transform hardware that forms the heart of TAPS can be used for many other signal processing applications than the required adaptive filtering functions. These include programmable matched filtering and prewhitening, as discussed and demonstrated in Section V. The feasibility of all these functions has been clearly demonstrated.

In summary, understanding the basic operating principles of the transform adaptive processing system is more complex than is the case for a conventional adaptive filter; but its physical implementation is considerably simpler, since it consists of a small number of chirp filters, several mixers, several amplifiers, and a timing generator. All these components are conventional and easy to build, in direct contrast to the overwhelming fabrication difficulties associated with the conventional tapped delay line approach. There

are some problem areas with the transform approach related to spurious signals and timing errors, as discussed in subsequent sections. However, it is fair to say that these problems are minor compared to the corresponding difficulties in the standard approaches and can be circumvented as described in Section IV of this report. In addition, the performance advantages of the transform approach are significant.

SECTION III

CHIRP TRANSFORM OPERATION

The heart of the Transform Adaptable Processing System is the chirp transform. This basic building block is realized by a linear FM filter, two linear FM generators, and two mixers, as shown in Figure 3. Implementation of the chirp-Z transform algorithm has been demonstrated utilizing CCD technology,[34] but considerable simplification is possible with surface wave devices. CCDs process signals at baseband and therefore must transform and process both in-phase and quadrature channels. Surface wave devices process magnitude and phase simultaneously at the carrier frequency in a single channel.

The operation of the chirp transform is discussed in this section. First a mathematical derivation is given, followed by a heuristic description of transform operation. Computer analyses and demonstration results are presented before proceeding to the system applications and TAPS prototype design and demonstration in subsequent sections.

A. Mathematical Description

The chirp transform is realized by a chirp filter, two chirp generators, and two mixers as shown in Figure 3. The output F(t) can be written from this schematic:

$$F(t) = \left\{\left[S(t) \bullet C_1(t)\right] \ast I(t)\right\} \bullet C_2(t) \ ,$$

where $\ast$ represents convolution. To see that F(t) is a true Fourier transformation of the input signal S(t), complex notation is used and signals of the following form are assumed with constant time delays omitted (the time origin is the center of each waveform):

$$S(t) = S'(t) \exp\left(j2\pi f_o t\right) \ ,$$

where S'(t) is bandlimited to ΔF;

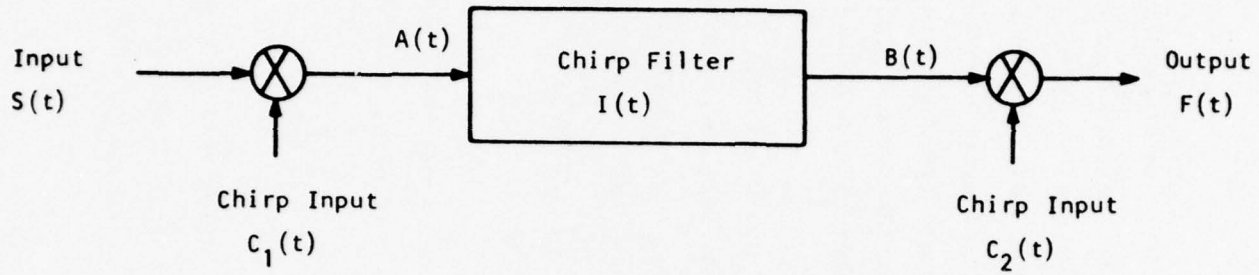

Figure 3 Basic Chirp-Z Transform Unit

$$C_1(t) = \begin{cases} \exp\left(j2\pi\left[f_1 t - \frac{\Delta F t^2}{2\Delta T}\right]\right), & |t| < \frac{\Delta T}{2} \\ 0, & |t| > \frac{\Delta T}{2} \end{cases}$$

$$I(t) = \begin{cases} \exp\left(j2\pi\left[(f_1 + f_o)t + \frac{\Delta F t^2}{2\Delta T}\right]\right), & |t| < \Delta T \\ 0, & |t| > \Delta T \end{cases}$$

$$C_2(t) = C_1(t) \ .$$

By simply putting these equations into the expression for F(t) and reordering and cancelling terms, one finds F(t).

$$F(t) = \exp\left[j2\pi(f_1 t - \frac{\Delta F t^2}{2\Delta T})\right] \bullet$$

$$\int_{-\frac{\Delta T}{2}}^{\frac{\Delta T}{2}} S'(\tau) \exp(j2\pi f_o \tau) \exp\left[j2\pi(f_1\tau - \frac{\Delta F \tau^2}{2\Delta T}\right]$$

$$\bullet \exp\left\{j2\pi\left[(f_1 + f_o)(t - \tau) + \frac{\Delta F(t - \tau)^2}{2\Delta T}\right]\right\} d\tau \ ;$$

$$F(t) = F(\omega(t)) = \exp\left[j2\pi(2f_1 + f_o)t\right] \bullet$$

$$\int_{-\frac{\Delta T}{2}}^{\frac{\Delta T}{2}} S'(\tau) \exp(-j\omega(t)\tau)\, d\tau \ ,$$

where

$$\omega(t) = 2\pi \frac{\Delta F}{\Delta T} \ t \ .$$

The limits of integration are set by the time length of the first multiplying chirp $C_1(t)$. A second constraint is given by the finite length of the convolving chirp filter I(t):

$$| t - \tau | < \Delta T.$$

This condition is only met for all τ in the range of integration if $| t | < \Delta T/2$. Hence, only for $| t | < \Delta T/2$ does the output represent the true Fourier transform of the input signal. The duration of the signal out of the filter is 3 ΔT, the length of the filter impulse response plus the length of the chirp signal. Therefore, only the center ΔT corresponds to a true Fourier transform of the input signal. The final mixing chirp has duration ΔT and acts as a gate to select the desired portion of the filter output. The output signal has the form of the Fourier transform of the input signal S(t) with the frequency of the transform given by the chirp slope times the time delay, $(\Delta F/\Delta T)t$.

B. Chirp Transform Heuristic Description

A qualitative understanding of the operation of the transformer can be obtained by examining the frequency-time diagram in Figure 4. The signal amplitude is not shown. Frequency is displayed on the vertical axis and time on the horizontal. The bandwidth of the signal corresponds to its height, and the duration corresponds to its length.

Figure 4(a) shows how signals are changed as they pass through the chirp transform subsystem. The frequencies of the input signals indicated in the figure were chosen to reduce spurious signals at the output. This choice is discussed in Section III.C. As shown in Figure 4(a), input signals S(t) in the range from 125 to 175 MHz are mixed with a linear frequency down-chirp $C_1(t)$ centered at 275 MHz. This mixing gates the input in time and superimposes a

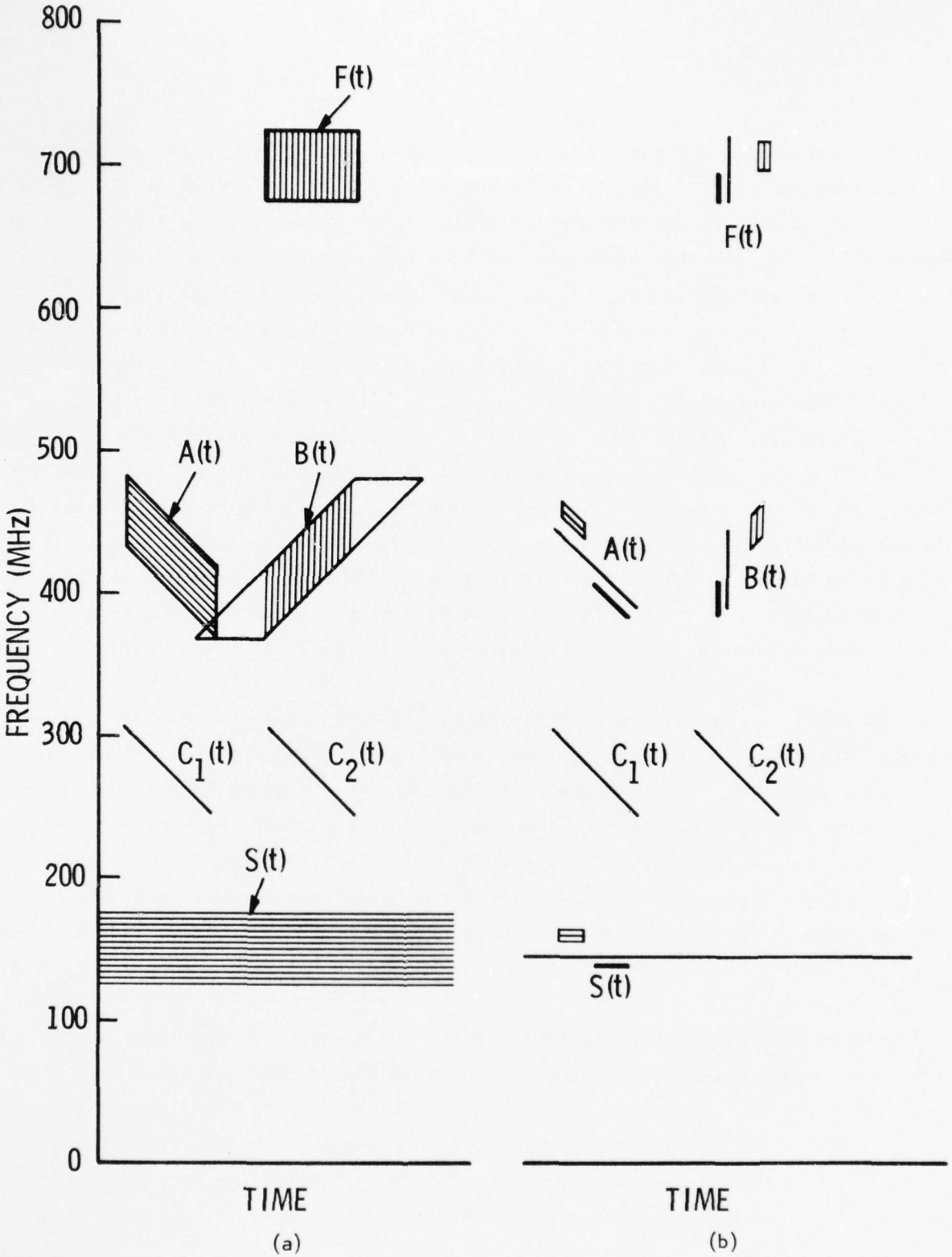

Figure 4 Frequency-Time Diagram of Chirp-Z Transform Unit. (a) Full band coverage; (b) three-tone example.

chirp on the signal. The sum frequency product term A(t) centered at 425 MHz is fed into the chirp filter shown in the block diagram of Figure 3. The chirp filter output B(t) covers the same frequency range as the input A(t), but it is delayed in time, and the dispersive up-chirp characteristic of the filter has introduced an up-chirp on the output. Since the linear FM filter I(t) must handle the sum of the bandwidths of S(t) and $C_1(t)$ and also possesses the same chirp slope as $C_1(t)$, then I(t) is twice the time length of $C_1(t)$. The duration of the convolution of A(t) and I(t) is therefore three times the length of the signal A(t). The only portion of the signal that corresponds to a true Fourier transform of the input is the center part that corresponds to the time when the entire signal is in the chirp filter. These time considerations are discussed in the mathematical analysis section, III.A. The slope of the chirp $C_1(t)$ is matched to the filter chirp slope so that the filter output consists of compressed pulses corresponding to the input frequency components. The chirp filter does not change the frequencies present in the input signal A(t).

As shown in Figure 3, the filter output B(t) is mixed with another down-chirp $C_2(t)$. This mixing gates out the useful portion of the output and cancels the chirp characteristic of the signal. The product term F(t) at 700 MHz corresponds to the true Fourier transform of the input signal S(t) over the duration ΔT of the chirp signals. The high frequency can be avoided by mixing with an up-chirp instead of the down-chirp $C_2(t)$ and using the difference product term only, but for an adaptive bandpass filter, the entire post-filter mixing step can be skipped. This is discussed in Section IV.

Figure 4(b) treats a three-tone example: a cw term and two pulsed signals, all at different frequencies. One can see that the narrow-band continuous signal mixes with the chirp $C_1(t)$ to give a higher frequency chirp signal, the center line in A(t). The chirp filter compresses this signal into a short, wide-band pulse. This compression is analogous to the pulse compression in chirped radar systems. Thus, at this point in Figure 4(b), the cw signal is represented by a

short pulse with a large bandwidth indicated by its height. For clarity, the sidelobes indicated by the unshaded portions of B(t) in Figure 4(a) are not shown in Figure 4(b).

The two shorter tones are also compressed in the chirp filter. Since the filter has an up-chirp dispersive characteristic, the compressed pulse corresponding to the low frequency chirped tone has the shortest delay and appears first in time, followed by the compressed cw tone and the compressed high frequency pulsed tone. Because of their larger bandwidth, the short tones are transformed to longer compressed pulses as indicated by their width in the figure. The relative center frequencies of these compressed pulses are displaced by the chirp characteristic of the signal B(t). This characteristic shows more clearly in Figure 4(a). Post-mixing with the chirp $C_2(t)$ removes the chirp characteristic. The difference of the center frequencies in the output signal F(t) corresponds to the position of the original pulses S(t) in time. Comparing S(t) and F(t) in Figure 4(b), one can see that the transformer has the effect of rotating the input signal clockwise by 90° in the frequency-time plane. Thus, the bandwidth (height) of each tone in the input S(t) determines the time width of the corresponding output signal F(t). The input tone duration determines the bandwidth of the corresponding output pulse.

Figure 4(b) clearly shows the separation in time of the three different input frequency components. This separation allows one to modulate the output F(t) in time to eliminate any of the three components. Note also that the three components are separated in time before the final mixing in B(t). The signal could be modulated at this point to obtain the desired filter function. This fact leads to a significant simplication in the adaptive bandpass filter application of the transformer in Section IV.

C. Chirp Transform Design

The objectives of this program included the requirements that the filter should handle signals over a 50 MHz bandwidth and achieve a minimum bandwidth of 1 MHz. The latter constraint prescribes that the transformer process no less than 1.0 μsec intervals of the input signal at a time. The chirp generator $C_1(t)$ then requires a linear FM signal of bandwidth 50 MHz and at least 1.0 μsec. To ensure that these goals were met, bandwidth and time length were increased by 20% to 60 MHz and 1.2 μsec, respectively. The chirp generation is provided by exciting the impulse response of a surface acoustic wave linear FM filter. Correspondingly, the SAW chirp filter I(t) has twice the bandwidth, or 120 MHz, to handle the sum of the bandwidths into the mixer. (Figures 7 and 13 show the block diagrams with the 1.2 μsec time lengths increased to 1.9 μsec for reasons to be described later.)

Selection of specific operating frequencies is predicated on the spurious performance of the mixers required by the transform and the device insertion loss that increases with fractional bandwidth. As well as giving the desired product signals, balanced mixers produce even-order harmonics of both inputs. The system must be designed to be insensitive to these spurious signals. In addition, the mixers generate signals at both the sum and difference frequencies of the inputs. In this system we want only one component of this product. To design a system free of these spurious signals the operating frequency range was chosen to be 125 to 175 MHz, and the multiplying chirp filters are centered at 275 MHz.

The reasons for this are illustrated in the frequency diagram of Figure 5. The frequencies of operation must be chosen such that the passband of the chirp filter I(t) includes the sum signal of the chirp $C_1(t)$ and input S(t) product, but does not overlap the unwanted mixer harmonics. If the operating frequencies were reduced, the undesired harmonics would be reduced and overlap the 120 MHz operating range at 425 MHz with the desired sum frequencies out of the mixer.

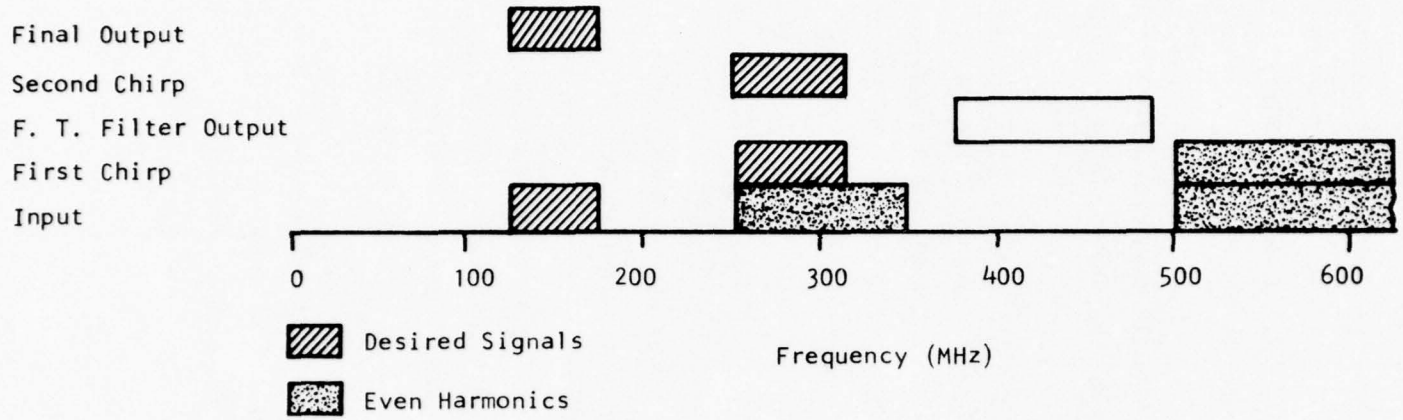

Figure 5 Frequency Selection due to Mixer Harmonic Considerations

With a small quiescent band on each side of the convolving chirp filter bandpass, the chirp filter provides the needed rejection of the even-harmonics and unwanted mixer products in the transformer. (Since there are two such convolving SAW chirp filters in the adaptive filter described in the next section, the rejection of these interfering terms is assured.)

The convolving chirp filter must have a bandwidth of 120 MHz at 425 MHz to cover the sum of the bandwidths of the input signal and the multiplying chirp out of the mixer. To perform the transform properly, the frequency-time slopes of the multiplying chirp and the convolving chirp must be equal; therefore, the SAW chirp filter must have a length of 2.4 μsec. These selections for operating frequencies and bandwidths make fabrication of the SAW devices at 425 MHz somewhat more difficult than might be desired. Nevertheless, use of a projection printing system; stepping each transducer separately; and reasonable care in photoreduction, crystal preparation, and fabrication are sufficient to achieve good patterning despite the widely varying electrode widths and spacings across each transducer.

The post-multiplying chirp $C_2(t)$ may be identical to the pre-multiplying chirp, but this produces a transform output whose carrier is at 700 MHz. This is not significant for the adaptable filter, since this operation is not needed (as described in Section IV), but for spectral analysis, one might choose to reverse the chirp direction in that SAW device and use the difference frequencies out of the final mixer. Either case provides the Fourier transform complete with phase and magnitude as desired.

A computer can be used to simulate analog operation of the acoustic transformer and compare the result with that obtained from conventional digital FFT routines. This analysis uses a three-frequency input signal as discussed earlier and illustrated in Figure 4(b). The amplitude and spectrum of the signal are

plotted as the signal is processed through each block of Figure 3. The input signal will be only the portion of the input corresponding to the duration ΔT of one repetition of the gating chirp $C_1(t)$. This approach allows separation of the desired portion of the transformed signal and the unwanted sidelobe responses. All the plot amplitudes are normalized to unity. The time axis is normalized to the gating chirp duration ΔT, and the frequency axis is normalized to the gating chirp bandwidth ΔF. The time origin has been placed at the waveform center as it was in the mathematical analysis of the previous subsection. The frequency origin is located at the center of the input passband. The digital simulation used in this subsection has an overall time-bandwidth product of 62, which is similar to that of the prototype system simulated. The mixing chirps $C_1(t)$ and $C_2(t)$ are unweighted, unity amplitude, linear frequency chirps. The chirp filter impulse response is also perfectly flat (unweighted).

The input and calculated waveforms are shown in Figure 6. The input signal S(t) and the filter input after mixing A(t) are shown in Figures 6(a) and 6(b). The left plot shows the amplitude of the waveform versus time and the right shows the spectrum as calculated by an FFT. The amplitudes of the three tones have been chosen to be equal. Figure 6(a) shows that the input signal S(t) consists of a cw signal at band center, a short pulse 12 MHz below band center, and a longer pulse 6 MHz above band center. Since we are considering only one repetition of the input chirp, the cw signal is truncated outside the time of interest. Because the mixing chirp is unweighted, the amplitude of the mixing product A(t) in Figure 6(b) is the same as that of the input, but the spectrum is changed. The filter output B(t) and the transformed signal F(t) are shown in Figures 6(c) and 6(d). This diagram clearly shows how the transformer accurately resolves the input frequency components in time, producing the Fourier transform. A comparison of Figures 6(a) and 6(d) shows that the signal amplitude versus time and the spectrum are interchanged when a signal passes through a direct chirp-Z transformer unit.

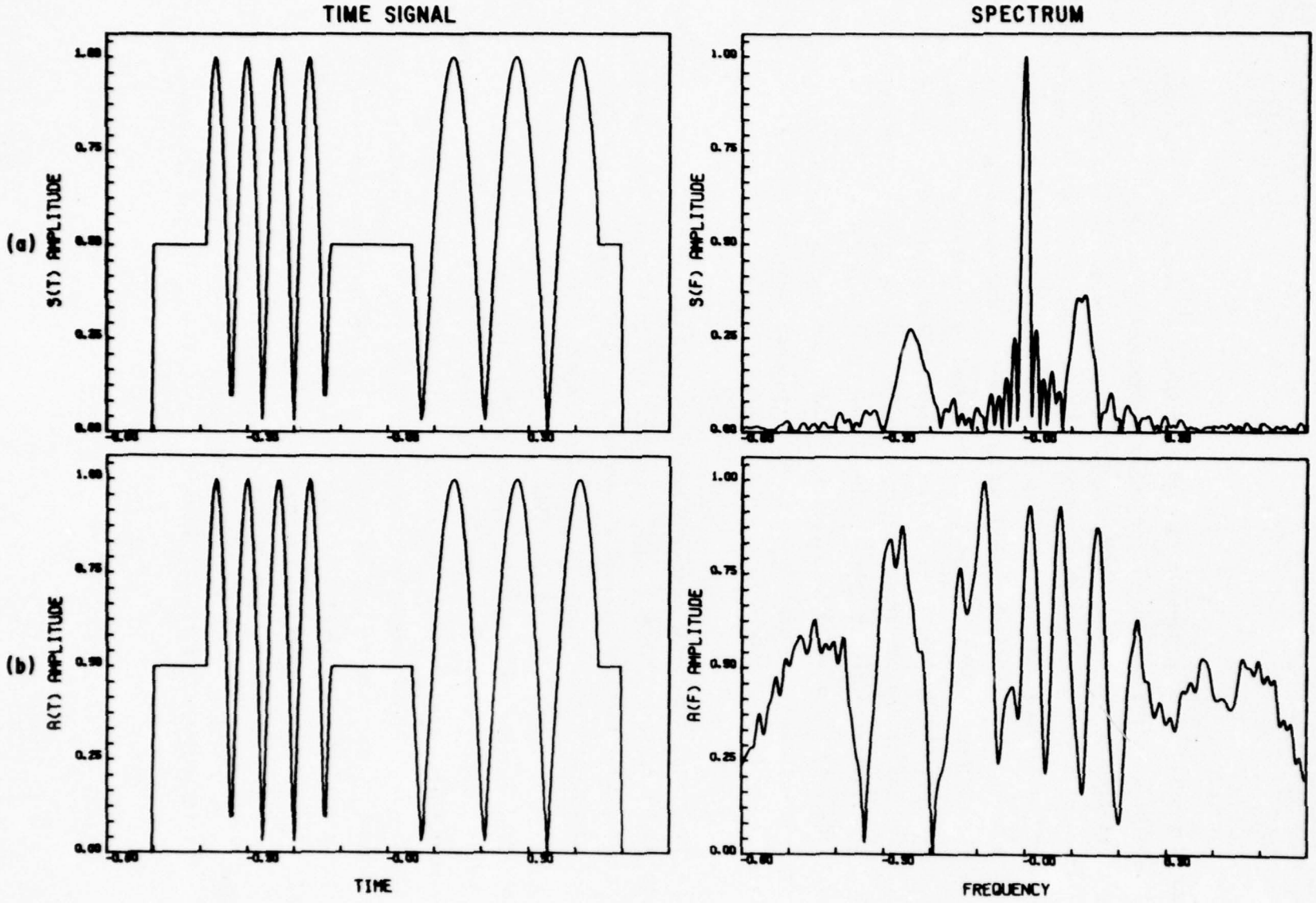

Figure 6 Chirp-Z Transform Unit Time Waveforms and Their Spectra. (a) Input signal S(t); (b) Mixing with down-chirp $C_1(t)$ produces A(t).

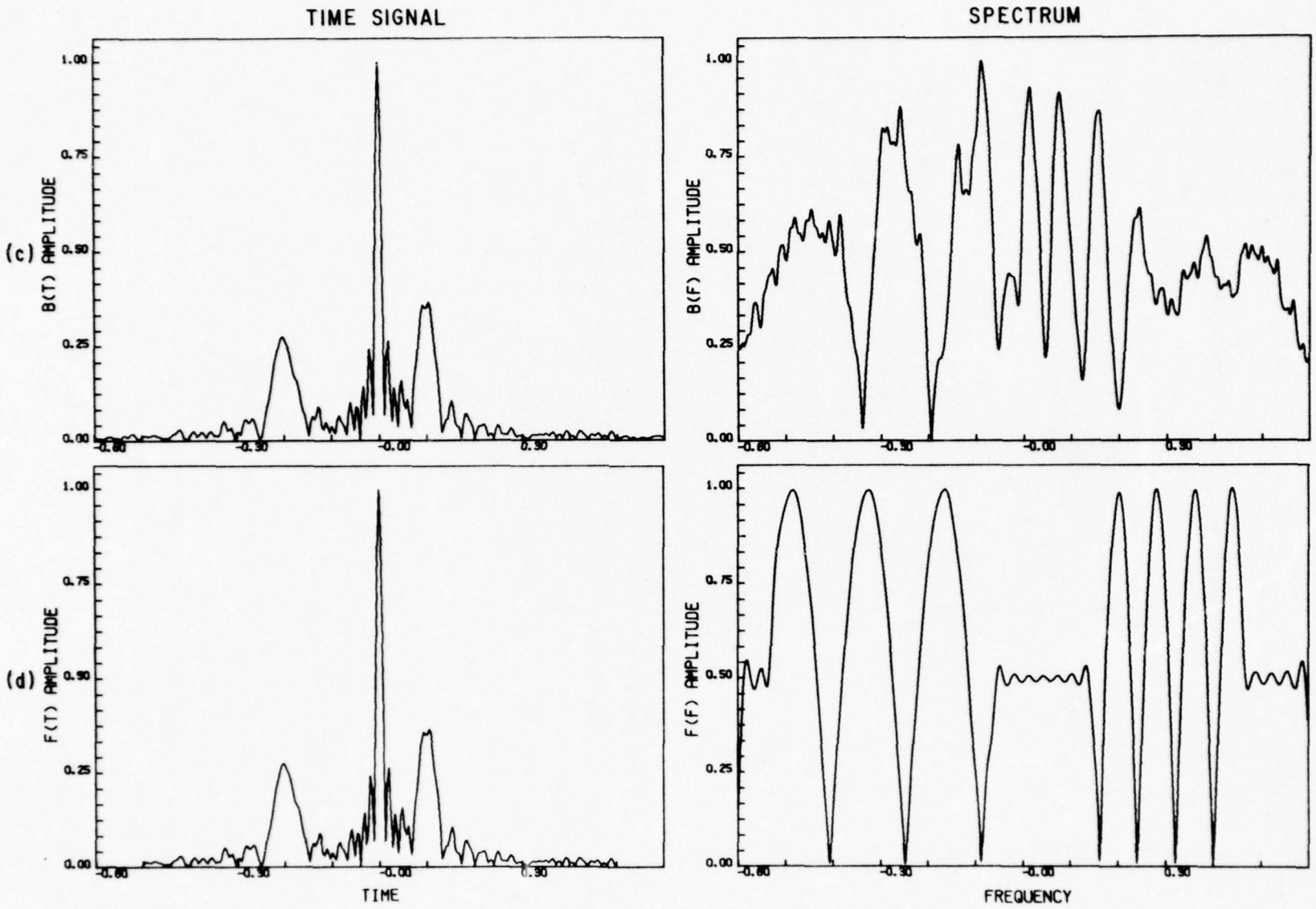

Figure 6 (continued) Chirp-Z Transform Unit Time Waveforms and Their Spectra. (c) Chirp filter output B(t); (d) Mixing with down-chirp $C_2(t)$ produces transformer output F(t).

Thus, the chirp-Z transformer resolves the frequency components in time so that the spectrum can be modulated directly with a time-varying waveform to produce the desired bandpass or bandstop filter characteristic. Note that the time separation of the three frequency components is present at the filter output in signal B(t) shown in Figure 6(c). Only the spectrum is changed in the postmixing with the chirp $C_2(t)$. More detailed analysis is presented later in this report.

D. SAW Chirp Transform Performance

The earliest SAW demonstration of the chirp transform was performed using existing surface wave pulse compression and expansion filters from a TI radar program. The devices used for this early breadboard were linear FM centered at 100 MHz with chirp bandwidth of 24 MHz and time lengths of 7.5 μsec. The details of this experiment are not described in this report, since the subsequent results from the prototype designed for this program are clearly superior and more capably demonstrate the transform performance.

The Transform Adaptable Processing System (TAPS) was designed and built with only one major modification to the transformer design. Subsequent analysis (Section IV) showed the desirability of using chirp devices with the greatest possible lengths. This raises the time-bandwidth product of the system and SAW devices and reduces the errors introduced by these analog operations. Further discussion is presented in the next section. The field-of-view of the projection printing system available for use prescribed that the transducers have lengths no more than 2.0 μsec, and design considerations for linear FM filters limit the useful chirp length to 1.905 μsec. With this modification the TAPS transform component was built as shown in Figure 7.

Demonstration of the chirp transform unit shown in Figure 7, the basic building block of the Transform Adaptable Processing System, is presented at this point. Figure 8 shows the actual chirp transform output for a succession of 7 cw input signals from 120 MHz to 180 MHz in 10 MHz steps. Since the chirp transform is designed to process 1.9 μsec blocks of time over exactly a 60 MHz band, the principal frequency component, or spectral main lobe, is shifted according to

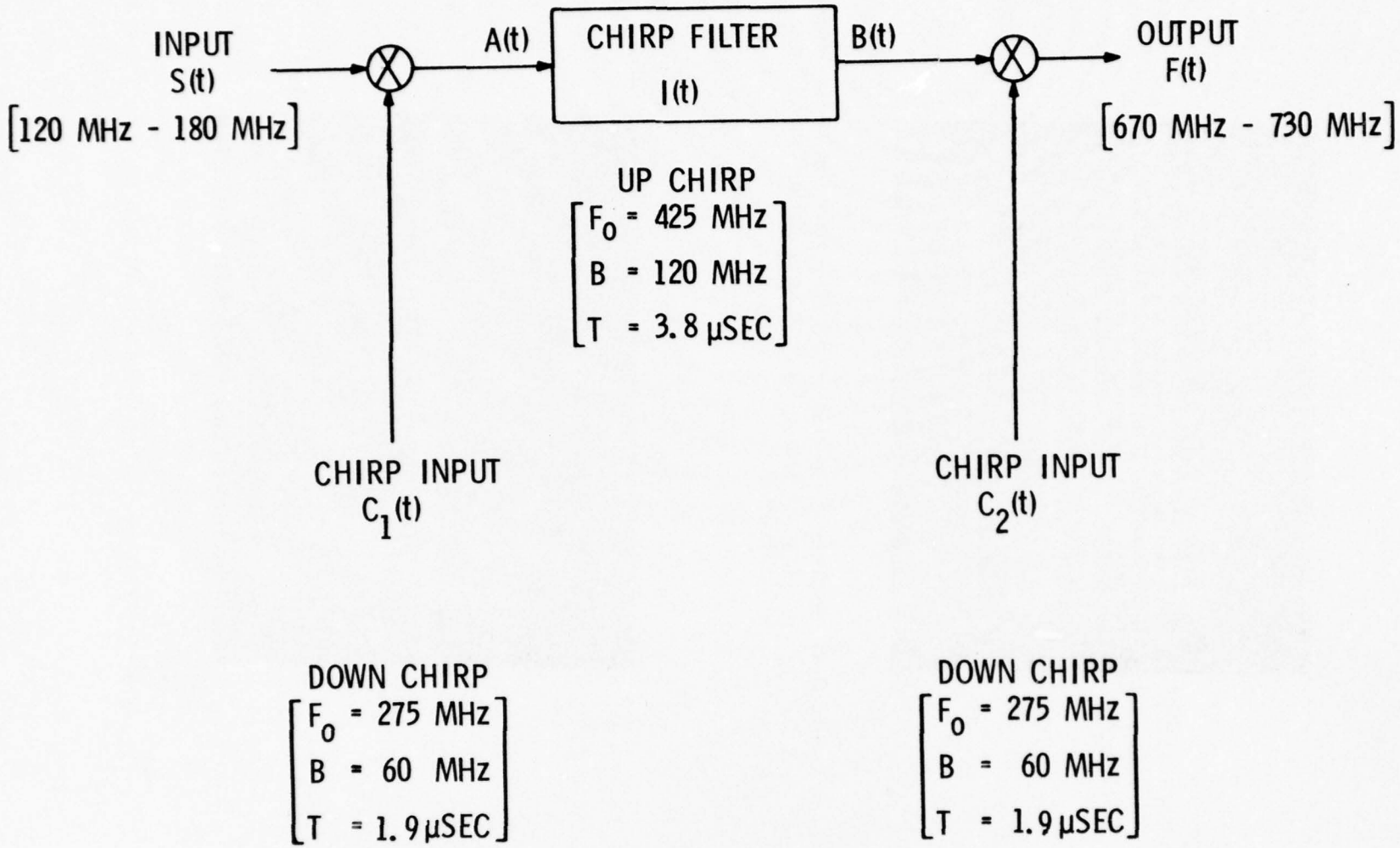

Figure 7 Implementation of a Prototype Chirp Transform System

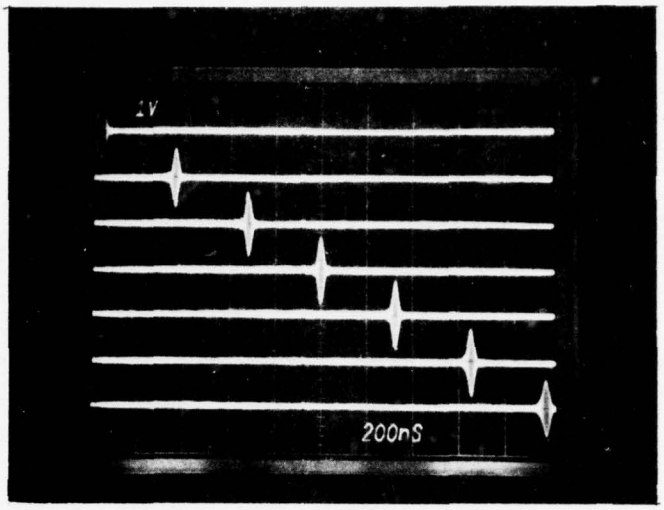

Figure 8(a) Prototype Chirp Transform Results for Seven Successive cw Input Signals Stepped from 120 MHz to 180 MHz in 10 MHz Steps

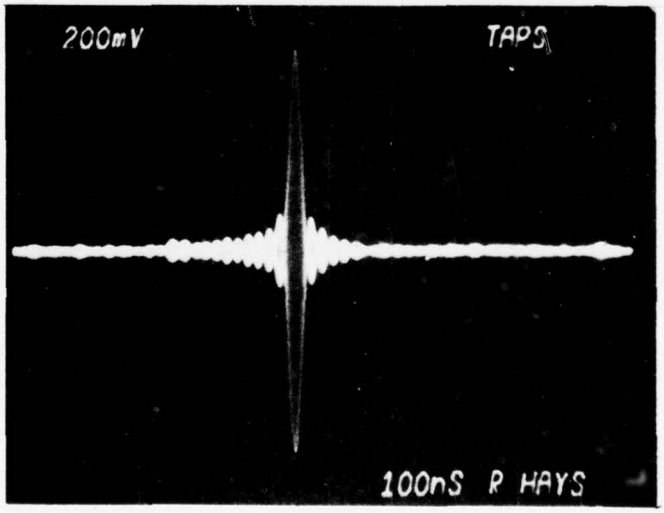

Figure 8(b) Prototype Chirp Transform for a Single cw Input Signal

the relation

$$\Delta t = \left(\frac{1.9\ \mu\text{sec}}{60\ \text{MHz}}\right) \Delta f = (0.032\ \mu\text{sec/MHz})(f - 150\ \text{MHz}) \quad .$$

Hence, for each 10 MHz step in frequency of the cw tone, the peak response moves 0.32 μsec, and the chirp transform output for the succession of cw signals in 10 MHz increments yields the linear translation shown in the figure. The amplitudes of all input signals were equal, demonstrating the flat bandpass response of the prototype over the designed 60 MHz bandwidth at 150 MHz center frequency. Each of these transform responses exhibits an essentially symmetric structure similar to sin x/x with -4 dB pulse width of 20 nsec compared to 17 nsec theoretical, which corresponds to 0.53 MHz, the width expected for the transform of a 1.9 μsec pulse.

For signals whose durations extend beyond a single 1.9 μsec time block, the chirp transform no longer represents identically the signal spectrum. This is easily seen by the fact that a true cw signal has only a single spectral line, not the sin x/x character of this system. This variation leads to special considerations to be noted subsequently. Pulsed signals of duration shorter than the time block of the system are handled precisely. Figure 9(a) shows the prototype transform results for three simultaneous input signals: 2 cw terms at 125 MHz and 145 MHz and a pulsed term at 165 MHz. The 165 MHz pulse width is 300 nsec. The frequency terms are all appropriately delayed according to their separation from the center frequency and the slope of the chirp filter; the spectral shapes are correct, including the sin x/x structure of the pulsed spectrum with null-to-null width of 0.21 μsec corresponding to 6.7 MHz exactly as required. Figures 9(b), (c), and (d) show three similar cases where the 165 MHz pulse widths are changed to 0.05, 0.1, and 0.8 μsec, respectively. The transforms show the inverse relationship of time length and bandwidth and the transform waveform has precisely the correct null-to-null widths corresponding to each of these rf pulse cases. The shortest pulsed signal that the system can handle without violation of the required bandlimiting condition is determined by the prescribed 60 MHz system bandwidth. This limit is nominally 20 nsec, depending on the character of the input signal, the configuration of the chirp transform processor, and the maximum acceptable aliasing or spurious levels.

(a) PW = 0.3 μsec

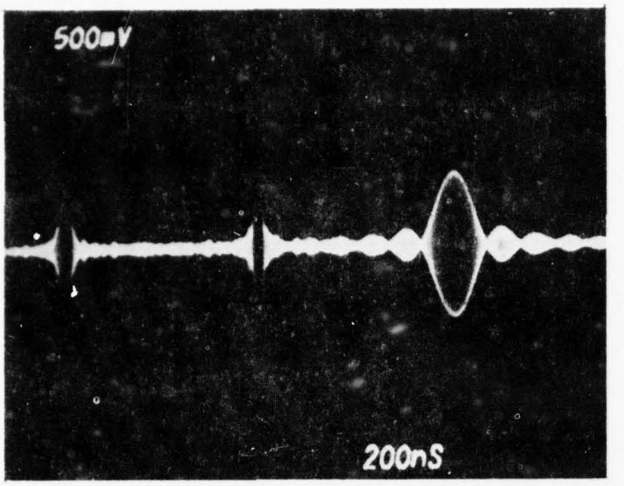

125 MHz 150 MHz 175 MHz

(b) PW = 0.05 μsec

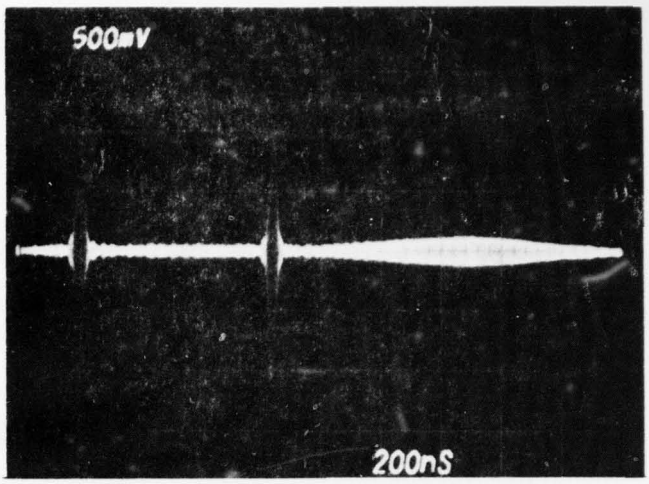

125 MHz 150 MHz 175 MHz

(c) PW = 0.1 μsec

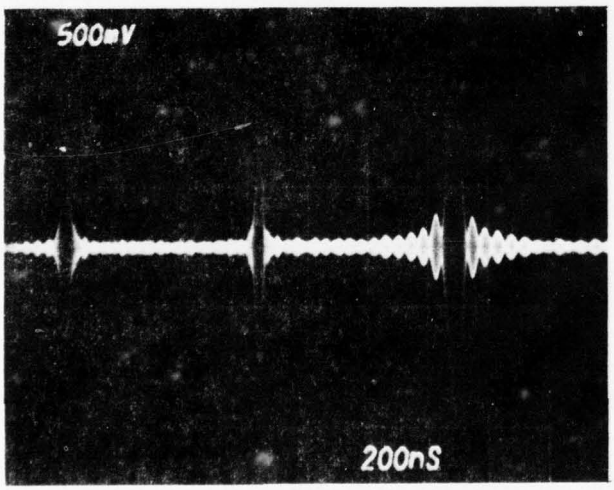

125 MHz 150 MHz 175 MHz

(d) PW = 0.8 μsec

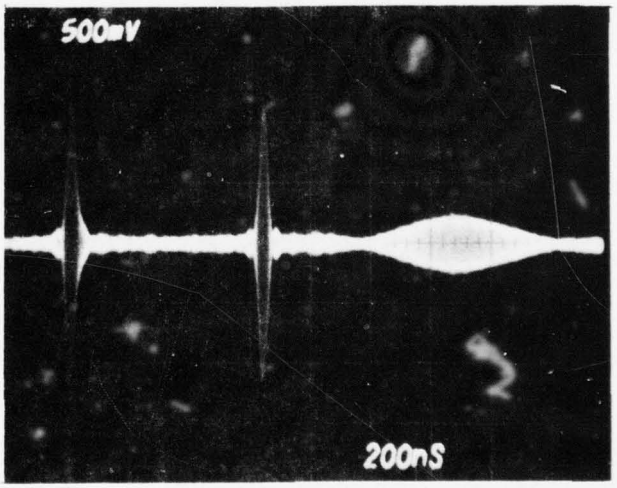

125 MHz 150 MHz 175 MHz

Figure 9 Chirp Transform of Three Simultaneous Input Signals Including cw Signals at 125 MHz and 145 MHz and a Pulsed Term at 165 MHz of Width PW

E. Chirp Transform Continuous Operation

The chirp transform is performed over an interval of time that corresponds to the duration of the first multiplying chirp $C_1(t)$ (1.9 μsec). For continuous operation, one must repeat this transform operation each 1.9 μsec to transform all the input signal. TAPS, therefore, operates on successive blocks of data entered via the input time signal. The TAPS system has been described as processing short rf signal blocks, but by dividing continuous input signals into short consecutive time blocks, processing each block separately, and finally summing (by inverse transforming) the processed signal blocks, continuous operation is achieved. This is discussed further in the sections on system applications of the chirp transform, but for the chirp transform alone, spurious considerations merit the most attention.

Obviously, the time length of the transformed output is $3\Delta T$, or 3 times the length of the processed signal input (ΔT) from the convolution with the chirp of $2\Delta T$ length. Since only the center ΔT interval (corresponding to the time when the input signal is entirely within the convolving filter) represents the true Fourier transform, the adjacent ΔT intervals contain undesired information. The remaining time contains only the sidelobes of the transform operation. In continuous operation, these sidelobes are present in the adjacent intervals of the time signal and cannot be directly gated off. The most obvious (and sometimes most desirable) configuration would have two parallel channels, each processing alternate time blocks and the accurate transform information is then available for successive time intervals at alternate channel outputs, automatically eliminating the unneeded end portions of the $3\Delta T$ convolution output.

A considerable simplification is possible, however. The transform is accurate over the bandwidth of the system (in our case 60 MHz) and if the input is truly bandlimited, the components outside this frequency range are small. The ΔT intervals on either side of the central time segment exhibit spurious responses comparable to the violation of the bandlimited assumption. Since one can certainly ensure that the input signals are bandlimited, the spurious responses may be sufficiently small to neglect that contribution compared to the actual transform data. This means that the transform process can be performed by the single channel shown in Figure 7 with the multiplying chirps impulsed each 1.9 μsec corresponding to their length and signal time block length for transform processing. The chirp transform output traces out the signal transform from 120 MHz to 180 MHz corresponding to 1.9 μsec, immediately repeats for the chirp transform of the next interval of time, and so on, with the spurious of alternate intervals neglected in comparison to the transform information present.

To demonstrate the continuous operation of the prototype, the three-tone input signal of Figure 9(a) was used. The period of the pulsed signal was selected to be 1.9 μsec so that it is present in every chirped interval. The trace of Figure 9(a) shows a single chirp transform interval out of the train of transforms continuously available in Figure 10. Figure 10 shows this transform information clearly repeated on 1.9 μsec intervals as necessary for continuous operation. Simulations of this continuous operation have been performed to determine the distortion introduced. These are included in the discussion of the TAPS system for adaptive filtering.

F. Chirp Transform Dual

The chirp transform diagrammed in Figure 7 suffers from two very basic limitations. There are two nonlinear elements (mixers) in the signal channel which define maximum signal levels and minimum distortion. In addition, the surface wave chirp filter in the path must have at least twice the bandwidth of the signal to be transformed, accompanied by nominally 12 dB more loss than

INPUT

CW: 125 MHz and 145 MHz
PULSE: 300 nsec at 165 MHz

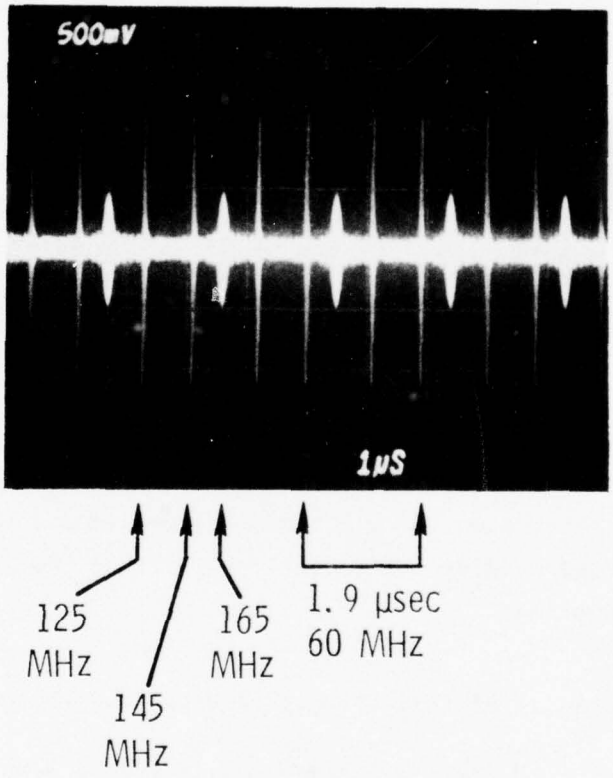

Figure 10 Transform Continuous Operation of the Prototype for the Three-Tone Input Used for Figure 9(a)

the usable bandwidth suggests. It would seem desirable to examine alternative configurations that would reduce the number of mixers and/or remove the "wasted" bandwidth from the filter in the signal path. The most logical substitute configuration for consideration would, of course, be the dual. The dual to Figure 7 is shown in Figure 11.

The output of the chirp transform is written as follows:

$$O_1(t) = \left[\left(S(t) \cdot C_1(t)\right) \; * \; I(t) \right] C_2(t) \; ,$$

where the expression for each element is given on pages 15 and 17. This reduces to the transform of S(t) over the center one-third $[(-\Delta T/2) < t < (\Delta T/2)]$ of the output signal.

$$O_1(t) \propto \int_{-\frac{\Delta T}{2}}^{\frac{\Delta T}{2}} S(\tau) \exp(-j\omega\tau) \, d\tau \; , \; \omega = \frac{2\pi\Delta F}{\Delta T} \, t.$$

Realistically, however, the output signal for this implementation approximates the transform of the input, and its accuracy depends on the validity of the "band-limited" assumption for all the SAW elements and the signal. Similarly, the spurious responses outside the center one-third of the output signal reflect this customary assumption.

The dual (Figure 11) of this circuit is described as follows:

$$O_2(t) = \left[\left(S(t) * C_1(t)\right) \cdot \; I(t) \right] * \; C_2(t).$$

If one looks at the Fourier transform of this expression, the duality requirements become more obvious and evaluation is simpler:

$$F \left\{ O_2(t) \right\} = \left\{ \left[\left(S(\omega) \cdot C_1(\omega)\right) * \; I(\omega) \right] \; C_2(\omega) \; \right\},$$

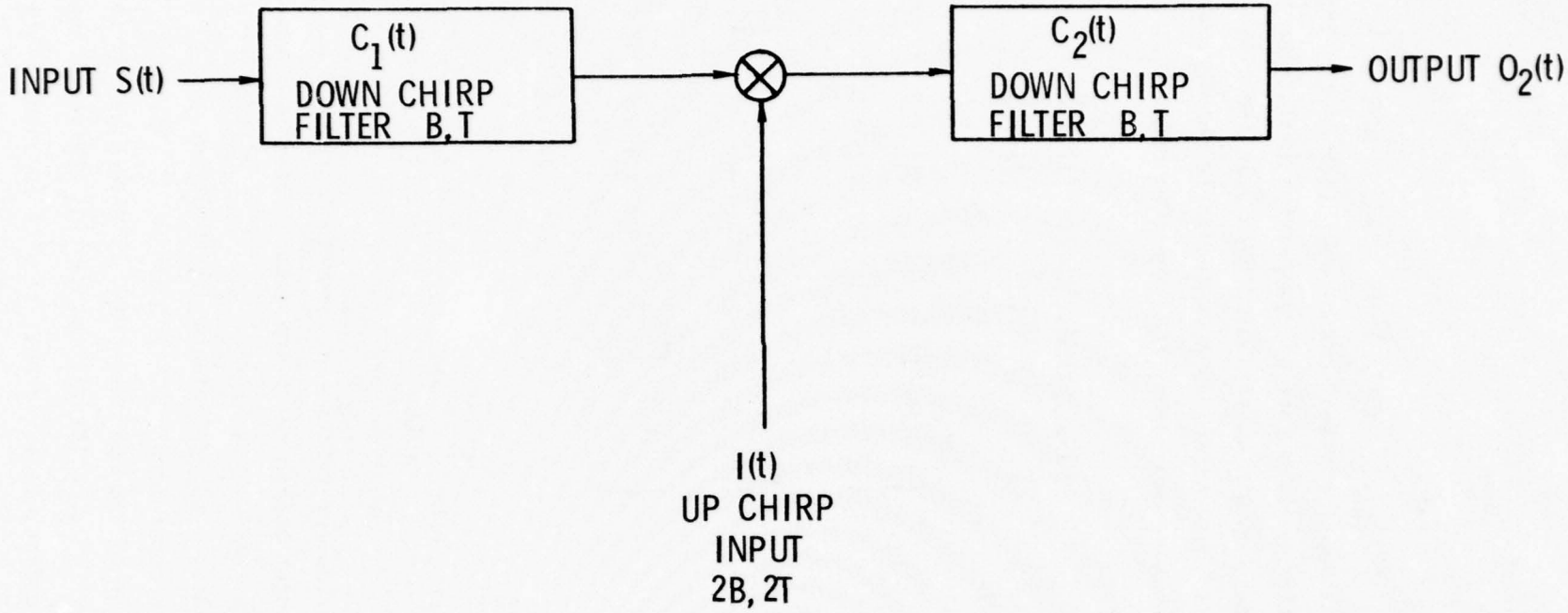

Figure 11 Chirp Transform Dual

where the elements are the Fourier transforms of each term of the preceding equation. Close examination reveals that the expression inside the brackets is the same in the frequency domain as that of Figure 3 in the time domain. Hence, the requirement is that the chirps have quadratic phase and rectangular shape in the frequency domain rather than the time domain. ($\omega = 2\pi f$)

$$C_2(\omega) = C_1(\omega) = \begin{cases} \exp(-jk\omega^2) & |f| < \frac{B}{2} \\ 0 & |f| > \frac{B}{2} \end{cases}$$

$$I(\omega) = \begin{cases} \exp(jk\omega^2) & |f| < B \\ 0 & |f| > B \end{cases}$$

$$F\{O_2(t)\} = \left\{ \left[(S(\omega) \cdot C_1(\omega)) * I(\omega) \right] \cdot C_2(\omega) \right\}$$

$$= \left\{ e^{-jk\nu^2} \int_{-B\pi}^{+B\pi} S(\omega) \exp(-jk\omega^2) \exp(jk[\nu-\omega]^2) d\omega \right\}$$

$$O_2(t) = F^{-1} \left\{ \int_{-B\pi}^{B\pi} S(\omega) \exp(-j\omega t) d\omega \right\}, \quad t = k2\nu$$

Again, the expression inside the brackets accurately represents a transform of $S(\omega)$ over only the center one-third of the output, or $|\nu| < 2\pi(\nu/2)$. The output $O_2(t)$, however, is the inverse Fourier transform of that expression, and that integration covers $-\infty$ to ∞, including the spurious region outside the center one-third. In other words, $O_2(t)$ does not exactly equal $S(\omega)$ anywhere, and the validity of the approximation is determined by the criterion that $S(t)$ be time-limited to $|t| < (\Delta T/2)$, the dual of the requirement of band-limiting discussed in the first case. Hence, if $S(t)$ is band-limited,

$$\int_{-B\pi}^{B\pi} S(\omega)\ \exp(-j\omega t)\ d\omega \approx \int_{-\infty}^{\infty} S(\omega)\ \exp(-j\omega t)\ d\omega$$

and if S(t) is appropriately time-limited,

$$O_2(t) \approx F^{-1}\ \{\ F\ (S(\omega))\ \} \approx S(\omega).$$

Apparently, it is possible to approximate the Fourier transform of a signal in either configuration under the appropriate restrictions. Which of the two is more accurate or is preferable for other reasons, such as insertion loss, requires further examination and/or simulation. One substantial factor is that SAW devices are truly finite in time length while satisfying the band-limiting approximation. Hence, "perfect" chirps cannot be obtained in the frequency domain as they may be in time. The distortion introduced in the analog transform operation by the requirement of time-limited input signals in the second case may be no worse than that due to the arbitrary partitioning of the input signal in the first chirp configuration. In either case, the band-limiting assumption is satisfied equivalently.

SECTION IV

TRANSFORM ADAPTABLE BANDPASS/BANDSTOP FILTER

Of the many important new signal processing applications made possible by the availability of spectral information in real time, the first to be discussed and demonstrated is the continuously variable bandpass/bandstop filtering.

Since the chirp transform converts the input signal piecewise into a time signal that is proportional to the Fourier transform of each signal block, adaptable filtering can be effected by simply multiplying each of the frequency components, which are now separated in time, by an appropriate amplitude and phase weighting coefficient with an rf mixer. This "modulated" chirp transform signal can then be inverse-transformed with a second chirp transform to reconstruct the "filtered" time signal. Figure 2 shows the block diagram of the system just described, consisting of three processing stages. By varying the modulation function G(t), the portion of the input spectrum that is passed or stopped can be arbitrarily selected in any combination of bandpass and/or bandstop responses. For programmable bandpass/bandstop filters the frequency weighting coefficients can be simple time gating. This section describes the filter operation, the prototype results, and the features significant to the design of this type of system.

A. Filter Description

An example of the type of filtering that can be done is shown in Figure 12. In this figure only the envelopes of the various signals are sketched. The input is chosen to consist of three equal amplitude tones: a continuous signal at frequency f_2 and pulsed signals at frequencies f_1 and f_3. Where the signals overlap, a beat pattern is produced as shown in the top line of this figure. The second line of the figure represents the spectrum F(t) produced by the chirp transformer, which resolves the signal into three separate time signals. The width of each of these signals is determined by the duration of the corresponding input tone and its spectrum. As the length of the input tone increases, the width of its transform decreases until it is limited by the maximum length input

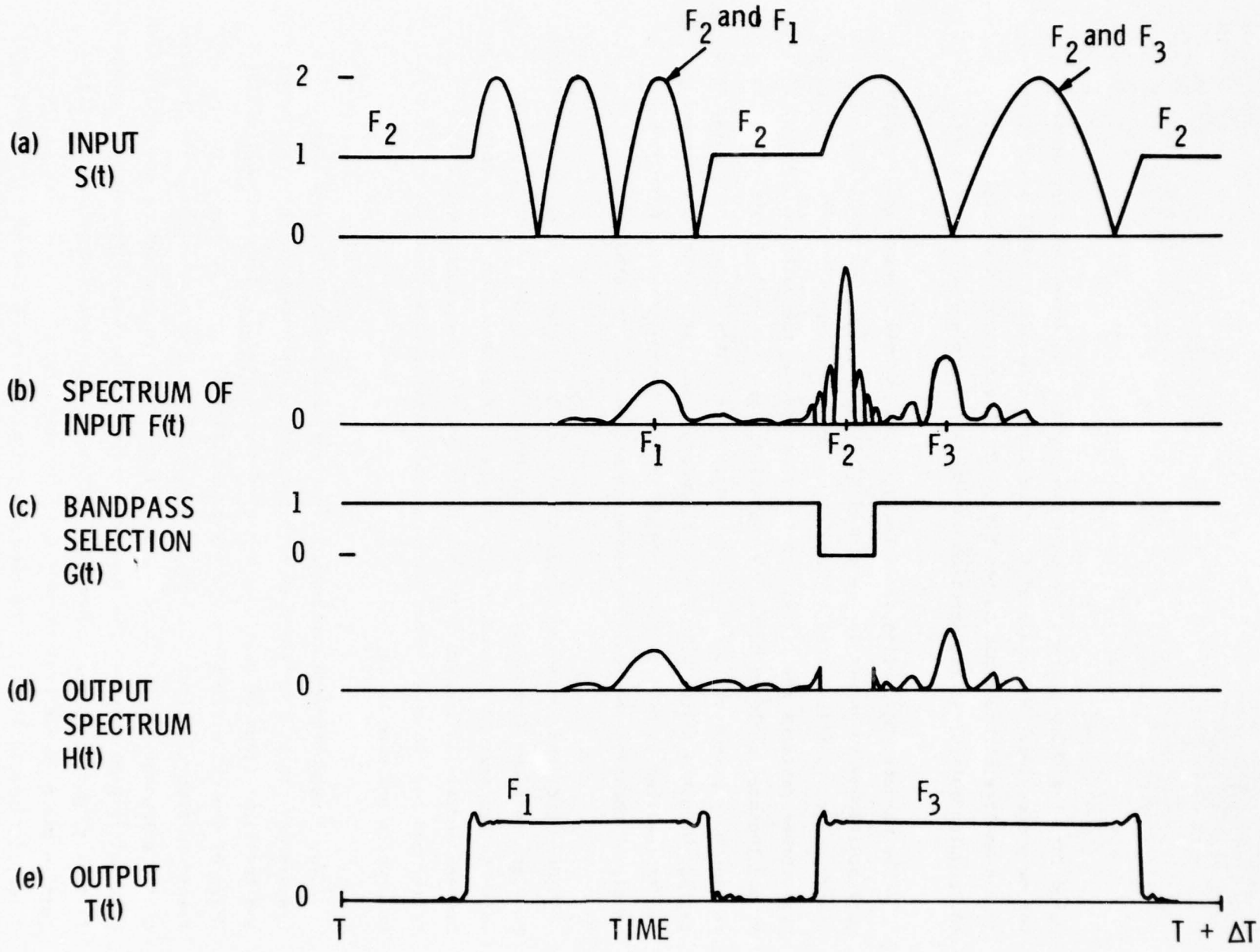

Figure 12 Transform Adaptable Bandpass/Bandstop Filter Illustration

pulse that the chirp-Z transform unit can process, an important consideration for cw processing. The shape of the time signals comprising F(t) are determined by the spectra of the input pulses S(t). In this example, the inputs are rectangular pulses, so the spectrum modulations are sin x/x or sinc functions.

The bandpass modulation function G(t) used in this example is a stopband gate positioned to remove the cw signal at frequency f_2. The resulting modified spectrum H(t) is illustrated in the fourth line of Figure 12. After the inverse transformer restores the signals to the time domain, the background signal at f_2 and the beat patterns caused by that signal are removed. In addition, the remaining rf pulses at f_1 and f_3 are distorted slightly, since the signals have passed through a filter with finite bandwidth. Similarly, bandpass operation can be realized as well as many combinations of bandpass/bandstop responses simply by changing the position and width of the gate or gates.

As noted, the processed output signal block is obtained from the modulated Fourier transform (frequency spectrum) by means of a second chirp transform which is properly configured to provide the inverse transform. The only differences between normal and inverse transform units are that the slopes of the chirp filter and the two chirp generators must be reversed, i.e., change up-chirp to down-chirp and vice versa.

The straightforward combination of transformer, modulator, and inverse transformer can be simplified by eliminating the last stage of the transformer and the first stage of the inverse transformer. That is, the post-multiplying chirp of the chirp transform and the pre-multiplying chirp of the chirp inverse transform from the block diagrams of Figures 2 and 3 are not necessary. The frequency components of the input signal are separated in time before the mixing with the post-multiplying chirp of the transform and, for the case of programmable bandpass filtering, gating at that point is all that is required. Removal of the dispersive phase in the transformed signal by multiplying by that chirp is therefore pointless in light of the need for reapplication of that exact dispersive

character to perform the inverse transform. This reduces the number of components required relative to the straightforward cascading of the complete transform units of Figure 7.

The block diagram of Figure 13 shows the principal components required for the adaptable bandpass/bandstop filters. The chirp slopes in the transform must match those in the inverse transform to avoid time compression or expansion at the output. Since one normally prefers that the filtered output T(t) exhibit no change in frequency from the input, the difference product term out of the final mixer is desired and is selected by the broadband filter. This further facilitates system design, since the two chirp generators (or multiplying chirps) are then identical because no weighting on the chirps is desired. (Weighting the chirps to reduce spurious levels is discussed in this section.) The complete adaptable filter requires but four surface wave devices: two chirp generators and two chirp filters. The broadband output filter is appropriately a low-loss lumped element bandpass filter, as is the broadband input filter (not shown) to remove input frequencies outside the 50 MHz operating band.

The frequency-time diagram for this complete system is shown in Figure 14. The processing of the input signal to the output of the first chirp filter B(t) is the same as that described in the transformer section relative to Figure 4(a). The output of the up-chirp filter B(t) is modulated in the programmable bandpass modulator and passes directly into the down-chirp filter. Thus, the input to this filter consists of the modified spectrum of the input signal S(t) modulating a chirped carrier signal. Because it has an up-chirp characteristic, it is matched to the inverse transformer down-chirp filter. The output D(t) is a filtered version of the input S(t) mixed with a down-chirp. It is delayed in time by the second filter. By post-mixing with a second down-chirp $C_3(t)$ and selecting the difference frequency with a bandpass filter, one obtains the desired filtered output signal T(t) at the same frequency as the input, but delayed in time.

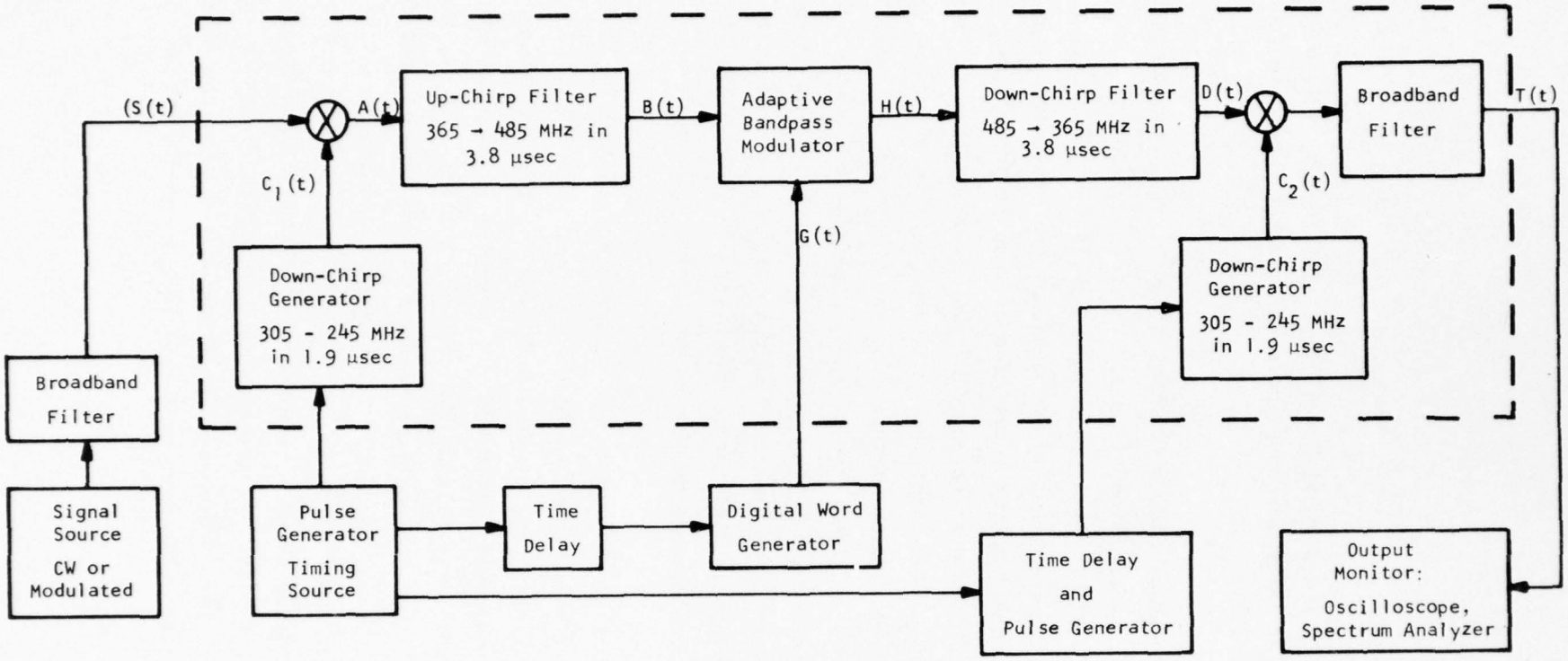

Figure 13 Block Diagram of the Acoustic Adaptive Transversal Filter Using Transform Processing.
(Prototype inside dashed lines, laboratory test equipment outside.)

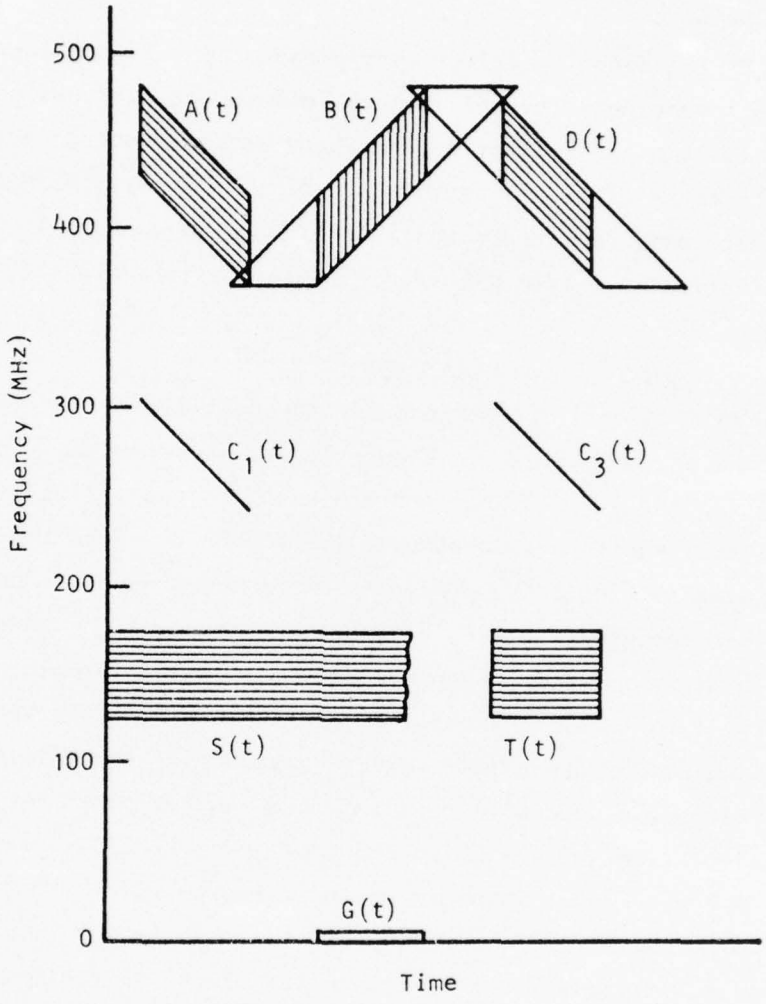

Figure 14 Frequency-Time Diagram of Transform Adaptive Processor System

B. Computer Analysis

Simulations of the adaptive filter as discussed in the last section have been performed to investigate several factors influencing TAPS design. Besides the revealing analysis of the effect of time-bandwidth product on the system performance, the effects of weighting the SAW chirp filters, timing errors between the two chirp generators, continuous operation involving cw signals, and modulation function selection have been examined. These topics are discussed in the following subsections.

The parameters originally prescribed for the preliminary design of the adaptive filter instead of those shown in Figure 13 are used for the simulations. That is, the SAW time lengths are 1.2 μsec and 2.4 μsec instead of 1.9 and 3.8 μsec, respectively. These results are subsequently incorporated into the final design detailed in the next section. The preceding simulations were performed at baseband, but all other computer analyses have been effected at the carrier frequencies of the prototype system. Nonetheless, the results are in general displayed in envelope form to avoid excessive plotting costs. Moreover, the purposes of these simulations are better served by examining the envelope and phase data where variations in successive runs are more easily identified. This is illustrated by simulations of the chirp transform of Figure 3 shown in Figures 15 and 16. The 1.2 μsec input waveform shown in Figure 15(a) is a cw term at 150 MHz, plus two pulsed rf terms: 0.35 μsec at 162 MHz and 0.51 μsec at 144 MHz. The two pulsed rf terms occur at the center of the time block, and their interference is clearly exhibited. The envelope is shown in Figure 15(b) for comparison with the plot with the carrier term present. Figure 16(a) shows the magnitude of the chirp-Z transform unit output at rf. The corresponding output in envelope form is shown in Figure 16(b). The costs of generating the amplitude with the carrier frequency are higher and the data are no more illuminating than is the case for envelope and phase information.

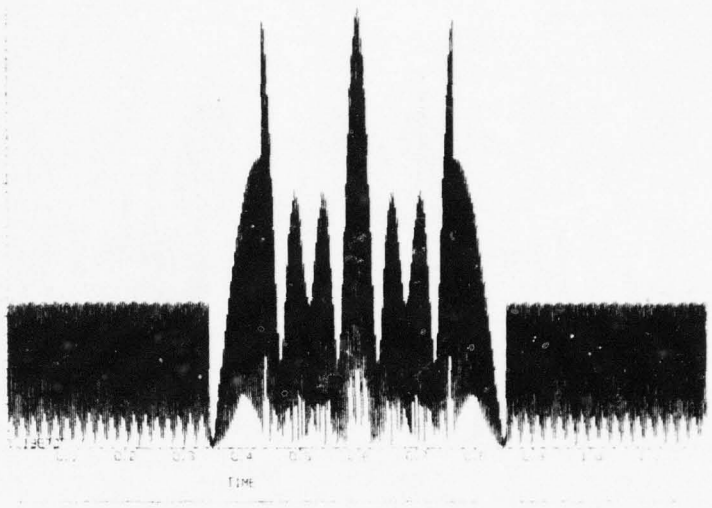

(a)

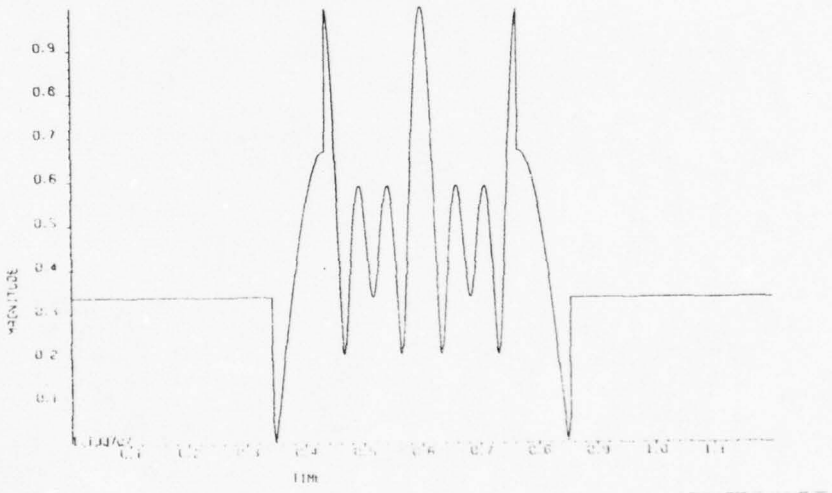

(b)

Figure 15 Magnitude (a) and Envelope (b) of a Three-Tone Input Signal to be Transformed

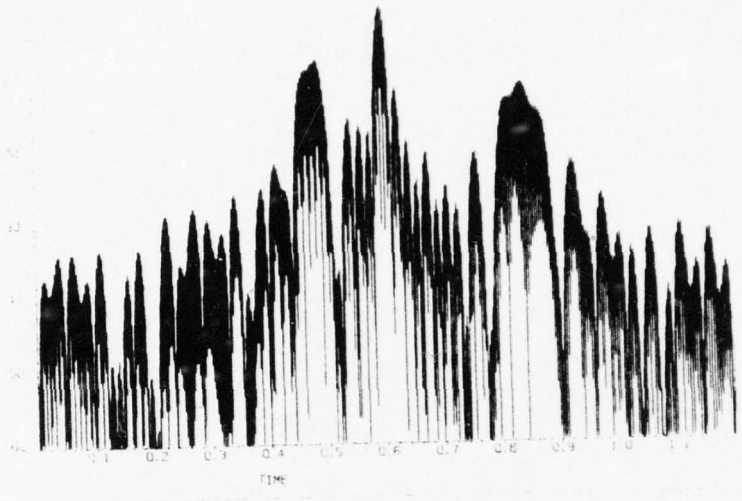

(a)

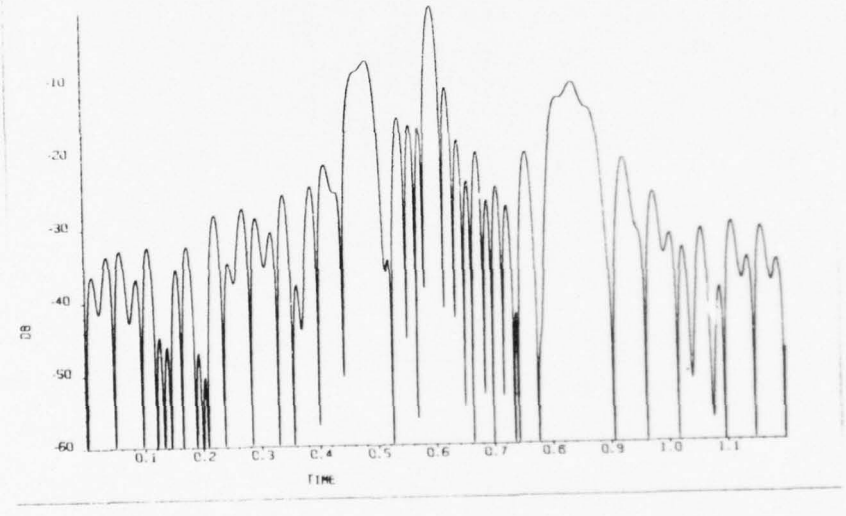

(b)

Figure 16 Magnitude (a) and Envelope (b) of the Chirp-Z Transform Signal of Figure 15

1. Transform - Inverse Transform Accuracy

A fundamental test of performance of this prototype system is the distortion introduced with no intervening modulation or filtering. The question to be answered is how well the input signal is reconstructed at the output of the TAPS system after both transformation and inverse transformation. In addition to the actual prototype results, simulations of the TAPS system yield instructive data. A 1.2 μsec, three-tone, bandlimited signal whose envelope is shown in Figure 15 was used as the input to the system shown in Figure 13. The simulations are performed at the carrier frequencies indicated in the block diagram, but in general the results are displayed in envelope form.

For these simulations, it is important that the input signal be bandlimited so that the processor output is not faulted for failure to reproduce the equivalent bandwidth larger than that of the TAPS system. To illustrate this, the familiar three-tone input is used. Figure 17(a) is a plot of the input signal envelope showing one cw term at 150 MHz and two pulsed rf terms, 0.35 μsec at 162 MHz and 0.51 μsec at 144 MHz. The time window is again 1.2 μsec for this system. Figure 17(b) is a plot of the system output following the transform and inverse transform with no filter modulation. The difference between the output and input normalized to the peak of the output is shown in Figure 17(c). The largest errors occur at the edges of the pulses and the time interval where the chirp filter bandlimiting has the greatest effect. Figure 18(a) shows the same input signal that has been bandlimited by a 2:1 shape factor filter with a 60 MHz bandwidth. The system output for this case is given in Figure 18(b), and the error introduced by the TAPS system is shown in Figure 18(c) normalized to the output peak. The large errors of Figure 17 are not present when the input signal is confined to the bandwidth of the system. Where the input signals are not bandlimited in future simulations, one should neglect this effect as seen here.

The preceding simulations of the preliminary prototype design of Figure 13 with no filtering or modulation show that the input [Figure 18(a)] is

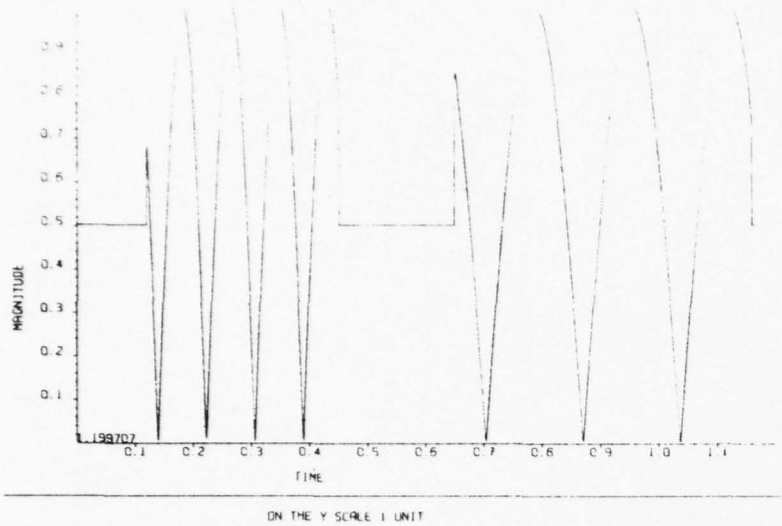

Figure 17(a) Envelope of the Three-Tone Input Signal Without Bandlimiting

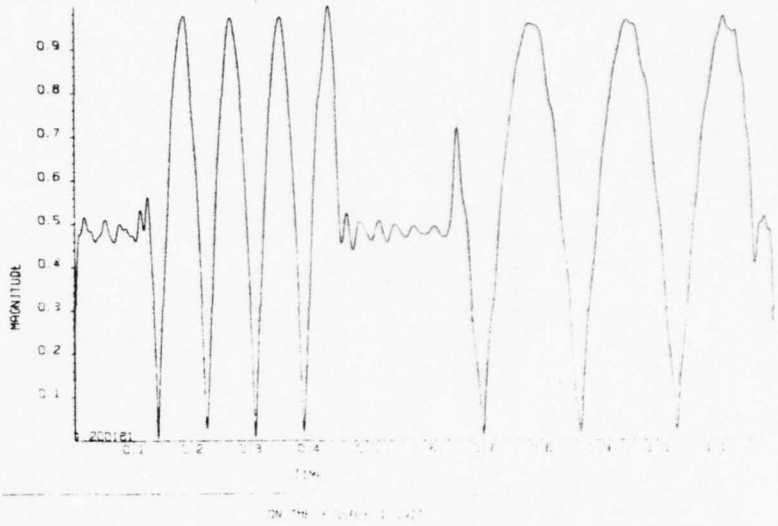

Figure 17(b) Envelope of the Output Signal After the Chirp Transform and Chirp Inverse Transform

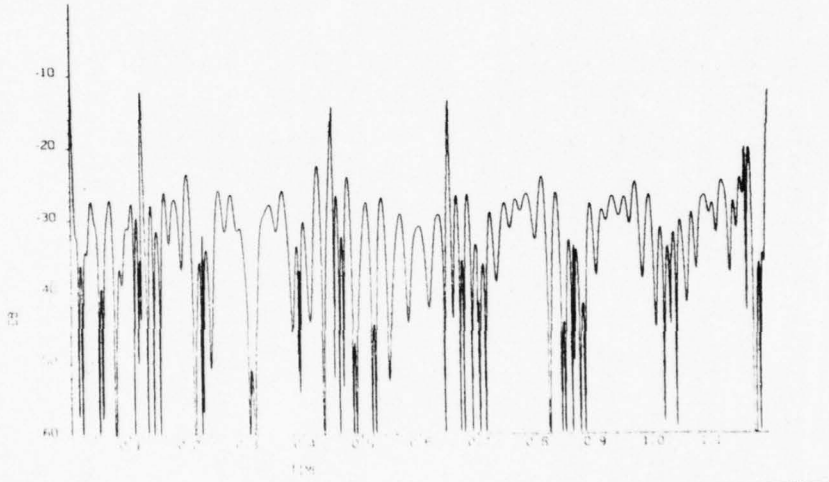

Figure 17(c) Errors Relative to the Input Without Bandlimiting Introduced by TAPS Transform - Inverse Transform Operations. (Difference between the TAPS output and input signals normalized to the signal peak.)

Figure 17 Transform Processor Accuracy Without Bandlimiting of Input

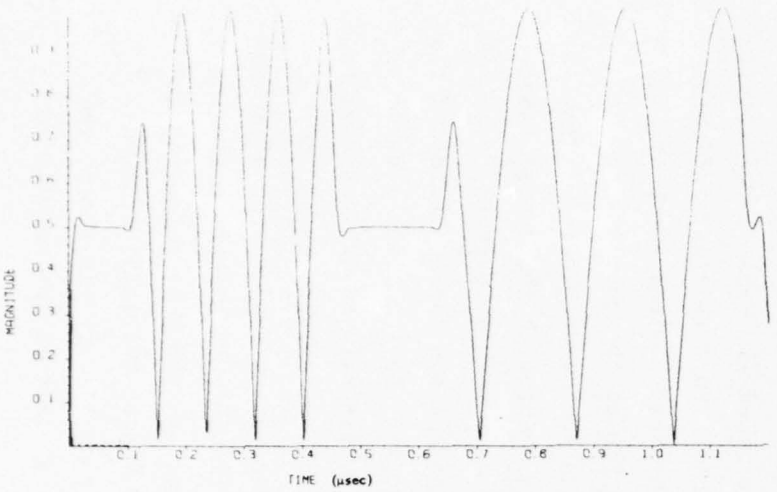

Figure 18(a) Envelope of the Three-Tone Input Signal With Bandlimiting Provided by a 2:1 Shape Factor, 60 MHz Bandwidth Filter

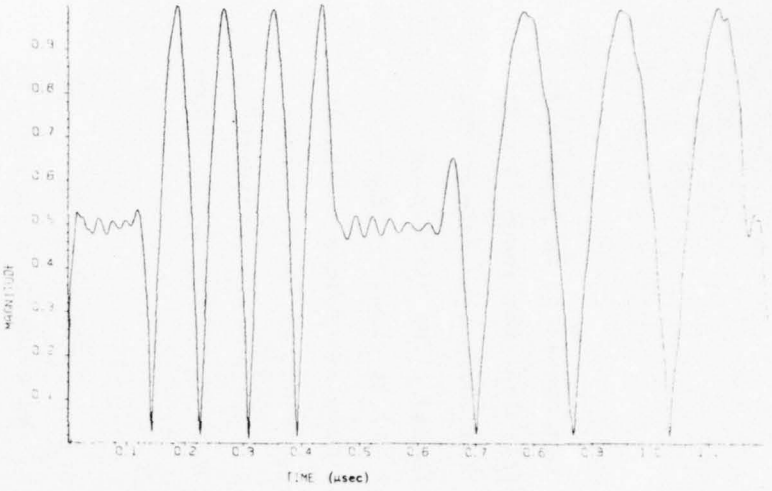

Figure 18(b) Envelope of the Output Signal After the Transform and Inverse Transform Operations

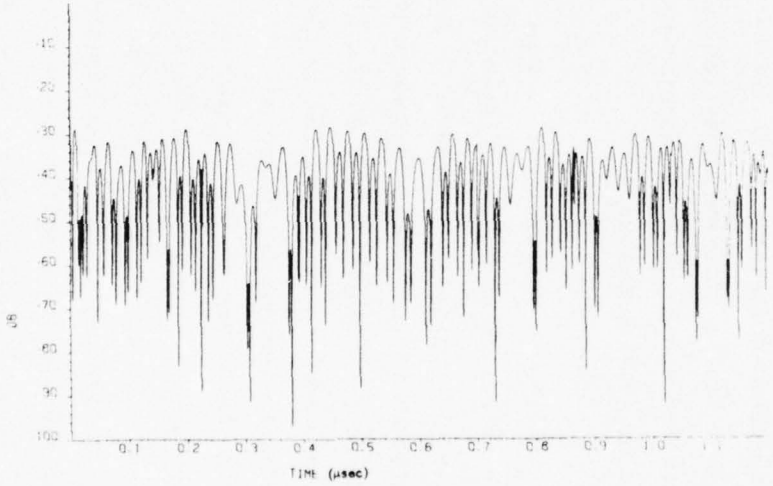

Figure 18(c) Errors Relative to the Bandlimited Input Introduced by TAPS Transform - Inverse Transform Operations. (Difference between the TAPS output and input signals normalized to the signal peak.)

Figure 18 Transform Processor Accuracy with Bandlimiting of Input

reconstructed after the transform - inverse transform operation to produce an output [Figure 18(b)] whose difference [Figure 18(c)] from the input is nominally -30 dB or better over its entire duration. The chirp transform of that input [shown in Figure 19(a)] is equally well performed. The difference between the chirp transform and that using a large FFT is shown in Figure 19(b) where the errors are seen to be below -30 dB down everywhere except at the cw spectrum component, which, as we have noted, is not perfectly represented in a finite time-length system such as this. (Further cw considerations are discussed subsequently.) Nonetheless, even the cw term is properly reconstructed as just discussed.

Although these results appear satisfactory for achieving the -25 dB spurious rejection demanded of the adaptive filter, improvement is possible by increasing the system time-bandwidth (BT) product. The errors introduced by the character of the linear FM components and accompanying Fresnel effects were found to be diminished rapidly as the BT product of the system was increased. Since the bandwidth of the system is already determined (50 MHz), and increasing the bandwidth further would add more insertion loss, the time length of the chirps is the object of this simulation. With the band-limited input of Figure 18, the transform-inverse transform operation was performed for multiplying chirp lengths of 1.8, 2.4, 3.6, and 4.8 μsec in addition to the original 1.2 μsec length. Comparison of the chirp transform of the input with the actual input spectrum revealed no dramatic improvement in accuracy with BT product, since the spurious level is influenced by the adjacent intervals and the character of the input signal as discussed under continuous operation. In fact, the average error varied between -35 dB and -50 dB for these cases with no obvious advantage in larger BT systems. Figure 20(a) illustrates this behavior. These inconclusive results are completely overshadowed by the system performance after the inverse transform, however. The TAPS output is visually identical to the input. The marked improvement in reproduction of the input is shown by comparing the output errors relative to the input signal for 4.8 μsec multiplying chirps [Figure 20(b)] to that for the 1.2 μsec case [Figure 18(c)]. In short, the average error decreased as 20 log BT as shown by the simulation results for

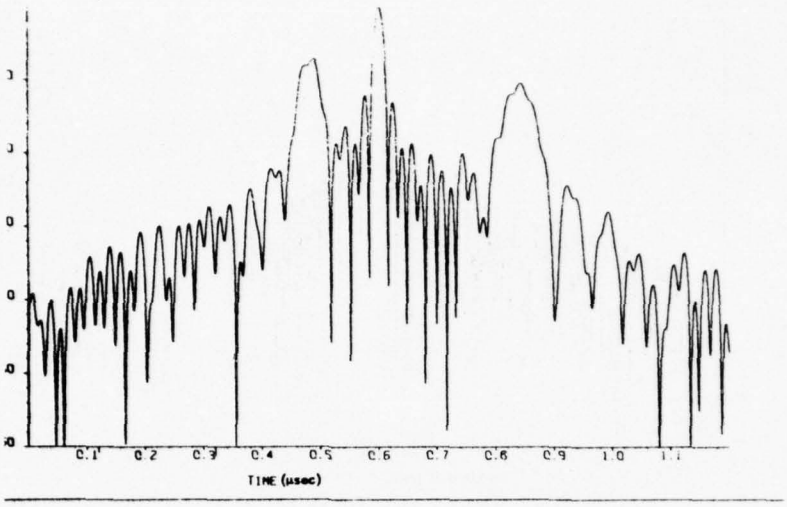

Figure 19(a) Typical Chirp Transform of the Three-Tone Input of Figure 18

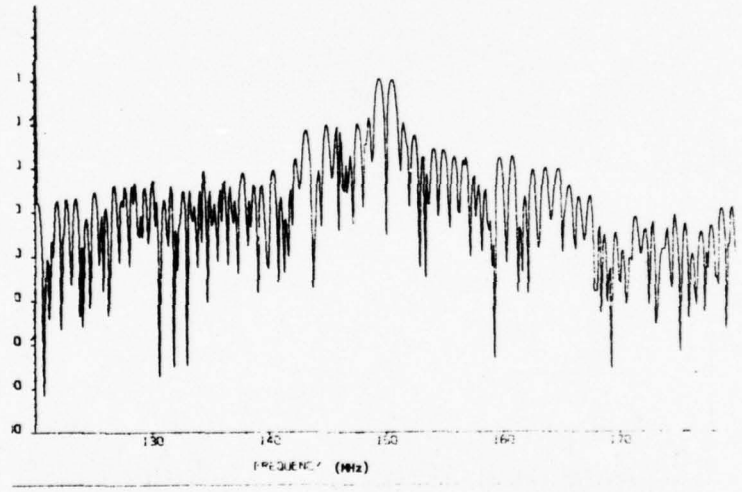

Figure 19(b) Normalized Error in the Transform for 1.2 μsec Multiplying Chirps

Figure 19 Chirp Transform Accuracy for 1.2 μsec Multiplying Chirps

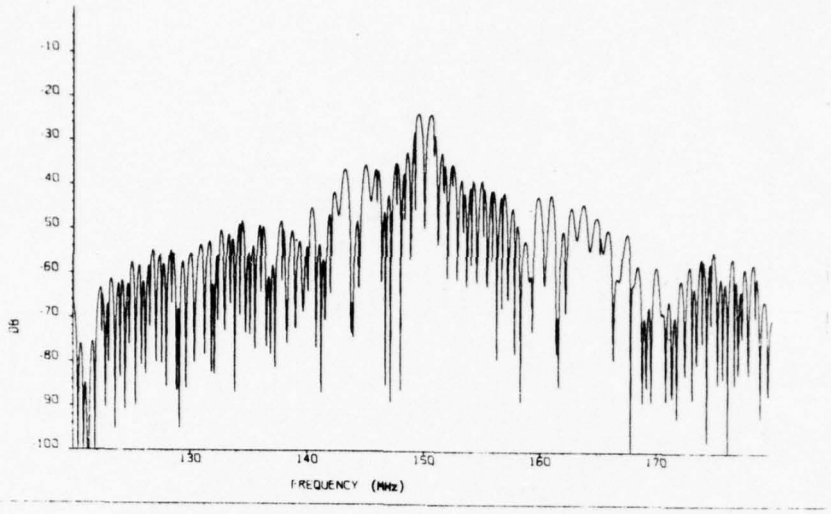

Figure 20(a) Normalized Error in the Transform for 4.8 μsec Multiplying Chirps

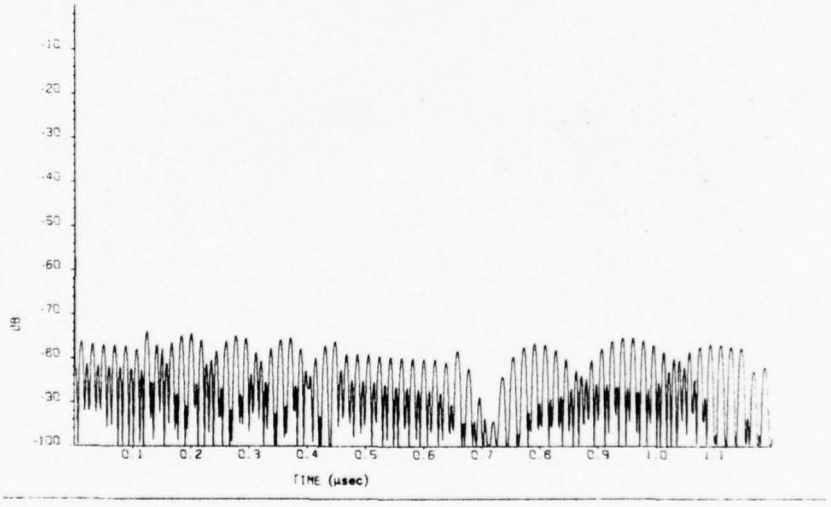

Figure 20(b) Errors Relative to the Input Introduced by TAPS Transform - Inverse Transform Operations for 4.8 μsec Multiplying Chirps

Figure 20 Chirp Transform Accuracy for 4.8 μsec Multiplying Chirps

average error plotted in Figure 21 along with the curve for 20 log BT. This dramatically illustrates the advantage of longer chirps for transform processing and is consistent with heuristic arguments based on other specific considerations such as cw filtering. With such clear evidence of the superiority of longer chirps, the chirp filters for the TAPS program were lengthened to the full field of view of the projection printing system available, approximately 2.0 μsec at these frequencies. The multiplying chirps are therefore 1.9 μsec and the convolving chirps are 3.8 μsec.

2. Spurious Signals

Spurious responses occur due to the continuous operation of a single channel in which the sidelobes of one interval are present in adjacent intervals, the shape of the bandpass modulation function, and the nonideal components used to implement the signal processing functions. The effects on design of the spurious performance of the mixers is described in Section III. In this section the emphasis is on distortion that is characteristic of the transform processor rather than the errors in phase or magnitude introduced by the nonideal SAW chirp generators and filters. The remaining two effects (continuous operation and modulation function selection) can be described in terms of the sidelobes generated by the corresponding signal processing function.

The importance of the selection of the filtering modulation function is easily seen in terms of a conventional filter analogy. If the modulation function is simply a square wave, the effect is similar to that of a perfect rectangular bandpass or bandstop filter which produces ringing in the response. In the chirp transform implementation of the adaptable bandpass/bandstop filter, the infinite bandwidth of the square wave is immediately limited by the chirp filter of the inverse transform. This chirp bandpass operation, which precedes the next mixing operation, reduces the distortion that would be caused

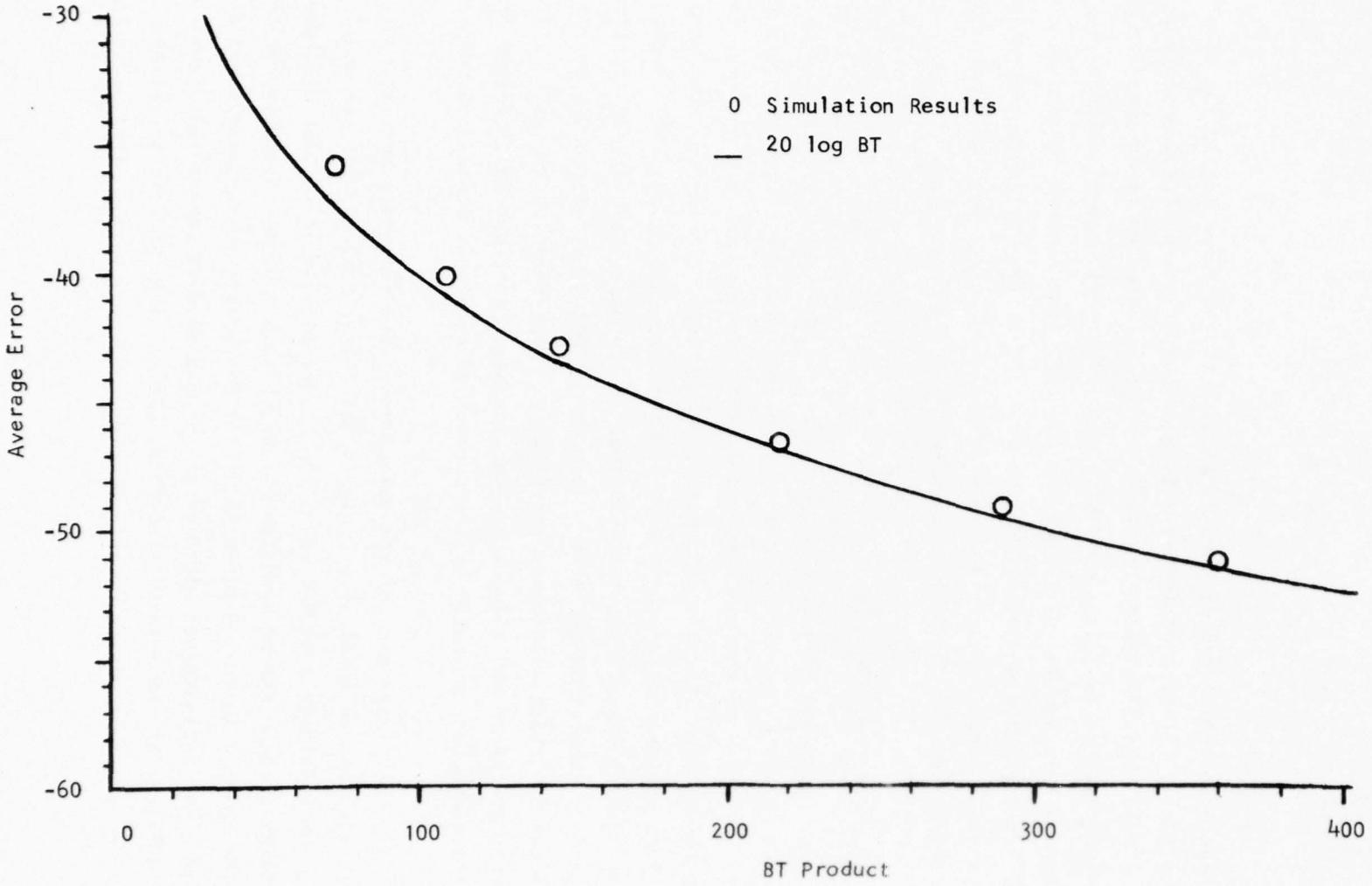

Figure 21 Average Normalized Error Introduced by TAPS for the Transform - Inverse Transform Operation as a Function of BT Product

had the mixer followed the gating. In other words, the simplification that permitted removing the postmultiplying chirp of the transform and the premultiplying chirp of the inverse transform has provided some immunity to the distortion that might have been introduced by an infinite bandwidth modulation function mixed with the processor bandwidth.

The protection afforded by this configuration against ringing (or sidelobes) introduced by modulation function rise and fall times that are too small for the processor bandwidth is best illustrated by simulations in which the cw signal of the previous three tone examples (Figure 18) is rejected by the adaptable filter. In the first case, the bandstop modulation of width equivalent to the mainlobe of the cw signal (1.6 MHz) and rise and fall times commensurate with a 200 MHz rate were used to reject a cw signal at 150 MHz. Figure 22(a) shows the reconstructed time signal. The ringing present due to the modulation is nominally 4 dB near the edges of the remaining two pulses. The cw term is removed more than 20 dB near the center of the interval, although somewhat less well at the edges, as discussed later. The distortion due to that effect does not pertain to the modulation function shape, although its width is certainly directly related to that error as well. Figure 22(b) shows the difference between the filtered signal where the cw term has been gated out and a pure two-tone signal in which the cw term is perfectly removed (i.e., never present). Figure 23(a) shows the spectrum of the filtered signal and Figure 23(b) the difference of that spectrum and a perfect spectrum without the offending cw term.

At the other extreme are modulations with rise and fall times that are too slow. This would correspond to filters with relatively high shape factors. The undesirable effect is that in addition to the cw term to be rejected, nearby signals are also attenuated. To illustrate this, rise and fall times commensurate with rates considerably less than the system bandwidth were used. The example included here is modulation with skirts equivalent to a 10 MHz rate.

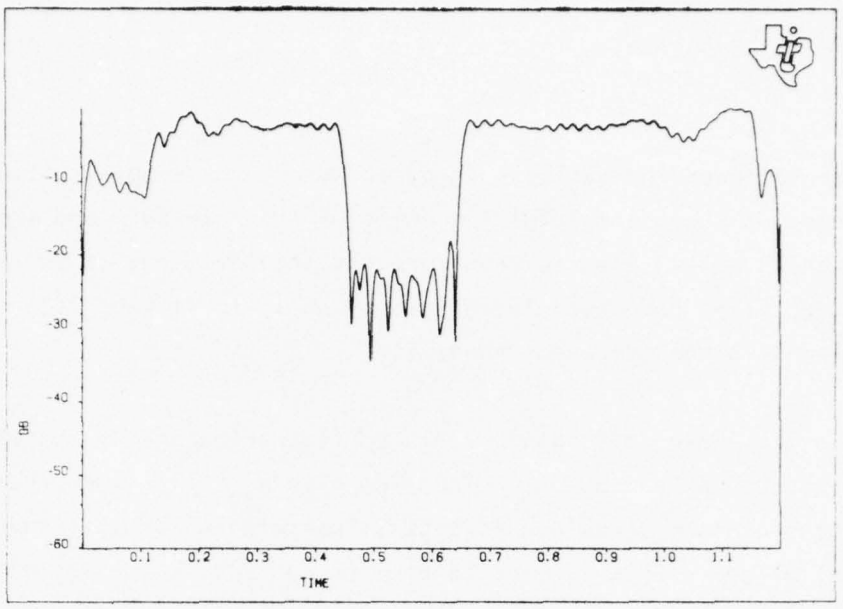

Figure 22(a) Filtered Time Signal With Modulation Rise and Fall Times Equivalent to 200 MHz

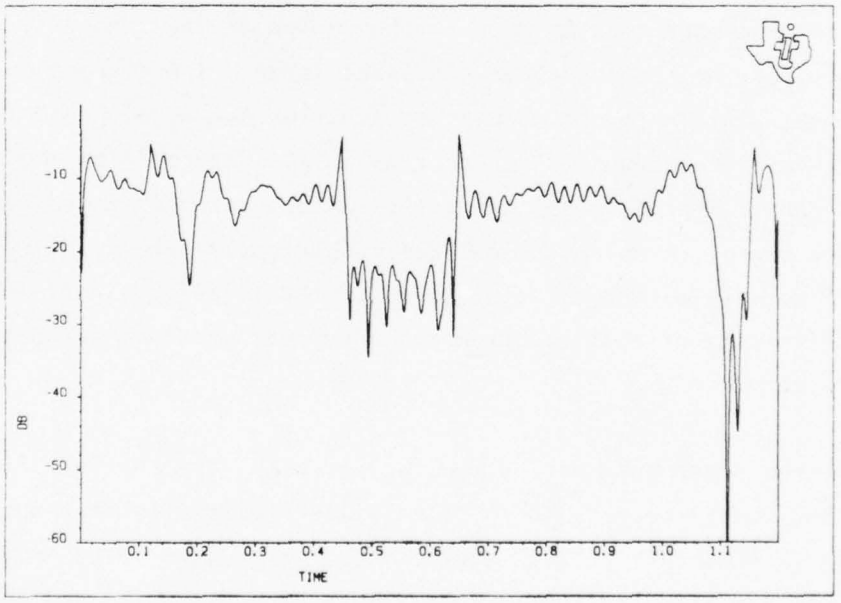

Figure 22(b) Difference Between the Filtered Signal and the Perfect Two-Tone Signal

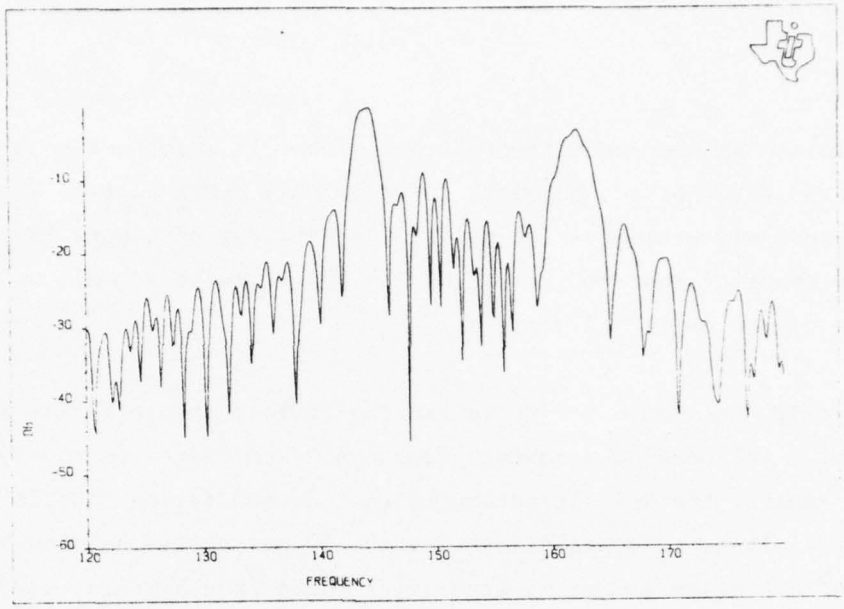

Figure 23(a) Spectra of the Filtered Signal of Figure 22(a)

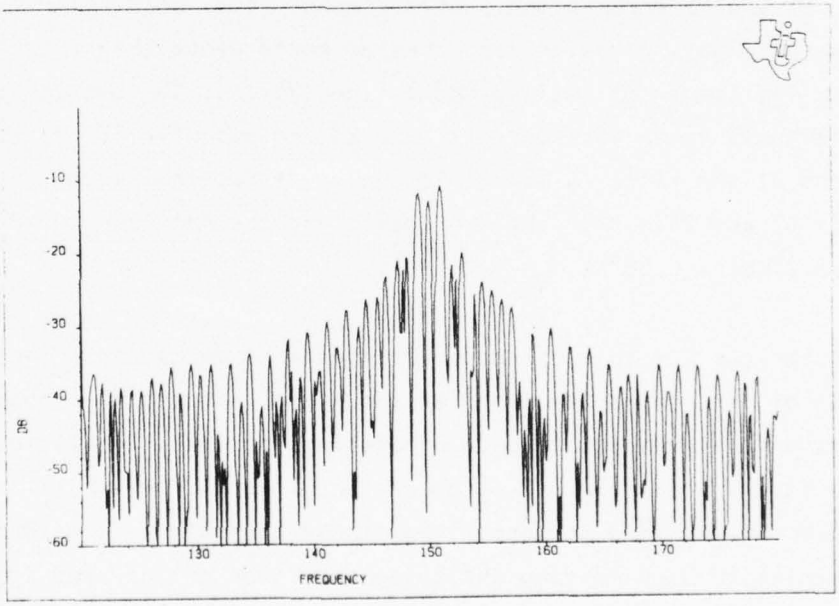

Figure 23(b) Difference Between the Filtered Spectra [Figure 23(a)] and the Perfect Two-Tone Spectrum

Figure 24(a) shows the reconstructed time signal in which not only is the cw term reduced, but the second pulse, which is only 6 MHz away at 144 MHz, has also been severely attenuated as well. The spectrum of Figure 24(b) gives further evidence of the removal of the 144 MHz rf pulse as well as the principal lobe of the cw at 150 MHz.

Generally, one would prefer to use the fastest possible rise and fall times without introducing frequency components too large for the system. As one might expect, the best selection is that of modulation functions whose rise and fall times are consistent with the 50 MHz system bandwidth. Simulations with modulation functions with skirts described by rates near 50 MHz illustrate somewhat improved gating performance over the square-wave case, although the improvement is less obvious due to the configuration already discussed. Figures 25 and 26 are the filtered time signals for modulation rise and fall times of 40 and 60 MHz rates, respectively. Although the fine structure of the filtered signals is different, they both exhibit nominally 2 dB worst-case gating distortion: better performance than those simulations with radically larger or smaller modulation skirts. The two spectra of the filtered signals given in Figures 27 and 28 are essentially identical. The comparisons of the filtered signal to a perfect two-tone signal are given in Figures 25(b) and 26(b) for the two cases, and the spectrum error is plotted in Figures 27(b) and 28(b).

The character of this distortion suggests correctly that the rise and fall times of the modulation function should not exceed the frequency handling capability of the system to avoid introducing spurious signals into the signal bandwidth from the ensuing mixing operation. The modulation will be performed with rise and fall times no larger than those equivalent to a 50 MHz rate and is implemented by bandlimiting the pulse generator output used for the filter gating.

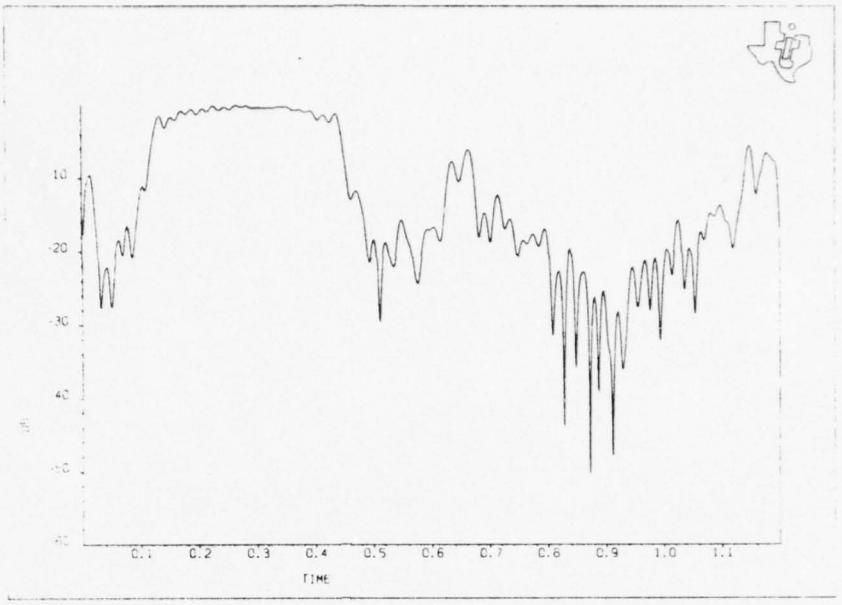

(a)

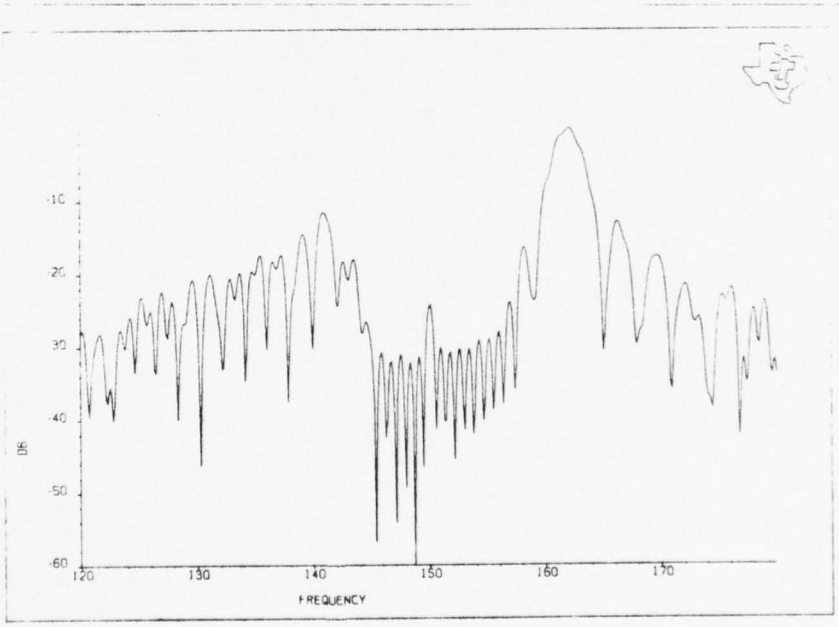

(b)

Figure 24 Filtered Time Signal (a) and Spectrum (b) with Modulation Rise and Fall Times Equivalent to 10 MHz

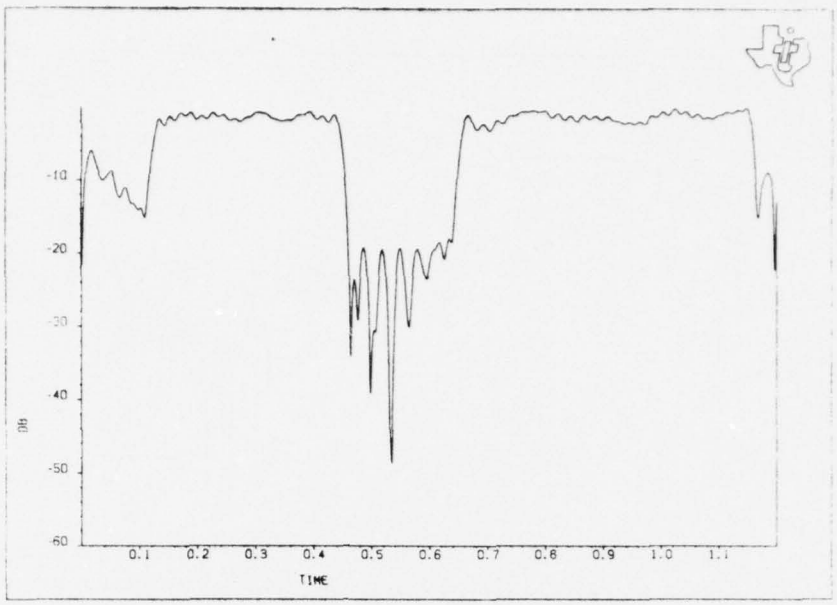

Figure 25(a) Filtered Time Signal with Modulation Rise and Fall Times Equivalent to 40 MHz

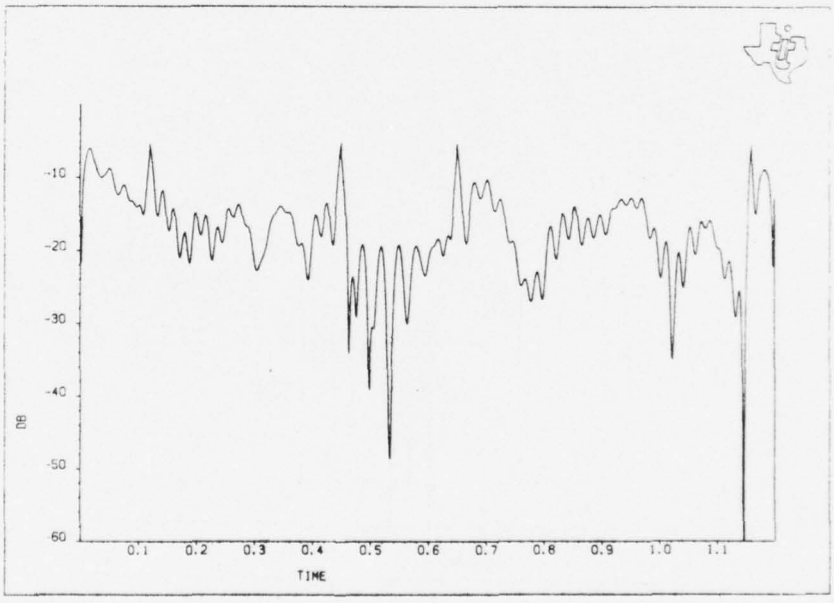

Figure 25(b) Difference Between the Filtered Signal and a Perfect Two-Tone Signal

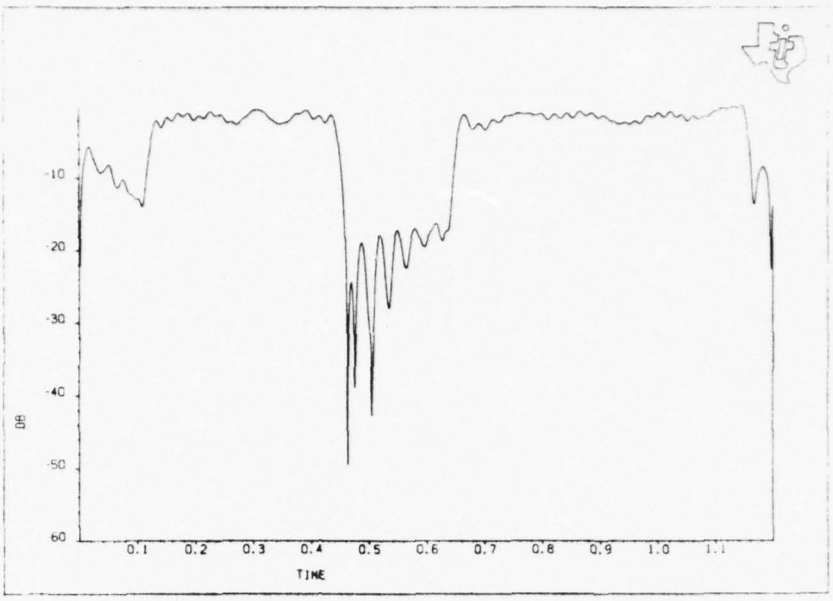

Figure 26(a) Filtered Time Signal with Modulation Rise and Fall Times Equivalent to 60 MHz

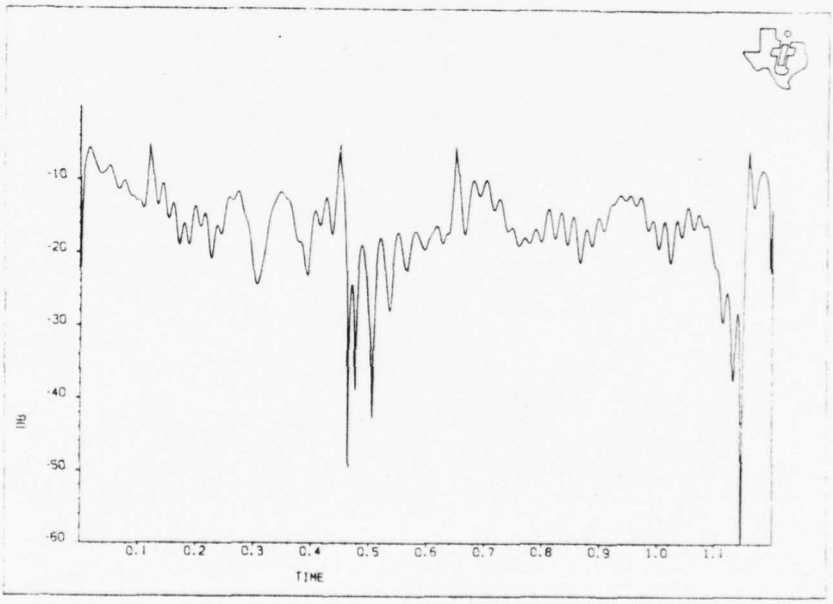

Figure 26(b) Difference Between the Filtered Signal and a Perfect Two-Tone Signal

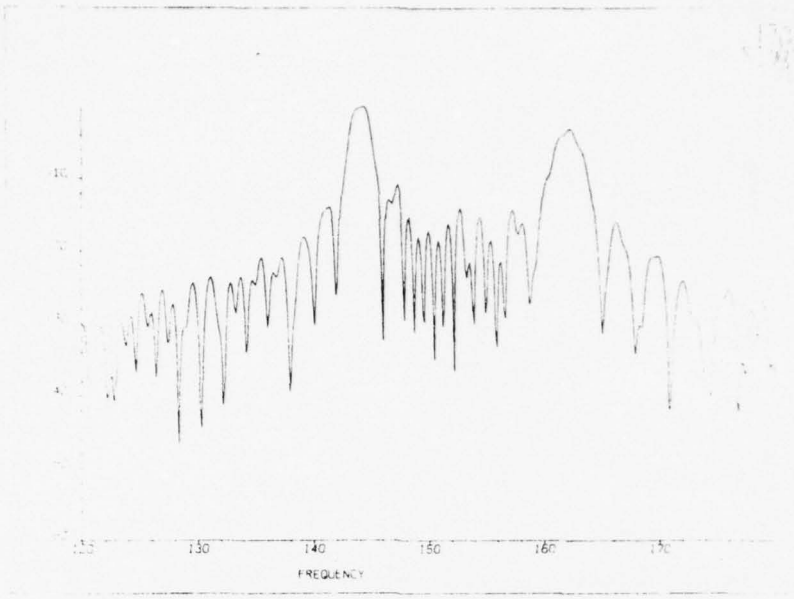

Figure 27(a) Spectrum of the Filtered Signal of Figure 25(a)

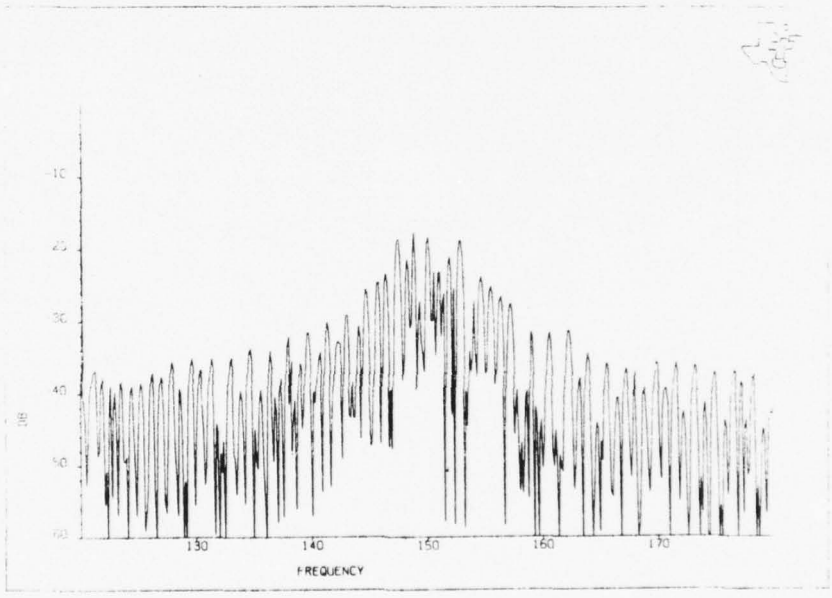

Figure 27(b) Difference Between the Filtered Spectrum and a Perfect Two-Tone Spectrum

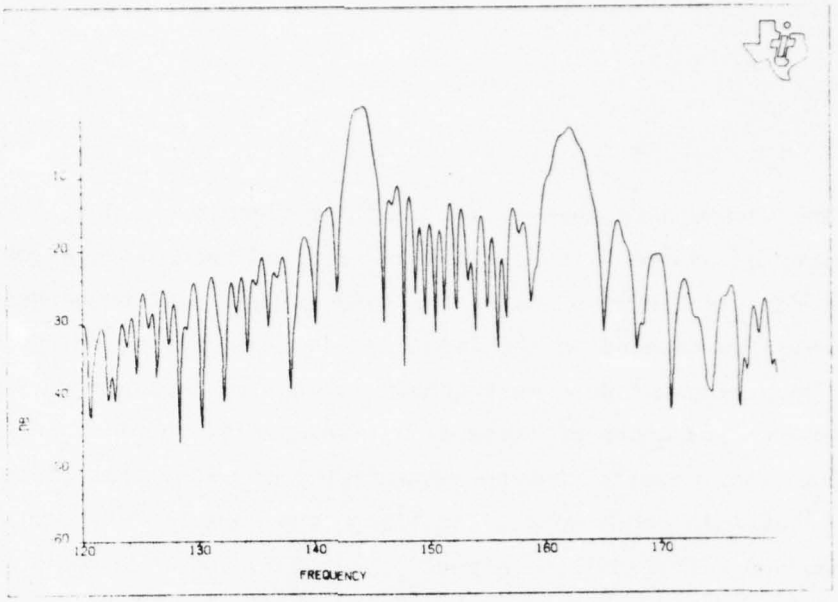

Figure 28(a) Spectrum of the Filtered Signal of Figure 26(a)

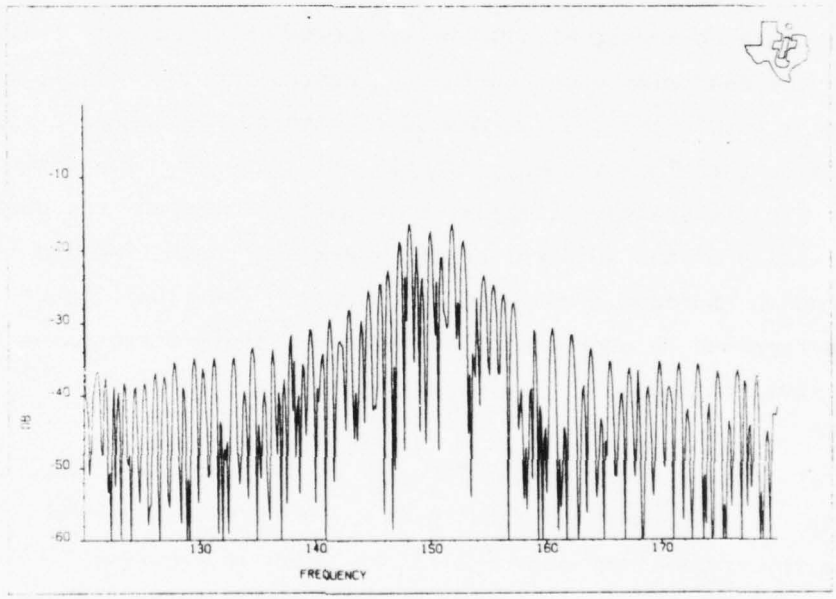

Figure 28(b) Difference Between the Filtered Spectrum and a Perfect Two-Tone Spectrum

The second sidelobe-related spurious signals are due to the continuous operation of the filter. TAPS operates on successive blocks of data entered via the input time signal. The input signal must be broken into time-intervals which correspond to the length of the multiplying chirp filter response. Each block of data must then be processed separately. Following operation on the transform of these signal intervals, the inverse transform is performed, and, ideally, the reconstructed time signal satisfies superposition principles. In other words, the time signal out of TAPS represents no more or less than the filtered input signal. Figure 29 shows schematically the continuous operation for the programmable matched filter case.

There are degradations associated with this operation, however. For example, consider the response of the transformer to a cw signal. The transformed signal will contain not only a compressed main lobe whose location depends on its frequency, but also the normal sidelobes associated with the compression of a chirp signal. While all principal frequency components for signals in the band will occur during the central chirp time ΔT, sidelobes will extend over a total time $3\ \Delta T$ as discussed before. This mode of operation is illustrated in the time-frequency diagram of Figure 30. The desired portion of the output B(t) is shaded. Clearly, this portion overlaps the unwanted (unshaded) tails of the adjacent output signals in both time and frequency, contributing to spurious signals at the output. The significance of this distortion is revealed through comparison of the transform processor for noncontinuous versus continuous operation.

The simulations again follow the block diagram of the transform processor with the same three-tone input signal previously used. The input signal and the transformer output B(t) are shown in Figures 31(a) and 31(b), but their spectra are on a log scale to show details over a wider dynamic range. The signal H(t) following the modulator is unchanged since no modulation is being applied. The reconstructed output in Figure 31(c) is very similar to

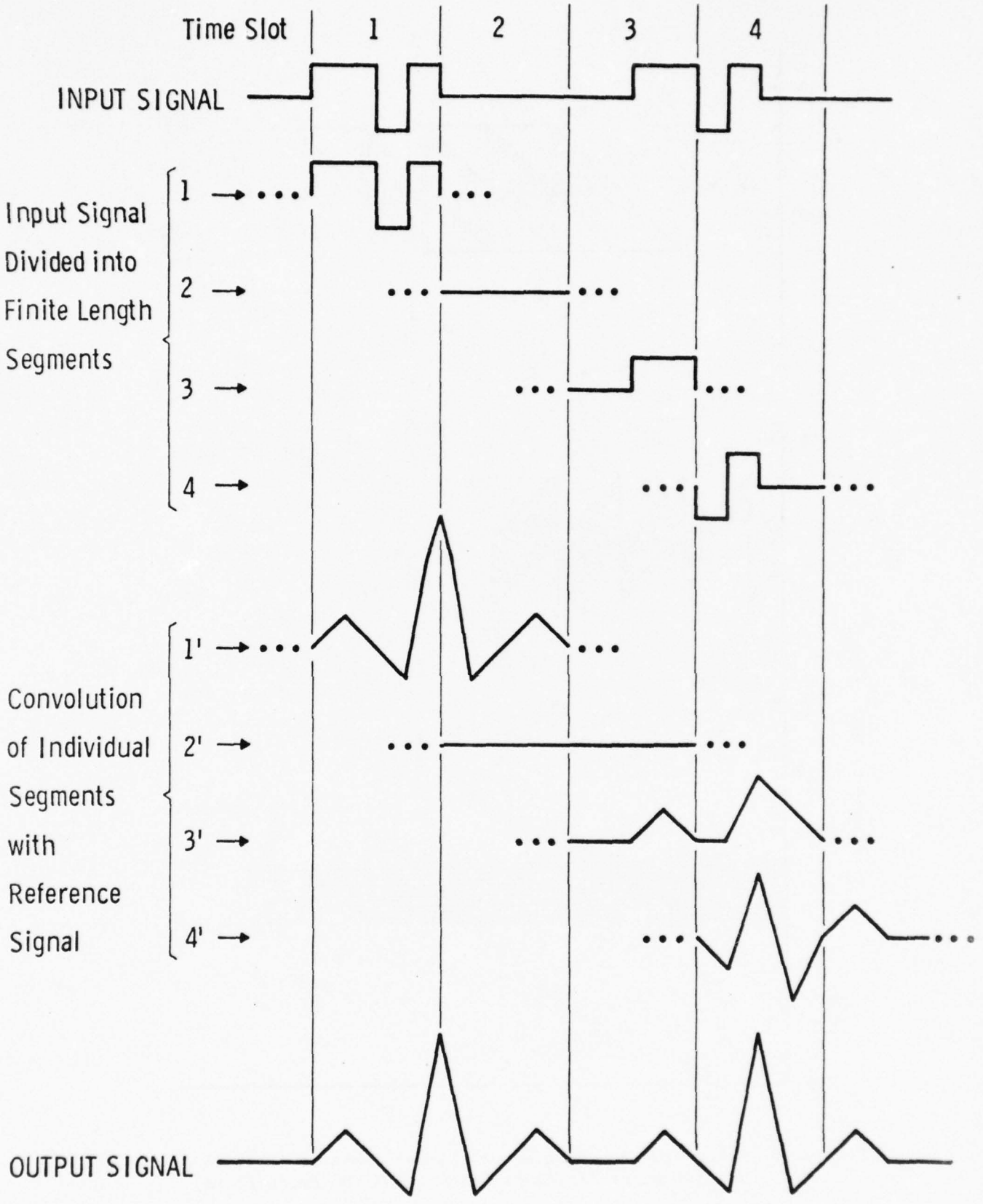

Figure 29 Continuous Signal Processing by Processing Finite Time Length Segments

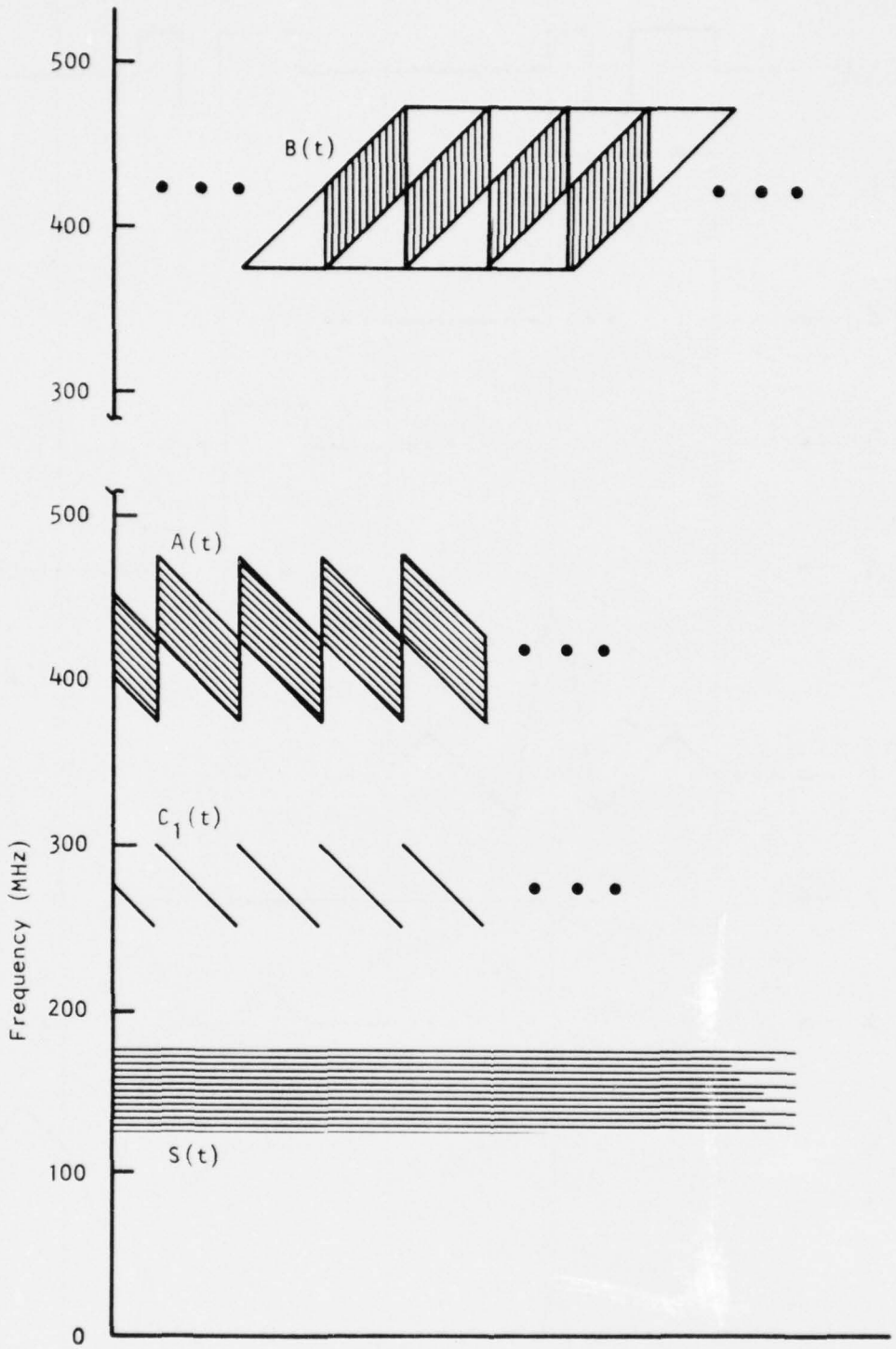

Figure 30 Frequency-Time Diagram of Chirp-Z Transform Unit Illustrating the Timing of Sidelobes Produced by the Chirp Filter

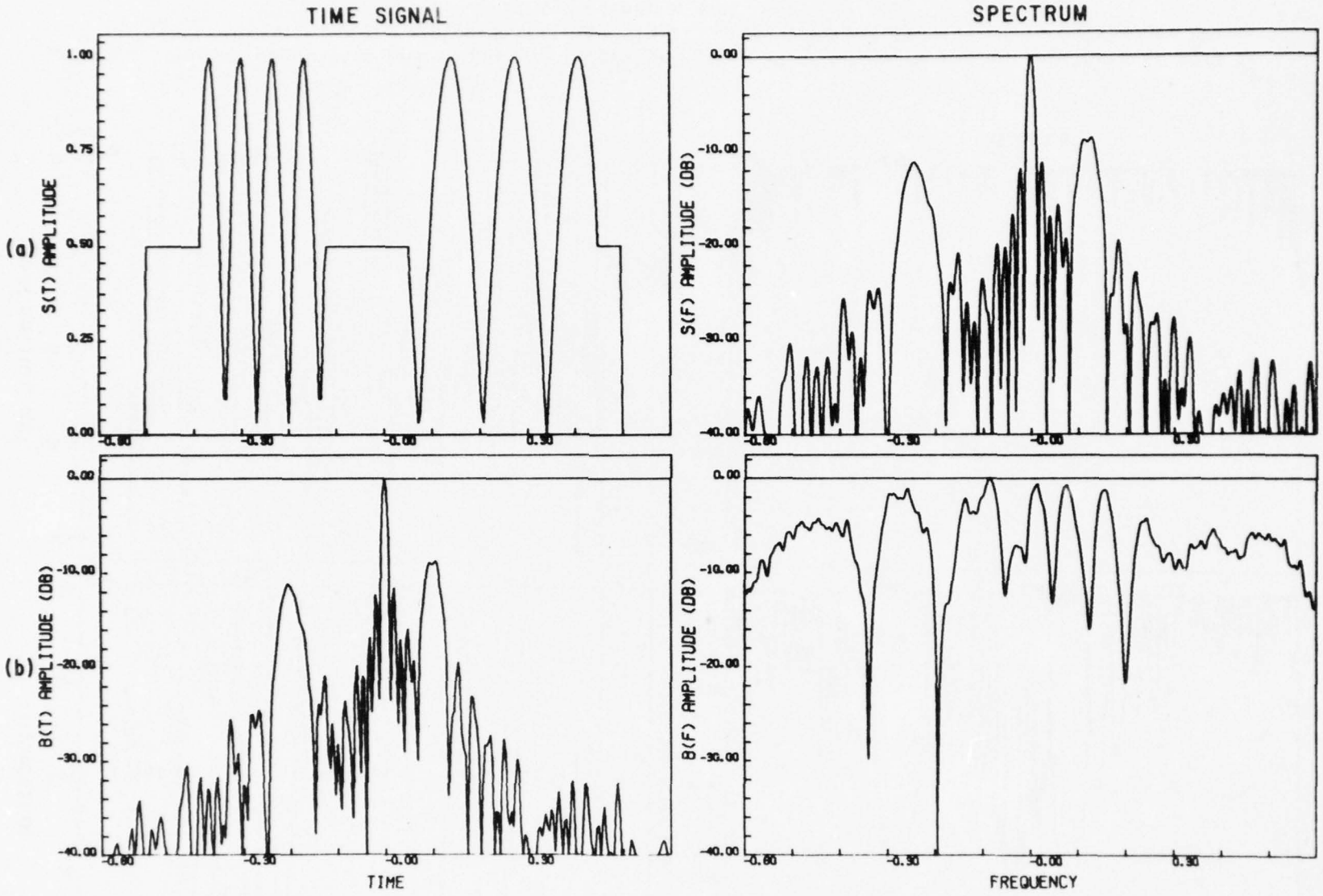

Figure 31 Transform Adaptive Processor System (TAPS) Time Waveforms and Their Spectra for a Three-Tone Unfiltered Signal. (a) Input signal S(t); (b) Transformer output B(t), unfiltered, equals H(t).

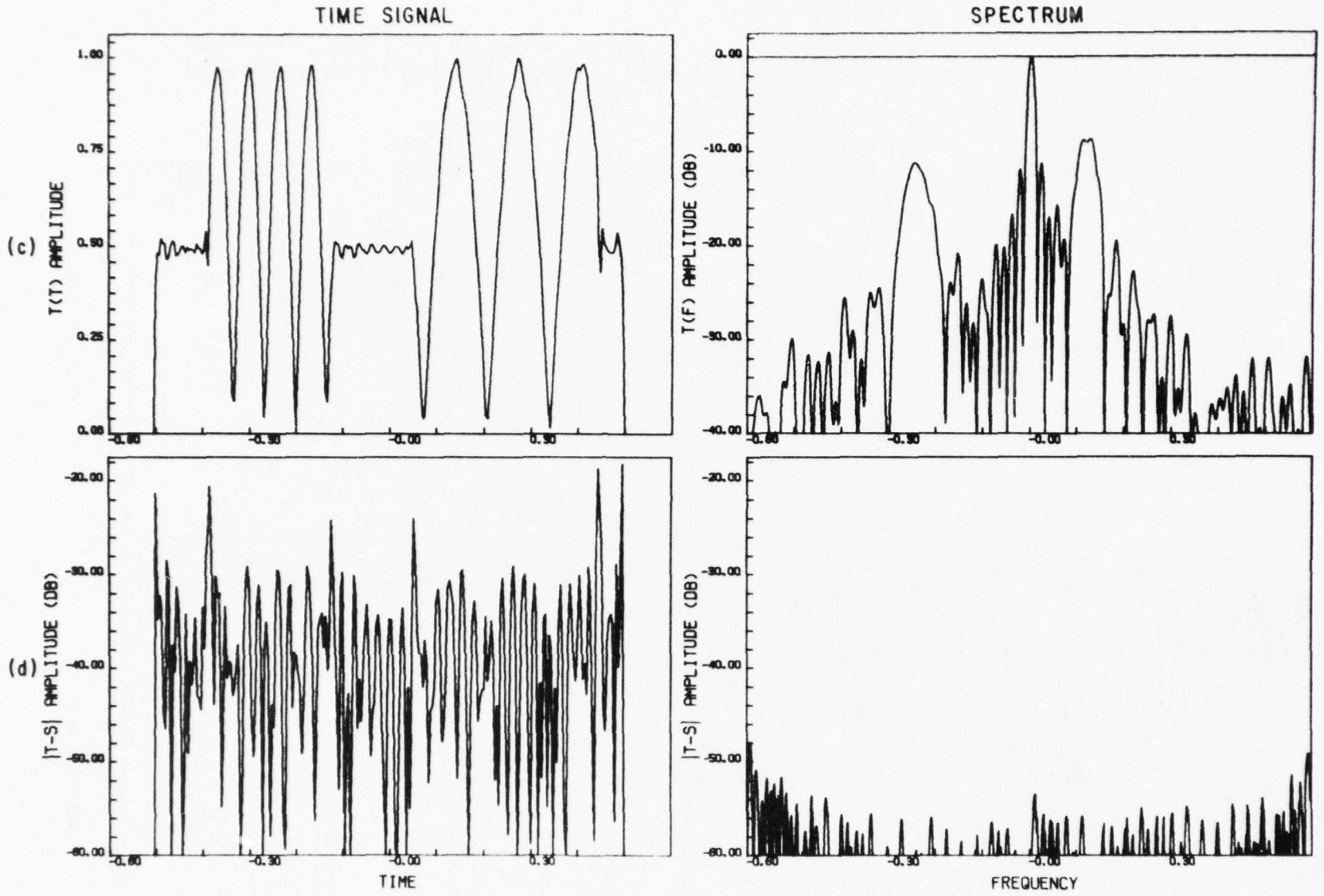

Figure 31 (Continued) Transform Adaptive Processor System (TAPS) Time Waveforms and Their Spectra for a Three-Tone Unfiltered Signal. (c) TAPS output T(t); (d) Difference between normalized input and output signal.

the input signal. The difference between the input and output is more than 30 dB down everywhere (except for the sharp spikes which are attributed to the comparison of a bandlimited output signal to the unbandlimited input rather than system errors), as shown in Figure 31(d). The spectra of the input and output are even closer, with the difference being more than 47 dB down everywhere.

The input signal used for simulated continuous operation consists of the same three-tone signal. The repetition rates of the pulsed signals were different, and each period was longer than the sampling time T (1.2 μsec) of the transform processor. A portion of the output containing both pulses was examined and compared with the example of noncontinuous operation in Figure 31. The input signal and its spectrum are shown in Figures 32(a) and 32(b). The chirp-Z transform of this signal is shown in Figure 33(a). The beating in the spectrum caused by the repetition of the pulses is not present in the chirp-Z transform, since only one pulse falls within the sampling time T. The input signal is recreated as shown in Figure 34(a) by an inverse chirp-Z transform. Figure 34(b) shows the difference between the input and output signals normalized to the input. The distortion level is between -20 and -30 dB down. (Again, note that the sharp spikes are not errors, but are introduced by the comparison of a bandlimited output to an essentially unbandlimited input.) In noncontinuous operation the distortion level was -30 to -40 dB down. Thus, cw operation has increased the distortion somewhat. The difference between the output and the input spectra is shown in Figure 33(b). The spectral distortion is always below -43 dB and is usually between -50 and -60. This is also about 10 dB worse than noncontinuous operation. As expected, then, cw operation introduces a low-level distortion which is seen to depend on the BT product of the system as discussed in Section IV.B.1.

One way to avoid this problem is to build a two-channel processor with successive periods of the chirp signal entering alternate channels. The

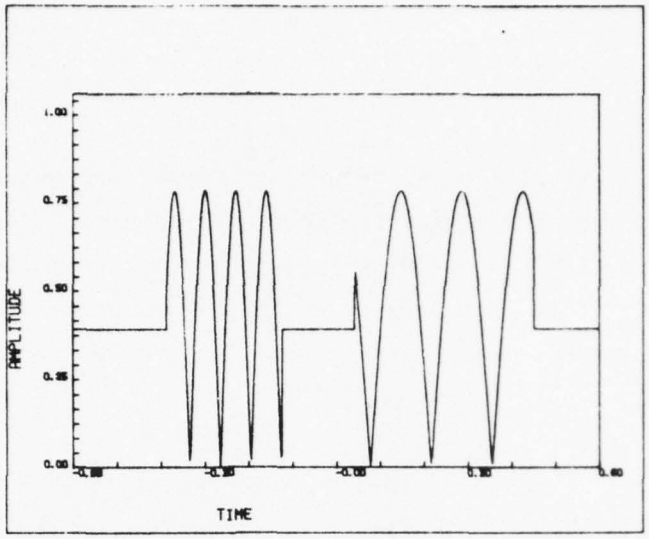

(a)

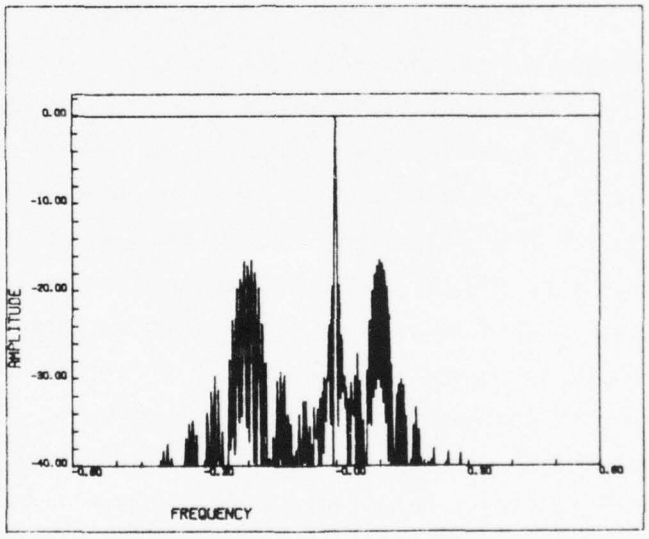

(b)

Figure 32 Input Signal (a) and Spectrum (b) for Continuous Operation Simulations

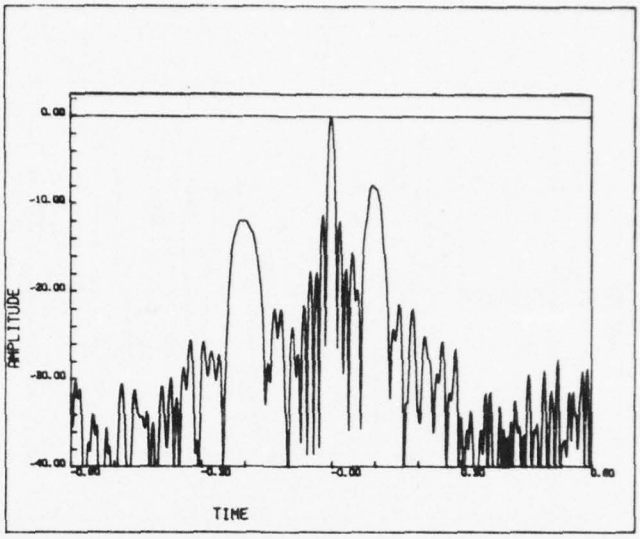

(a)

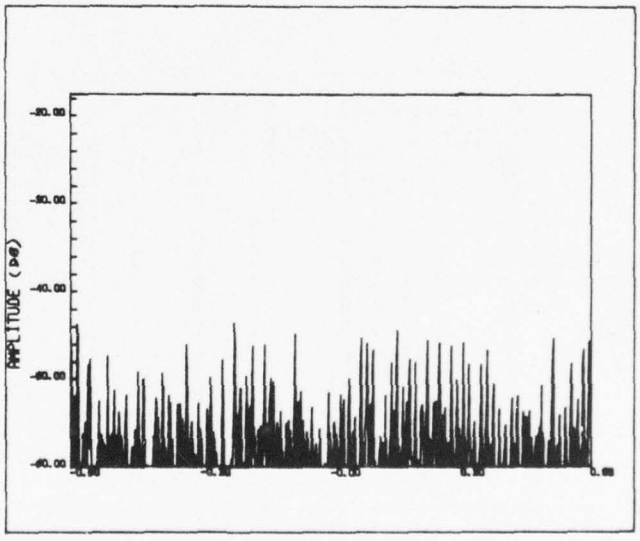

(b)

Figure 33 Chirp-Z Transform (a) and Spectrum Distortion (b) Introduced in Continuous Operation

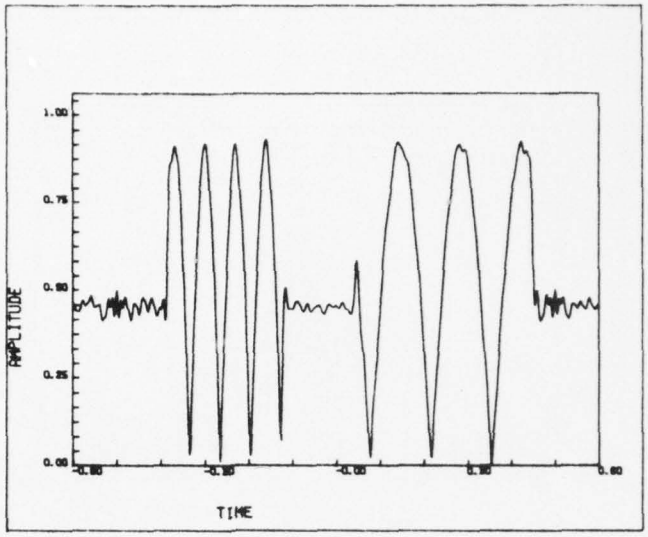

(a)

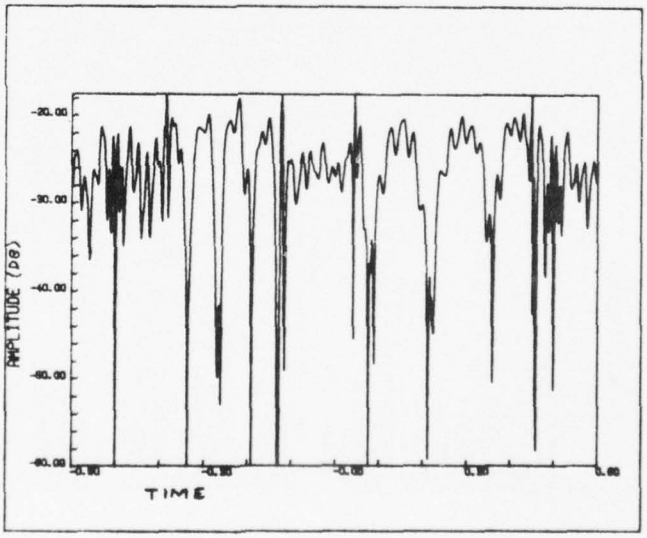

(b)

Figure 34 (a) TAPS Output in Continuous Operation Without Filtering and (b) the Signal Distortion Introduced

outputs can be gated before being summed to provide continuous operation. This two-channel transform doubles the system complexity and makes the timing problems more severe, since the summation must be coherent at the carrier frequency. Alternatively, since the tails on the signal correspond to sidelobes of the compressed input tones, they may be reduced by standard weighting techniques applied to the input mixing chirp.

There are several drawbacks to this approach. Since the actual Fourier transform of the input signal block would contain these sidelobes at levels comparable to the SAW chirp transform without a weighted multiplying chirp, weighting that first chirp will create additional frequency domain error. This error is not of predominant interest for the filter, however, since it is ultimately the reconstruction of the time domain signal after filtering and inverse transforming that is of concern. The success of weighting that chirp depends on its reduction of adjacent time interval sidelobe interference and resultant facilitation of filtering frequency components more optimally. Unfortunately, neither is strictly true. The character of the input signal most particularly influences the sidelobe suppression achieved by the weighting. That is, a short pulse that arrives early in the transform processing interval is simply monotonically attenuated by the shape of a single half of the weighted multiplying chirp. Had it arrived at the center of the interval, the pulse symmetry would have been preserved, but the amount of weighting applied would have been inconsequential. In other words, different signals would have been influenced differently by such weighting according to time of arrival and pulse length. Only the special case of a cw signal would be properly weighted for the desired sidelobe suppression and, as will be discussed in Section IV.C., this special case is not properly handled by a single-channel system for other reasons.

In addition to the relatively inconsequential error introduced into the frequency domain by weighting the first chirp, the reconstructed time

signal is also weighted by the chirp weighting function, as shown in the plots that follow. The examples included here are weighting on the multiplying chirp with Gaussian weighting of 0, -9, and -15 dB attenuation at the edge of the time interval relative to mid-interval. The input signal is the unbandlimited input of Figure 17(a). Figure 35(a) corresponds to the chirp transform of the input without weighting the chirps. The difference between the chirp spectrum and the actual spectrum determined by an FFT routine is given in Figure 35(b) normalized to the spectrum peak. Figures 36 and 37 correspond similarly to the chirp transform and the deviation from the actual spectrum for Gaussian weighting on the first multiplying chirp of -9 and -15 dB attenuation at the SAW chirp edges, respectively. Following the inverse transform, the reconstructed time domain signal is given in Figures 17(b), 38(a), and 39(a) for 0 dB, -9 dB, and -15 dB Gaussian weighting, respectively. Although the difference of this output compared to the input [Figures 17(c), 38(b), and 39(b)] is given in terms of the unbandlimited input signal, the overall variation (neglecting the spikes related to the unbandlimited signal as demonstrated earlier) is clearly evidenced. The time interval is shaped by the Gaussian weighting function, as expected. Of course, compensation for this weighting can be made in the final stage of the inverse transformer by properly weighting the last mixing chirp, but this presages higher loss for a complexity that has no actual advantage in the role of adaptable filtering.

The expectation that weighting for sidelobe suppression might improve filtering performance rests on the particular case of cw filtering. This is more easily seen in terms of a filtering example when bandpass modulation is applied to remove or pass the cw signal in the example of Figure 31. This expectation is not realized, as discussed next.

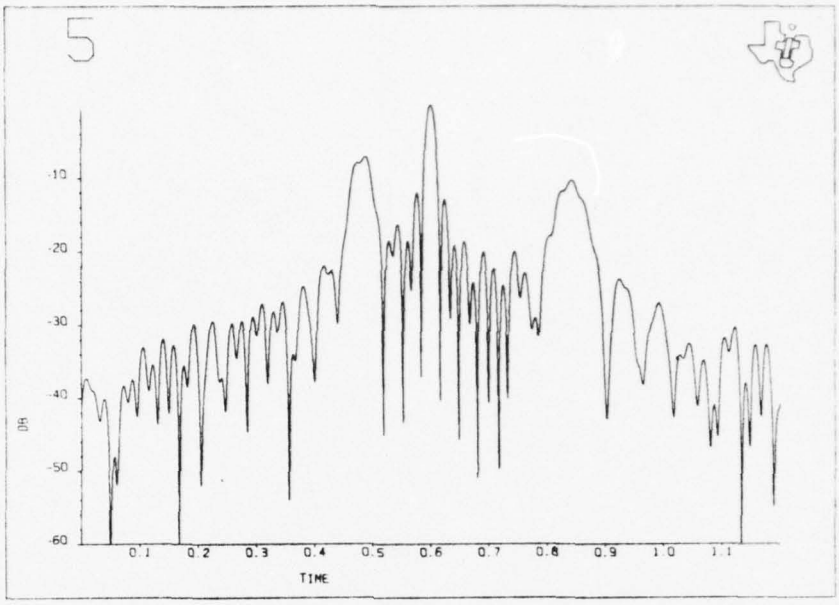

Figure 35(a) Envelope of the Chirp Transform of the Three-Tone Input Signal of Figure 32(a)

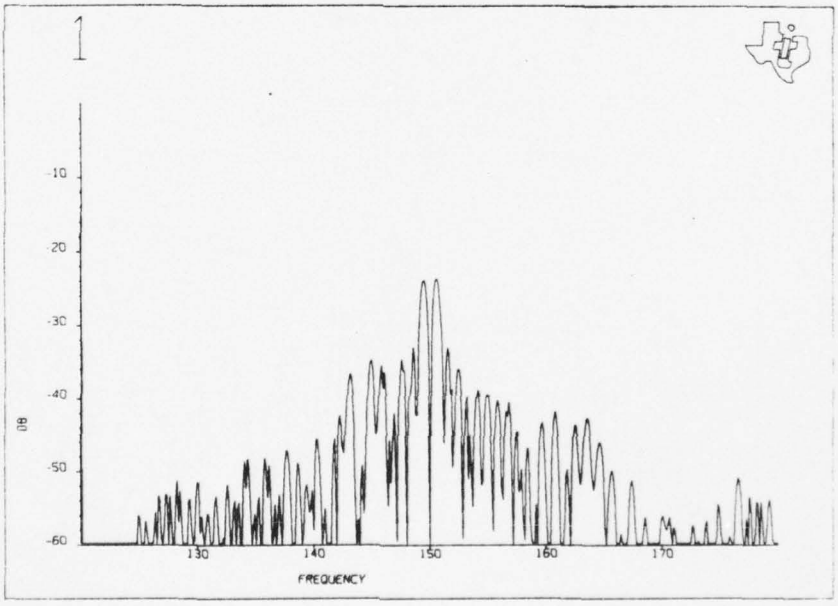

Figure 35(b) Difference Between the Chirp Transform and the Actual Signal Spectrum Normalized to the Spectrum Peak

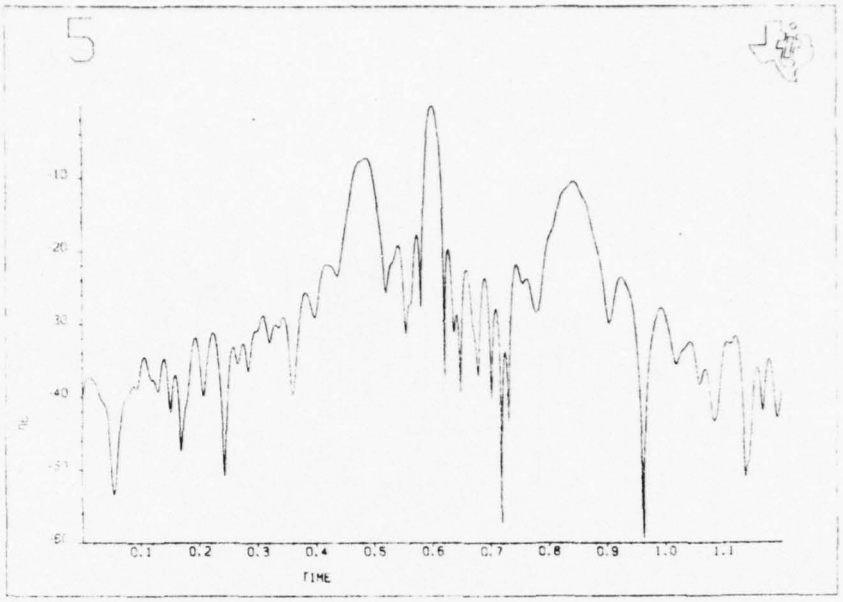

Figure 36(a) Envelope of the Chirp Transform of the Three-Tone Input Signal of Figure 17 with -9 dB Gaussian Weighting on the First Multiplying Chirp

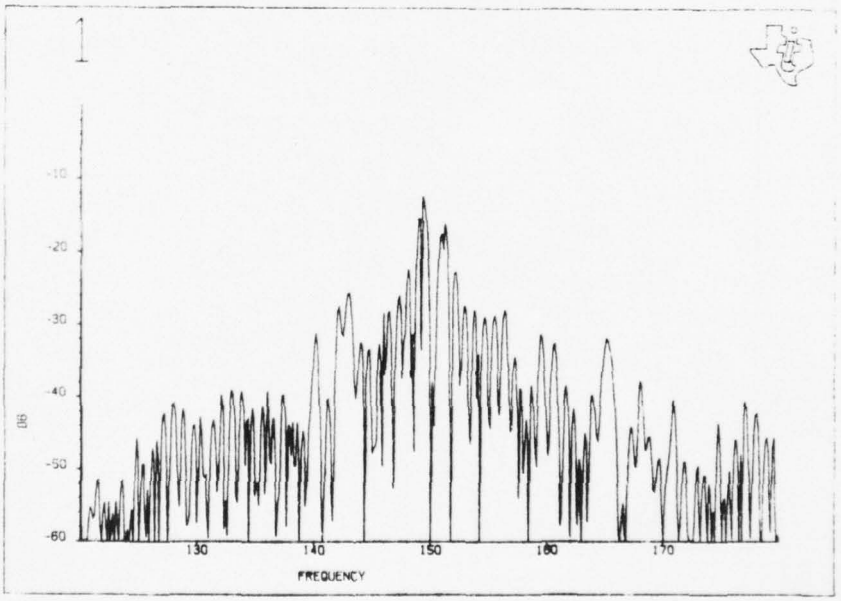

Figure 36(b) Difference Between the Chirp Transform and the Actual Signal Spectrum Normalized to the Spectrum Peak for -9 dB Gaussian Weighting

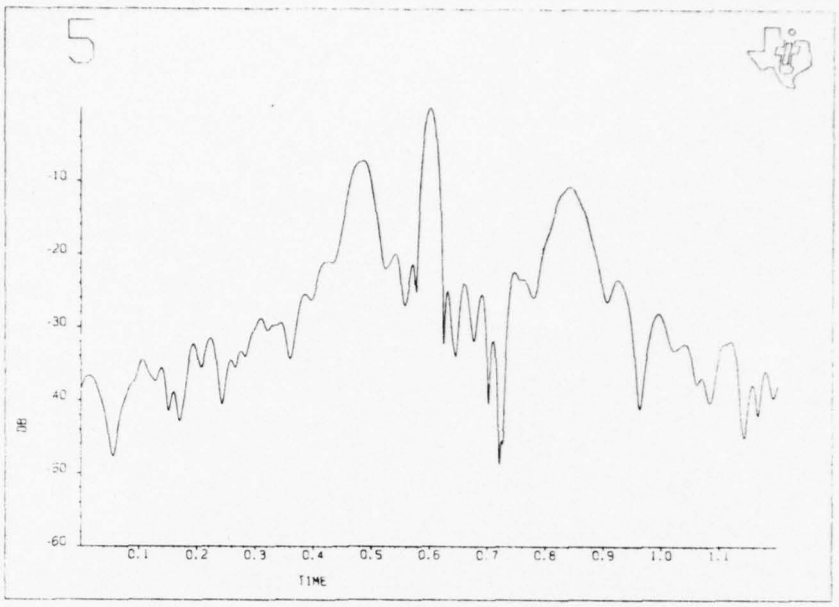

Figure 37(a) Envelope of the Chirp Transform of the Three-Tone Input Signal of Figure 17 with -15 dB Gaussian Weighting on the First Multiplying Chirp

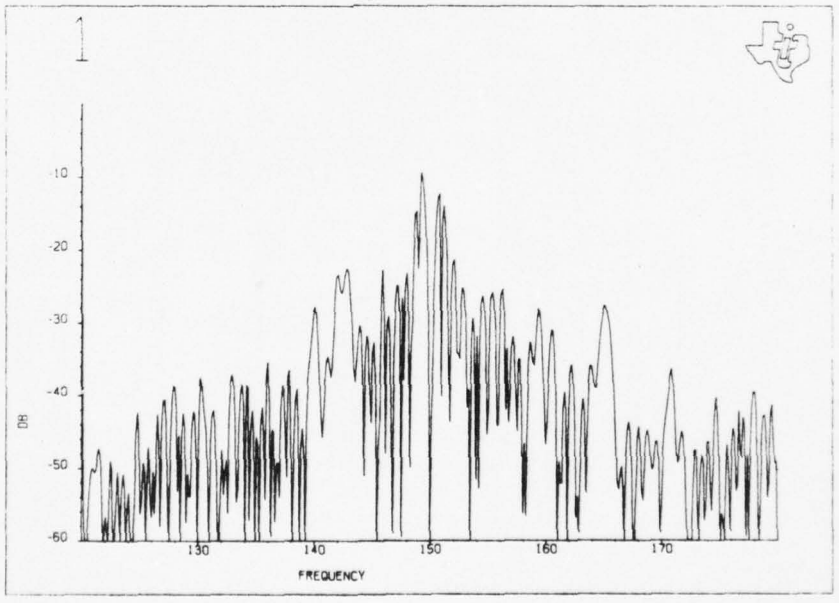

Figure 37(b) Difference Between the Chirp Transform and the Actual Signal Spectrum Normalized to the Spectrum Peak for -15 dB Gaussian Weighting

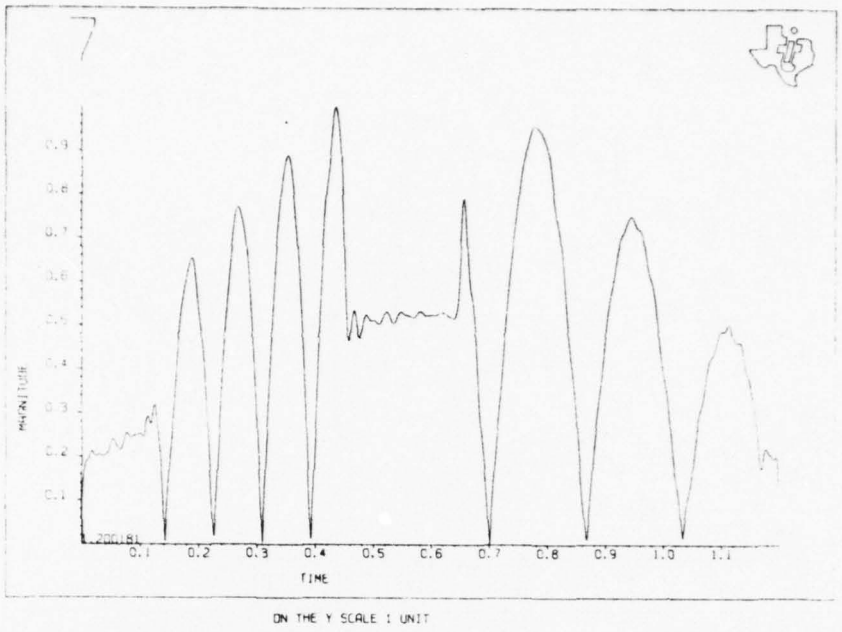

Figure 38(a) Envelope of the Time Domain Output of the TAPS System for the Three-Tone Input Signal of Figure 17 with -9 dB Gaussian Weighting of the First Multiplying Chirp

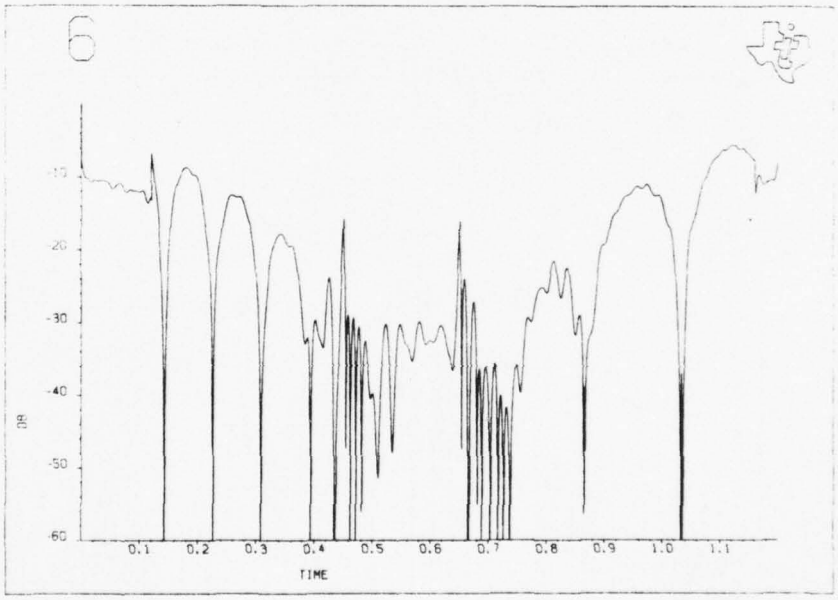

Figure 38(b) Difference Between the TAPS Input and Output Signals Normalized to the Signal Peak for -9 dB Gaussian Weighting

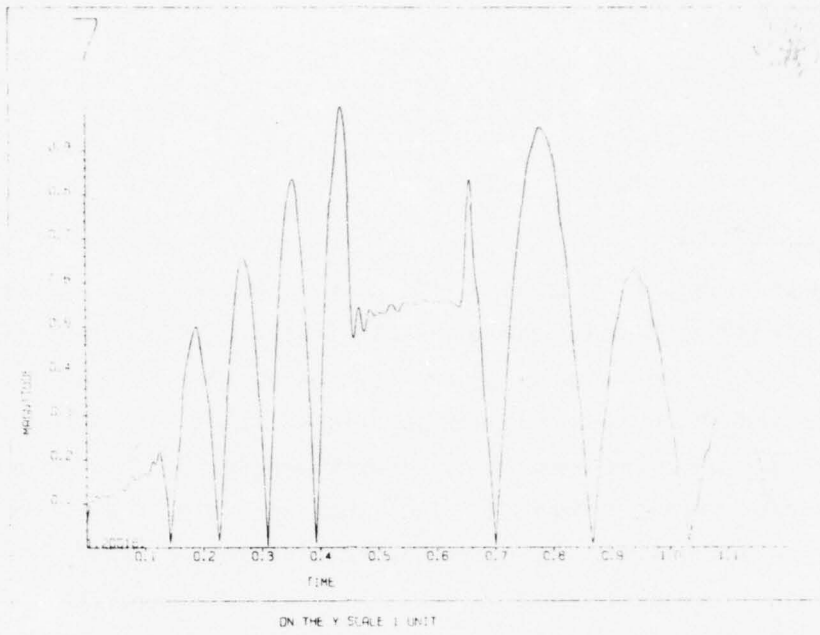

Figure 39(a) Envelope of the Time Domain Output of the TAPS System for the Three-Tone Input Signal of Figure 17 with -15 dB Gaussian Weighting

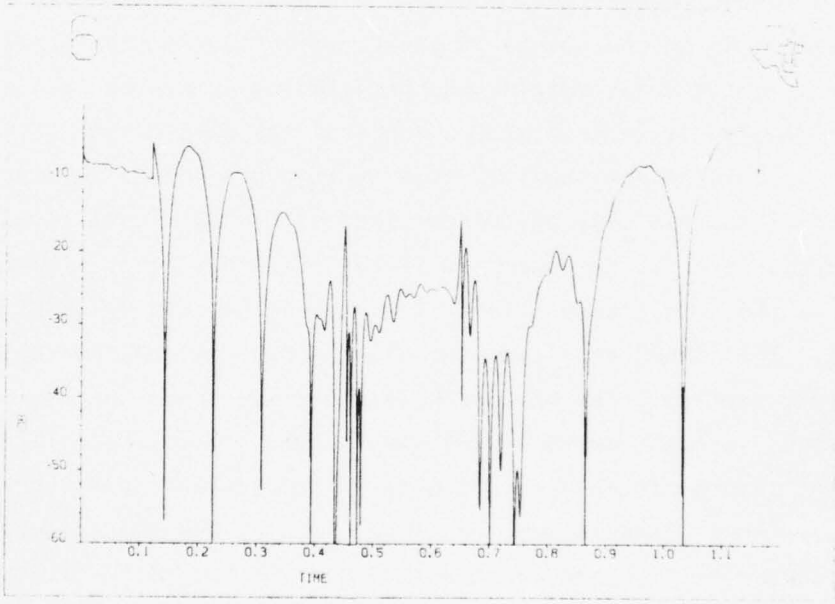

Figure 39(b) Difference Between the TAPS Input and Output Signals Normalized to the Signal Peak for -15 dB Gaussian Weighting

3. cw Filtering

The principal limitation of the single channel TAPS system is that of filtering cw signals. Whereas the adaptable filtering for pulsed signals is achieved with similar performance to that of conventional fixed-tuned filtering as is demonstrated shortly, cw signals (or signals that span more than one transform interval) require special considerations due to effects at the edges of the partitioned signal intervals. To illustrate this, a worst-case example is simulated for discussion. Using the input of Figure 31 and a modulation function to remove the compressed pulse in B(t) corresponding to the cw signal at bandcenter, Figure 40 shows the result of this bandstop operation and Figure 41 shows the complementary bandpass function. The modified signal H(t) showing the central lobe of the sinc function removed is shown in Figure 40(a). This filter modulation corresponds to a 1.6 MHz bandstop filter characteristic. The output T(t) for this filter is shown in Figure 40(b). The beating present on the pulses in the input signal and the cw signal level has been reduced. The ripple remaining on the pulses is generated by the residual energy of the cw frequency. In the areas outside and between the pulses one can see that this residual energy is largest at the edges of the sample time ΔT and smallest in the center. This effect shows up clearly if the bandpass modulation function is modified so that only the center lobe of the cw signal is passed. This case corresponds to a 1.6 MHz bandpass filter characteristic. The modified signal H(t) is shown in Figure 41(a). The normalized output T(t) is shown in Figure 41(b). The smooth amplitude variation shows that the two pulses have been completely removed. The variation in amplitude shows the loss of energy in the cw signal near the edges of the sample time. Simulations of continuous operation over several intervals more clearly demonstrate this effect. Figure 42 is a simulation of bandpassing the cw term at 150 MHz and rejecting the remaining frequencies: pulsed terms at 144 and 162 MHz with widths of 0.51 μsec and 0.33 μsec and repetition periods of 1.2 μsec and 1.8 μsec, respectively [Figure 42(a)]. At the edge of each of the three intervals, part of tne cw energy is lost, causing the scalloped effect shown in Figure 42(c). Figure 42(d) shows the opposite case: bandstopping the cw term over one interval.

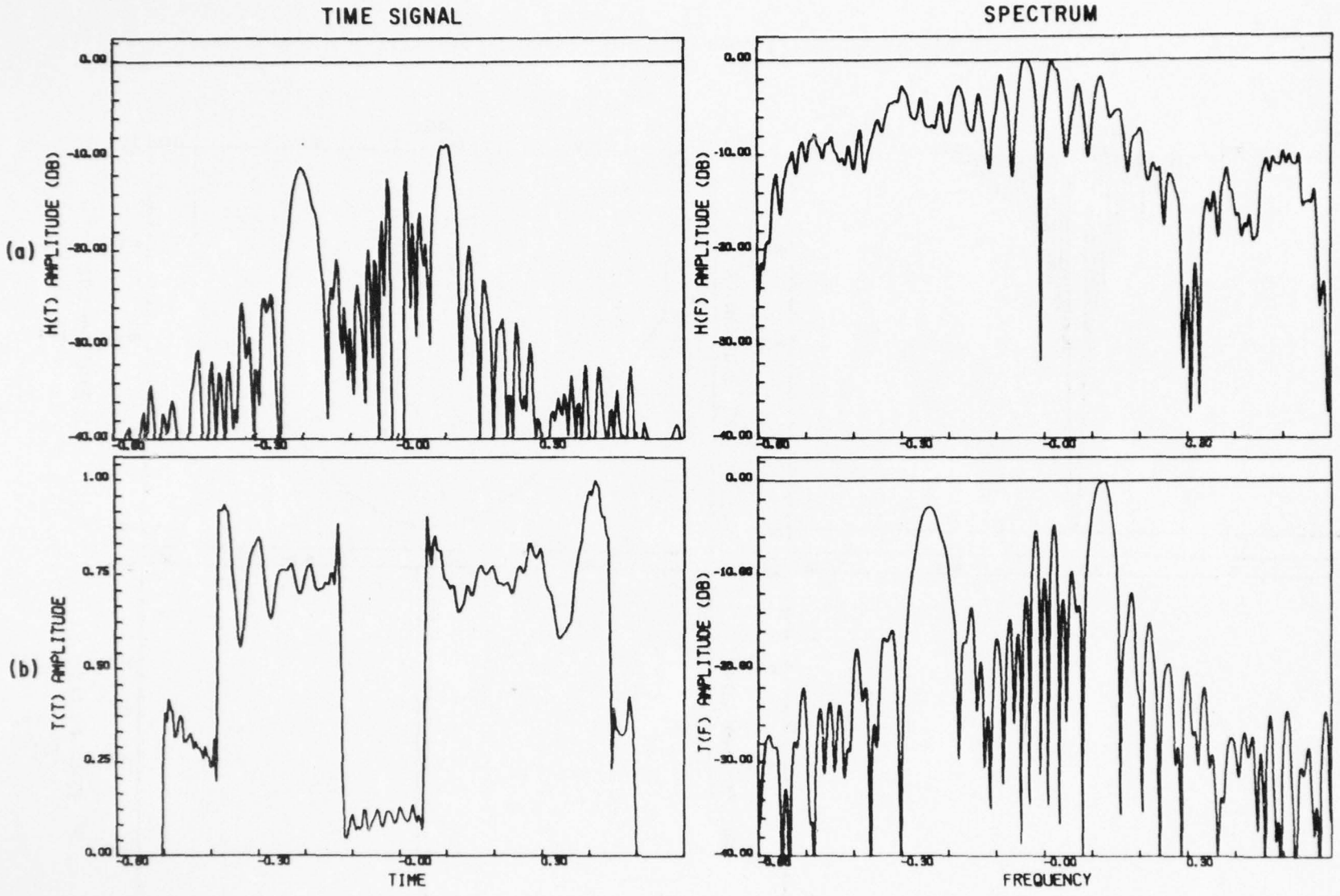

Figure 40 TAPS Output for Filtered Signals. (a) Bandstop filtered transform signal; (b) TAPS output T(t).

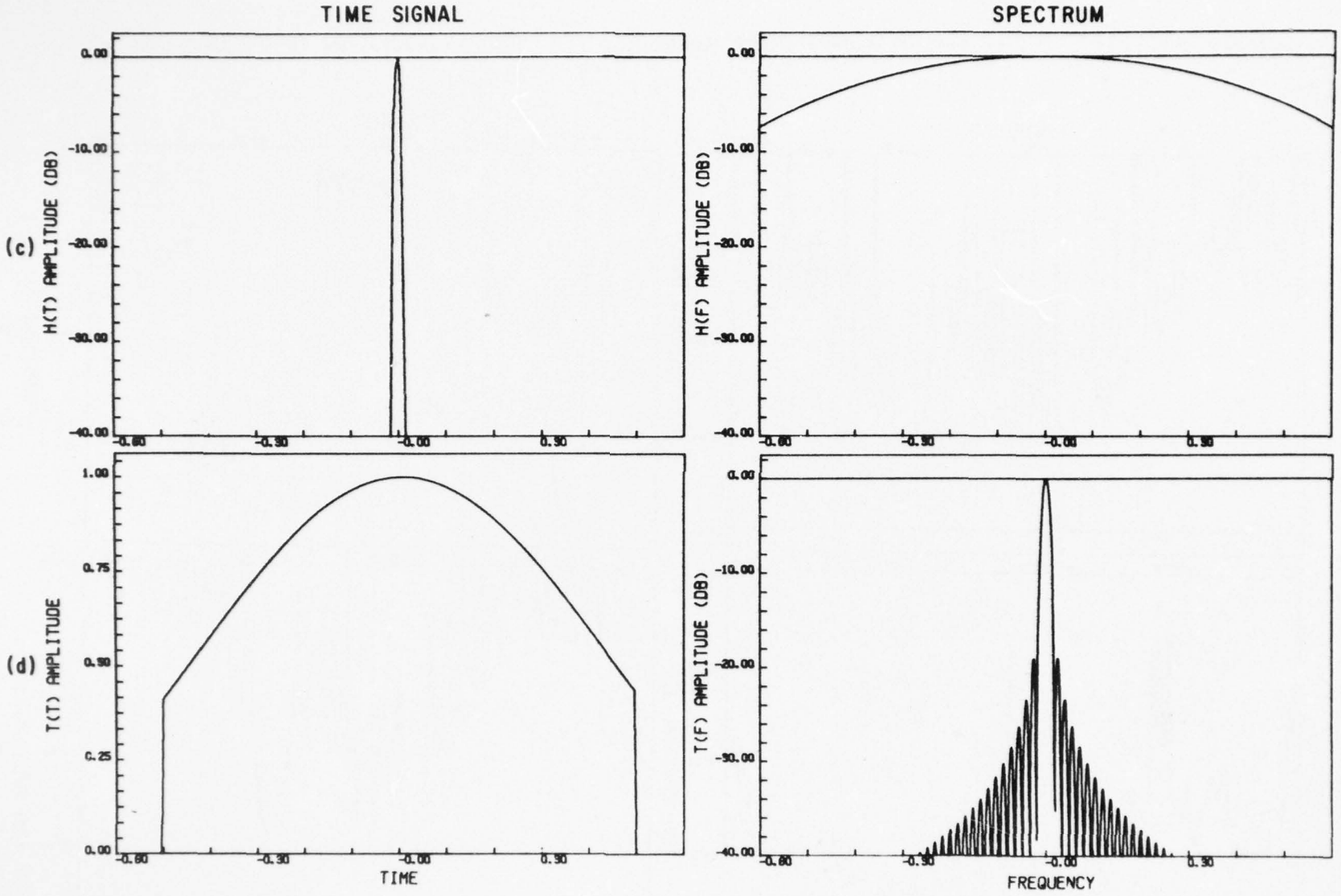

Figure 41 TAPS Output for Filtered Signals. (c) Bandpass filtered transform signal H(t); (d) TAPS output T(t).

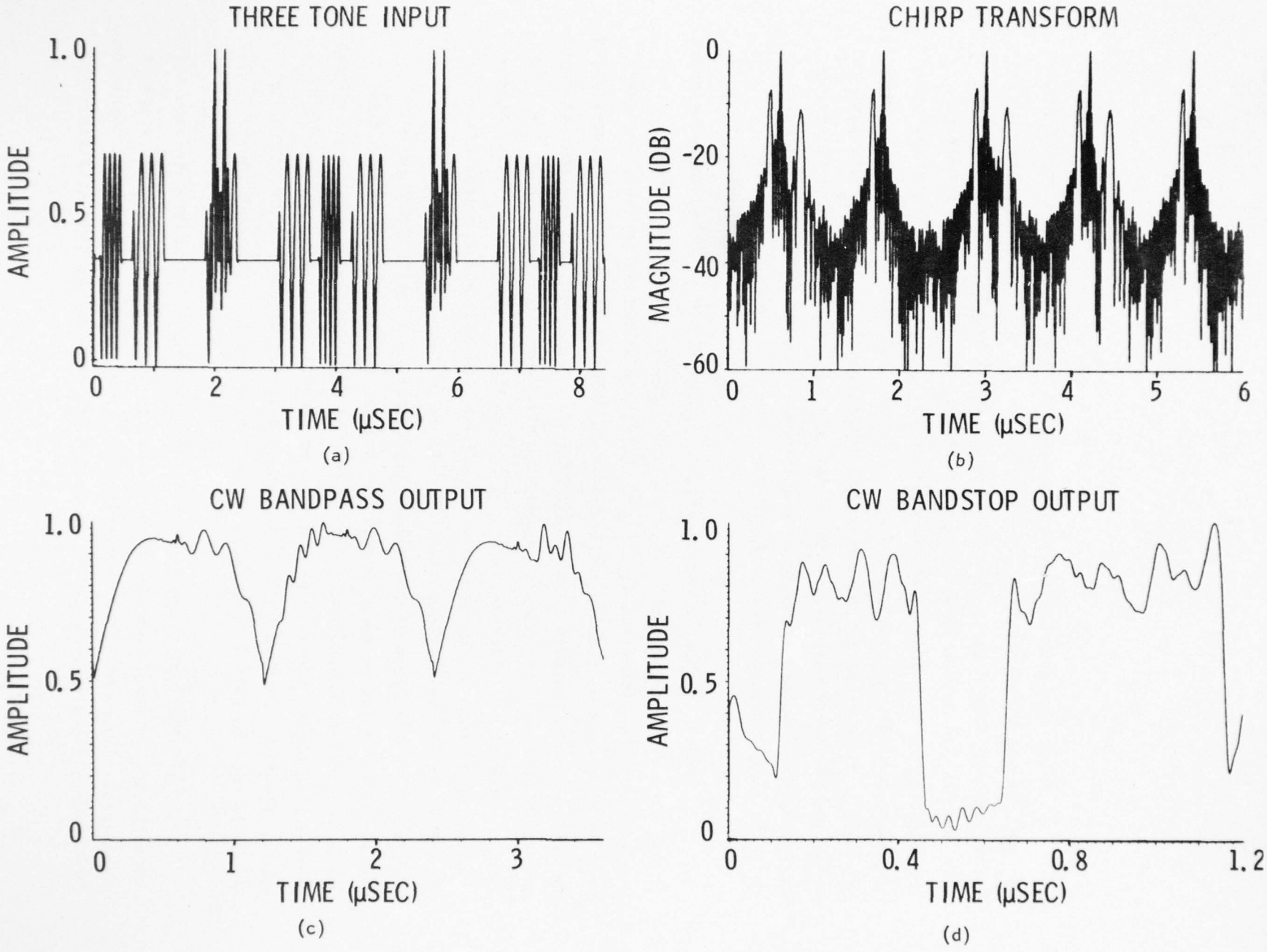

Figure 42 TAPS Filtering of cw Signals

Among the alternatives considered for reducing this distortion effect was that of weighting the first multiplying chirp. It has already been ascertained that no advantage to this weighting accrued to the TAPS system unless some benefit for cw filtering was established by permitting more complete localization of cw energy in the compressed pulse and reducing the transform sidelobes outside the modulation function. Unfortunately, the filtering performance is more directly related to the modulation function width and just as weighting the first multiplying chirp failed to appreciably improve filtering performance for pulsed signals, no significant improvement can be attributed to this design variation for cw filtering.

Figure 43 shows a representative comparison of weighted and unweighted chirps for use in cw bandpass filtering and bandstop filtering. Clearly, the character of the distortion is changed, but there is not appreciable improvement in the bandstop example for either case. The flatness of the reconstructed cw signal in the bandpass case is improved with the weighting, but the scalloped effect is not weakened, merely narrowed so that a smaller fraction of the time is distorted at the interval edges. The same effect can be achieved by changing the gate width of the modulation function with unweighted chirps also. In fact, weighting the multiplying chirp reduces the sensitivity of TAPS to variations in the width of the modulating signal, and this may be the only argument for including such weighting. Arguments against it include higher loss, the need to compensate for this shaping by inversely weighting the output multiplying chirp, and its introduction of sensitivity to time of arrival of pulsed signals. Such weighting, at least exclusive of two channel operation which is seen to fulfill the needs of cw filtering, is reasonably futile.

Alternatively, one might consider overlapping adjacent intervals such that the two intervals add to unity in the region where the amplitude drops at the edges. Figure 44 shows a time-frequency diagram for this type of operation. With the multiplying chirps $C_1(t)$ overlapping, one can see that A(t) exhibits

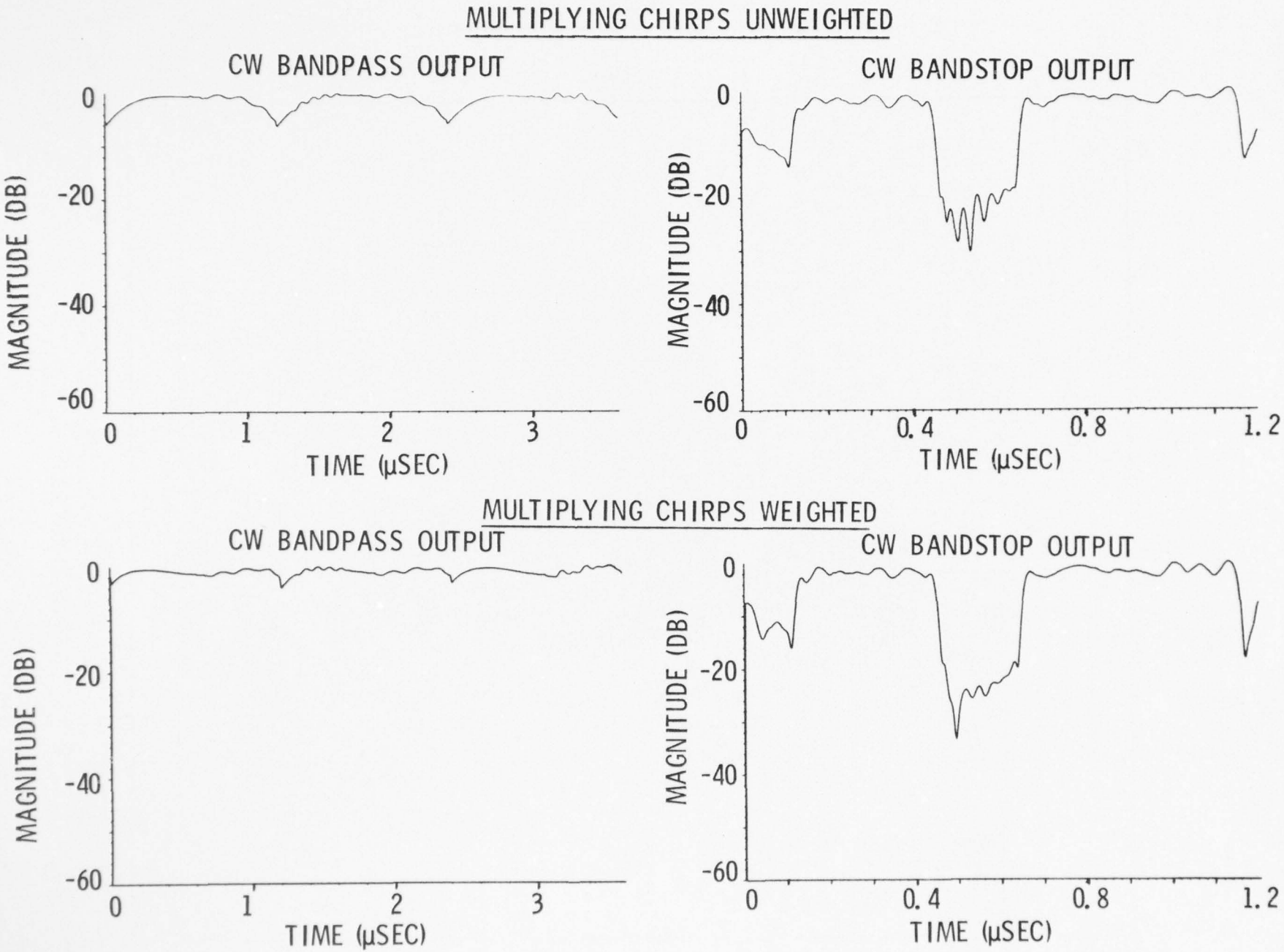

Figure 43 Effect of Weighting First Multiplying Chirp on TAPS Filtering of cw Signals

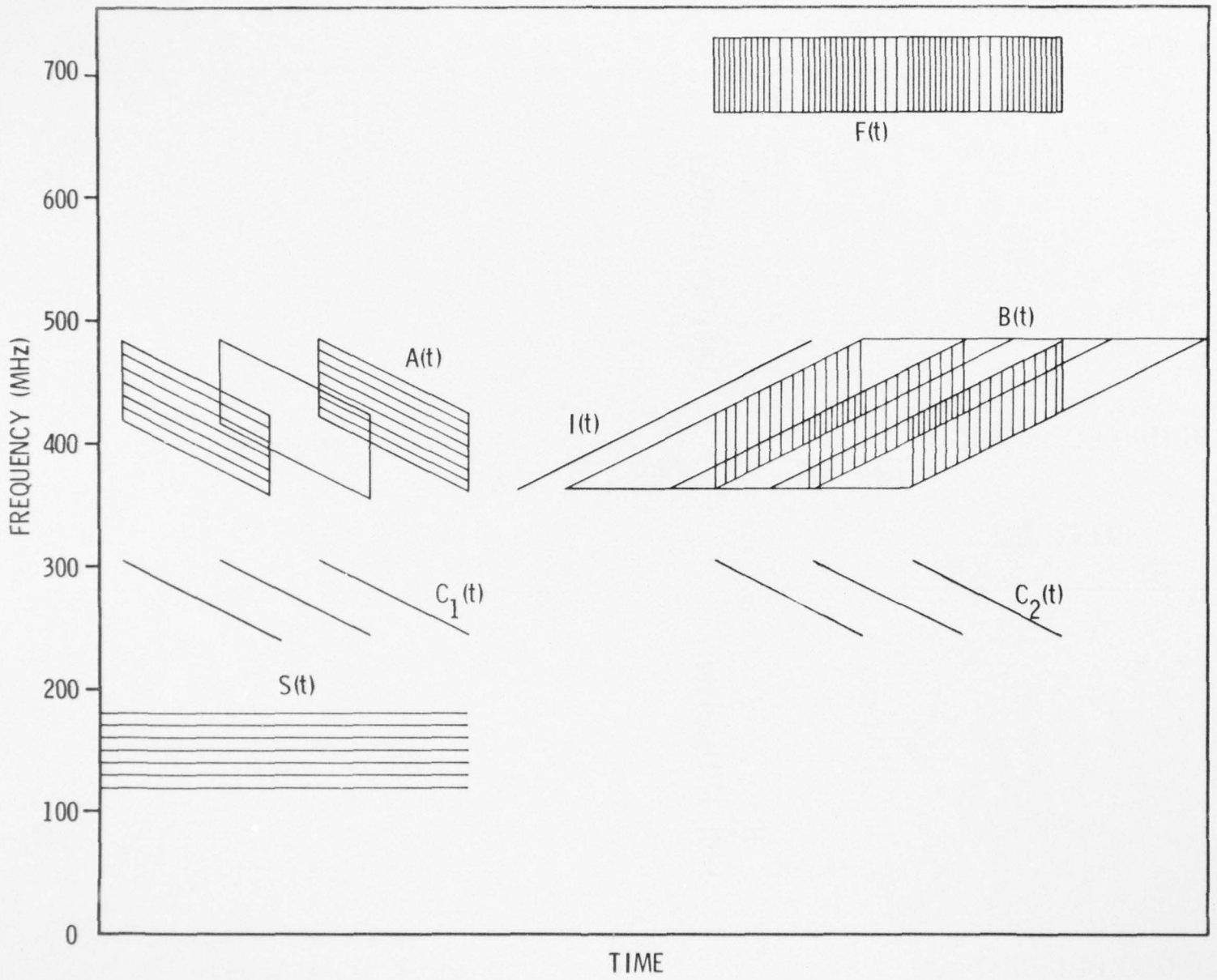

Figure 44 Overlapping Intervals Cause Chirp Transform Ambiguity in Single-Channel Continuous Operation

AD-A031 063 TEXAS INSTRUMENTS INC DALLAS CENTRAL RESEARCH LABS F/G 20/1
ACOUSTIC ADAPTIVE TRANSVERSAL FILTER.(U)
SEP 76 R M HAYS DAAB07-75-C-1309
UNCLASSIFIED TI-08-76-50 ECOM-75-C-1309-F NL

2 OF 2
AD
A031063

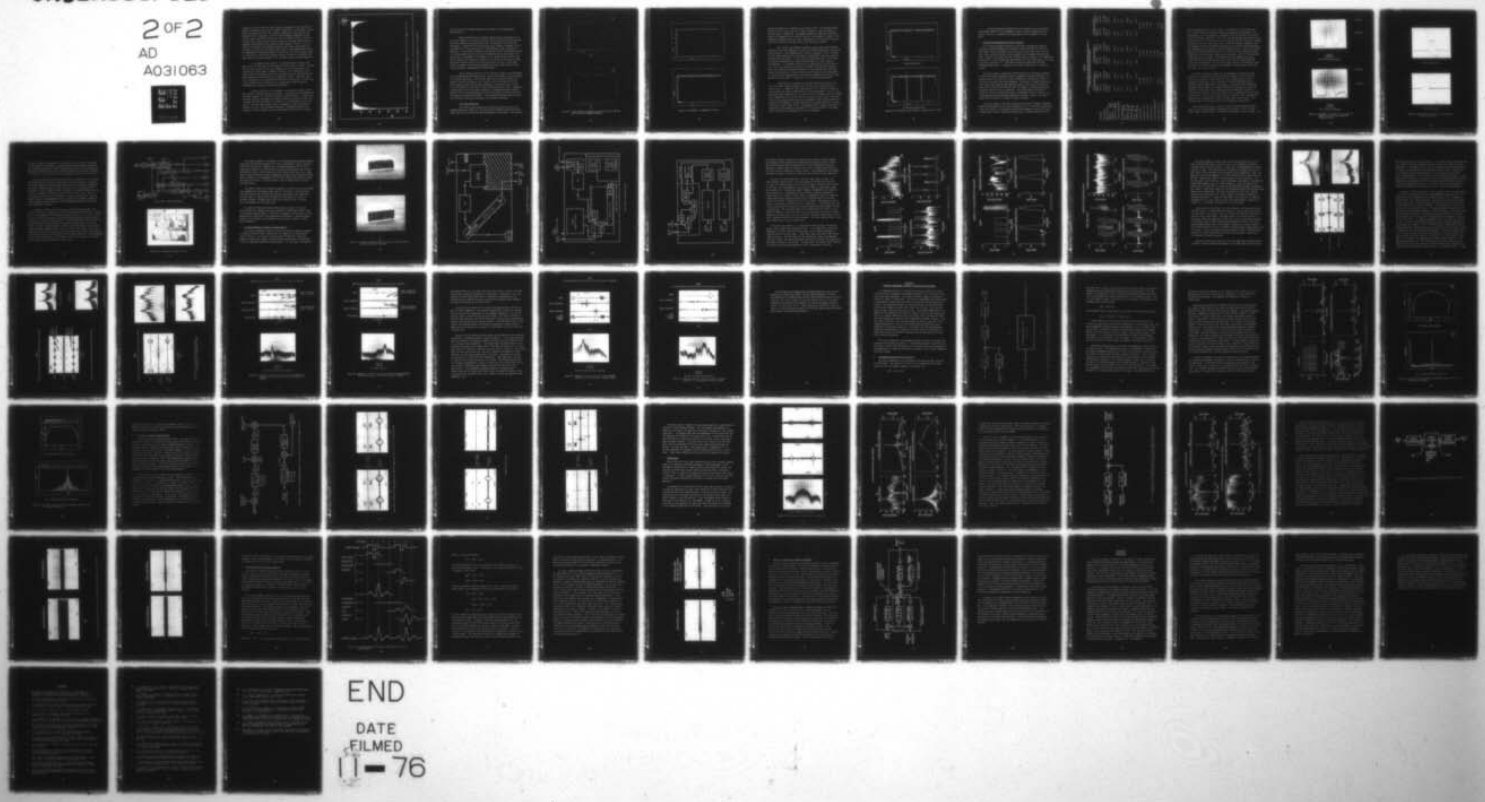

END

DATE
FILMED
11-76


1.0
1.1
1.25
1.4
1.6
1.8
2.0
2.2
2.5
2.8
3.2
3.6
4.0
4.5
5.0
5.6
MICROCOPY RESOLUTION TEST CHART
NATIONAL BUREAU OF STANDARDS-1963-A

intervals of time in which the high frequency components of one interval are present simultaneously with lower frequency components of an adjacent interval. After convolution with I(t), the frequency components of each interval are ordered in time as necessary, but now the high frequency components of one interval occupy exactly the same time as the low frequency terms of the next. In other words, the real-time transform output can no longer resolve the full frequency band because of the aliasing between adjacent intervals. To circumvent this problem, the bandwidths might be made larger than desired, but this adds insertion loss and leaves "dead" zones in the transform that cannot be unambiguously inverse-transformed to reconstruct a continuous output signal. To illustrate this interference between adjacent intervals, a simulation was made without the output broadband filter to remove the out-of-band frequencies.

At the edge of every interval, the reconstructed cw of one "time burst" rolls off such that a finite portion of that interval's signal is spread into the next interval at the wrong frequency just as the sidelobes of the transform contribute spurs in adjacent intervals. This spread part of the signal exhibits frequencies that are at the opposite end of the band from the proper frequencies contributed by the subsequent interval. Figure 45 shows this interference for cw operation and filtering in one channel. If the interfering frequencies are filtered off, the reconstructed output shows the scalloped effect familiar from previous discussion.

The only solution to this problem is a two-channel system in which each channel is used for alternate intervals. The outputs of both channels are not added, however, for then the interference would be present. Instead, the intervals should be overlapped far enough to account for the dip at the interval edges, and then the output is switched to first one channel and then the other so that the reconstructed output is composed of signal from only one channel at a time. The two-channel approach is acceptable theoretically, although it requires nearly twice as much hardware and timing errors become

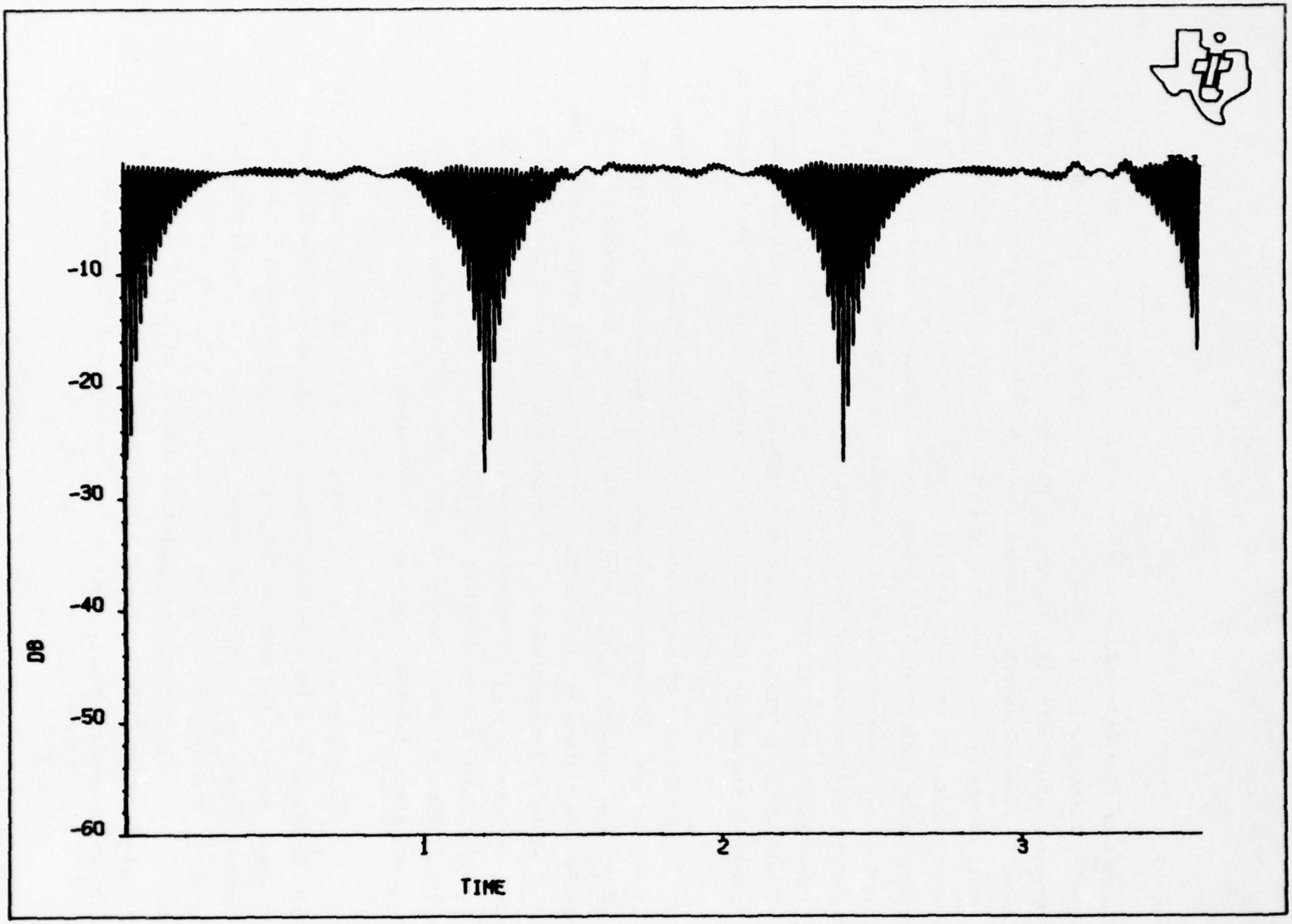

Figure 45 Adjacent Interval Interference for cw Operation in One Channel

more critical since coherent operation is desired to avoid large phase discontinuities.

Before demonstrating two channel operation with simulations for cw filtering, however, it is useful to mention again the earlier observation that the filter modulation function width itself is important to the filtering performance. Figure 46(a) and (b) show the single channel cw bandpass filtering example for filter gate widths for 0.83 MHz and 2.5 MHz, respectively. Certainly, if one wishes to achieve a pre-selected level of amplitude variation in the two channel case with the least overlapping of the two channels, the second case is preferable. For example, for a 1 dB amplitude variation, one must overlap the two channels by nominally 0.3 μsec out of the total 1.2 μsec processing interval in the first case, but by only 0.2 μsec in the second. Figure 47 compares the two-channel operation for the 2.5 MHz filter to that of the one-channel implementation of Figure 46(b).

The two channel solution for cw filtering is clearly required regardless of accompanying techniques such as interval overlapping or chirp weighting for sidelobe suppression. On the other hand, once two channel operation is adopted, interval overlapping is an integral part of the solution and even chirp weighting might be effectively employed to reduce sensitivity of the filter performance to varying the filter modulation function width. Regardless, implementation of the two channel processor is straightforward and feasible based on the filtering performance of the single channel prototype system and the extensive simulations performed. Timing becomes the major area of concern and required accuracy can be achieved with available technology.

4. Timing Considerations

The relative times between the transform mixing chirp $C_1(t)$, the bandpass modulation signal $G(t)$, and the inverse transform mixing chirp $C_3(t)$ (see Figure 13) are critical to optimum operation of the system. The transform

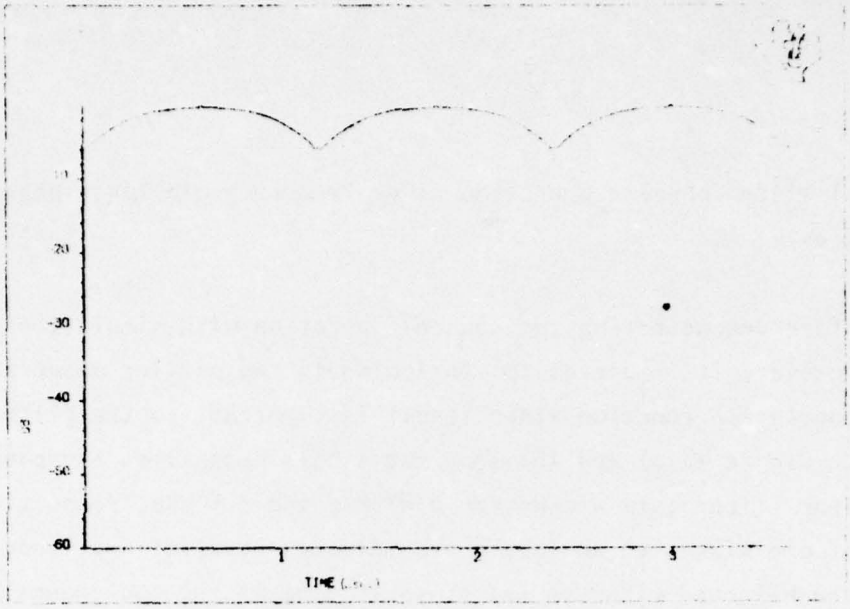

(a)

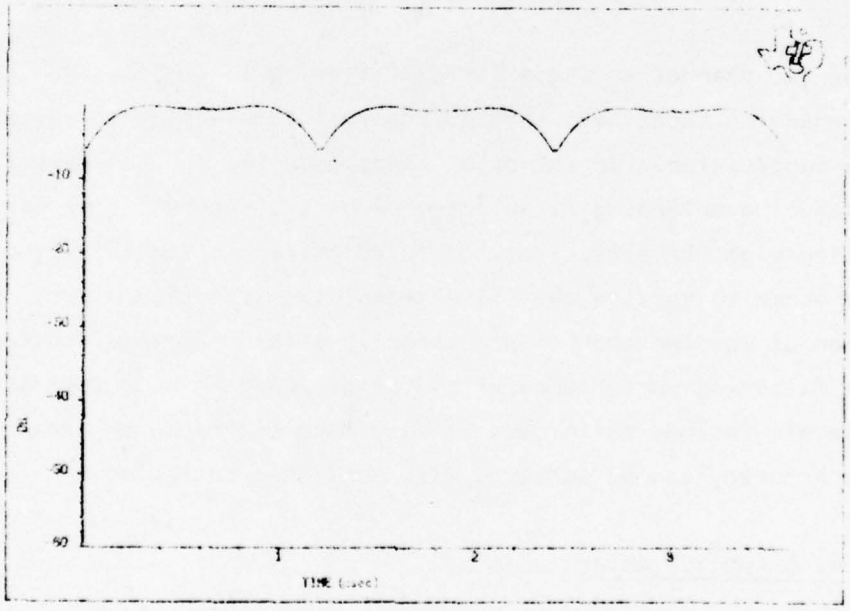

(b)

Figure 46 Single-Channel cw Bandpass Filtering for (a) 0.83 MHz and (b) 2.5 MHz Bandpass Response

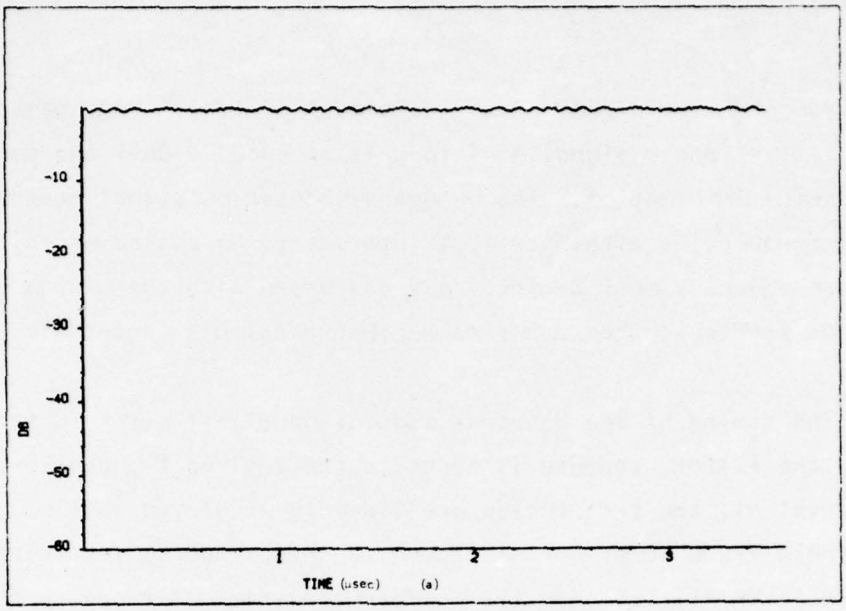

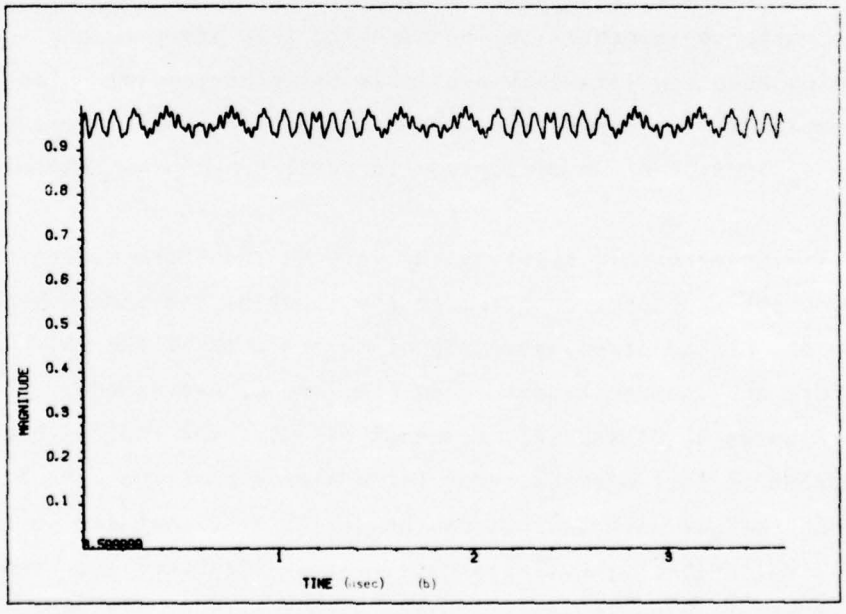

Figure 47 Two-Channel cw Bandpass Filtering

mixing chirp gates out a portion of the signal ΔT long. This passes through the chirp filter, and a signal 3 ΔT long is produced. Only the center ΔT contains useful information. The bandpass modulation signal must accurately select the frequencies within this ΔT interval to be passed or rejected. This interval subsequently must be inverse transformed with the mixing chirp $C_3(t)$ occurring at precisely the same time as that particular interval.

The timing of the bandpass modulation signal simply determines how accurately the filter response is tuned to the desired frequencies. Within any given interval ΔT, the frequencies are linearly displayed in time. The rate at which these frequencies are displayed is determined by the chirp slope of the SAW linear FM filters. In the prototype system described in this report, the linear FM parameters are 1.905 μsec and 60 MHz for a chirp slope of 31.5 MHz/μsec. If the modulation function is generated 10 nsec too early or late, the filter response is shifted by 0.3 MHz from the desired frequency. The filter response is otherwise identical to that selected and since nanosecond timing accuracy is easily available using commercial pulse generators for the feasibility demonstration, the expected frequency errors smaller than 30 kHz are insignificant in comparison to the 1 MHz minimum bandwidth.

Timing errors in starting the inverse transform mixing chirp will shift the output frequency compared to the input by the same 0.3 MHz for 10 nsec error. In addition, some signal may be lost if the chirp signals of the transform and inverse transform do not line up everywhere. This is illustrated by Figures 48(a) and (b), respectively, for the radical case of a 40 nsec error compared to that with no error for a simple cw signal input. Since the delay of the surface wave devices can be designed so that the chirp gates are triggered simultaneously, reliable gate timing is assured such that no signal loss occurs and only small shifts in the output carrier frequency can occur in proportion to the accuracy of the SAW chirp filter fabrication. Once again, shifts of 30 kHz per nanosecond of error are acceptable.

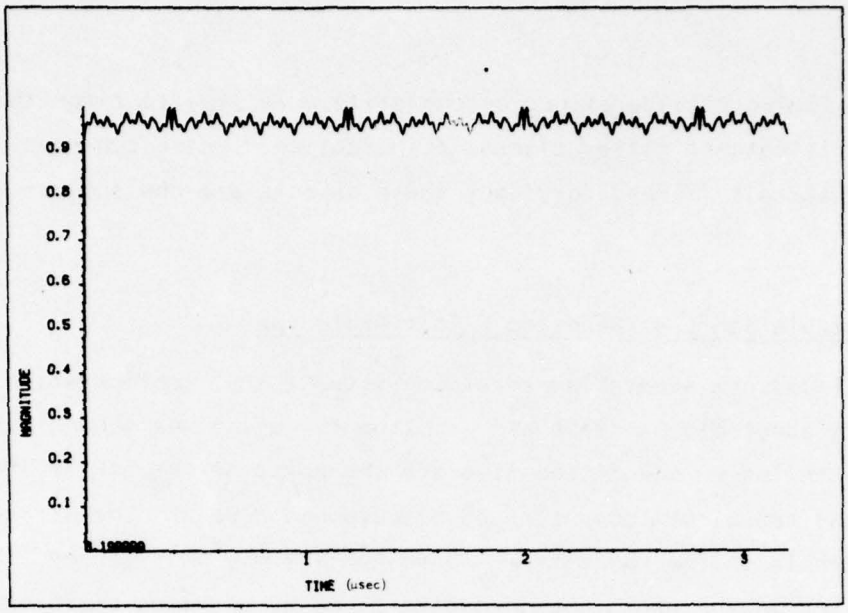

(a) No Timing Error

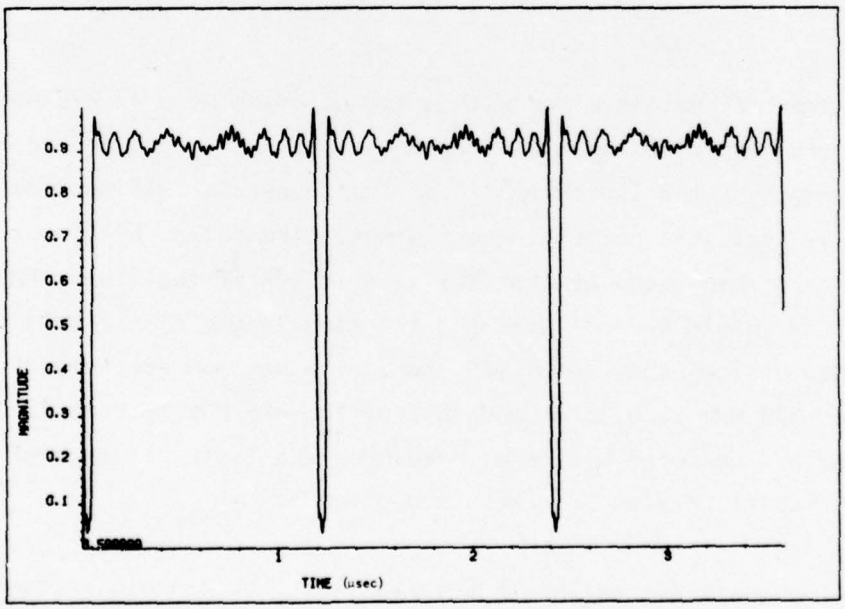

(b) 40 nsec Timing Error

Figure 48 Simulation of the Effects of Timing Errors in TAPS

Timing considerations become still more important for the transform programmable matched filter discussed in Section V where coherence over successive intervals is mandatory, but these aspects are the subject of future work.

C. Adaptable Bandpass/Bandstop Filter Prototype

The Transform Adaptable Processor System (TAPS) configuration required to perform adaptable bandpass and bandstop filtering was shown in Figure 13. The elements inside the dotted line are the parts of the TAPS filter, and the other boxes represent laboratory test equipment used to demonstrate the prototype. Signals in the range from 120 to 180 MHz may be filtered. The frequencies of operation in the prototype were determined by spurious performance of the mixers discussed in Section III.C. The mixers are Watkins-Johnson M6E low-level, double-balanced mixers. In operation, the input to the mixers is limited to -5 dBm.

The input signal is mixed with a 60 MHz down-chirp at 275 MHz to produce a signal with upper fundamental frequency components from 365 to 485 MHz. The maximum length of the SAW chirp filter transducers at 425 MHz was limited to 2.0 μsec by available patterning equipment. The design of linear FM two-transducer filters then requires that the time length of the linear FM convolving chirp filter should be 3.81 μsec and the time length of the multiplying chirp SAW devices half of that, or 1.905 μsec. The maximum aperture of the SAW filters at 275 MHz is 0.98 mm and that of the 425 MHz filters is 0.86 mm. The calculated and measured mid-band impedances and losses of each of the three linear FM SAW filters on ST quartz are given in Table I.

The input signals to the TAPS system must not contain frequency components beyond the bandwidths of the devices (Section IV.B.1). The surface wave devices within the system will attenuate the out-of-band components, but since a mixer precedes these filters, out-of-band frequencies can create products that fall

Table I

Calculated and Measured Mid-Band Impedances and Losses of Three Linear FM SAW Filters on ST Quartz

	275 MHz Down-Chirp		425 MHz Up-Chirp		425 MHz Down-Chirp	
	Trans. 1	Trans. 2	Trans. 1	Trans. 2	Trans. 1	Trans. 2
Bandwidth	60 MHz	60 MHz	120 MHz	120 MHz	120 MHz	120 MHz
Time Length	0.95 μsec	0.95 μsec	1.91 μsec	1.91 μsec	1.91 μsec	1.91 μsec
Aperture (eff.)	0.98 mm	0.55 mm	0.86 mm	0.35 mm	0.86 mm	0.46 mm
Radiation Impedance (Parallel Eq.) R_p	4.4 kΩ	7.8 kΩ	1.4 kΩ	3.4 kΩ	1.4 kΩ	2.6 kΩ
Radiation Impedance (Parallel Eq.) X_p	-41.1 Ω	-73.0 Ω	-9.8 Ω	-24.0 Ω	-9.8 Ω	-18.3 Ω
Parasitic Resistance	1.0 Ω	1.2 Ω	0.6 Ω	0.7 Ω	0.6 Ω	0.7 Ω
Calculated Series Impedance R_{sc}	1.4 Ω	1.9 Ω	0.7 Ω	0.9 Ω	0.7 Ω	0.8 Ω
Calculated Series Impedance X_{sc}	-41.1 Ω	-73.0 Ω	-9.8 Ω	-24.0 Ω	-9.8 Ω	-18.3 Ω
Measured Series Impedance R_{sm}	1.1 Ω	2.1 Ω	0.6 Ω	0.7 Ω	0.6 Ω	0.8 Ω
Measured Series Impedance X_{sm}	-40.0 Ω	-73.4 Ω	-9.9 Ω	-24.1 Ω	-10.7 Ω	-20.1 Ω
Mismatch Loss	25.8 dB		32.1 dB		32.1 dB	
Apodization Loss	2.5 dB		3.9 dB		2.7 dB	
Propagation Loss	0.7 dB		2.0 dB		2.0 dB	
Diffraction Loss	1.2 dB		1.5 dB		1.7 dB	
Scattering Compensation	--		5.0 dB		--	
Bidirectional Loss	6.0 dB		6.0 dB		6.0 dB	
Total Insertion Loss	36 dB		51 dB		44 dB	

within the passband of the chirp filters. Introduction of interfering terms at this point cannot be corrected by post-mixer operation on the signal. For this reason, it will be necessary to include a filter at the input to eliminate undesired frequency components. This filter has the same desired characteristics as the output filter. The output filter is required to select the lower frequency component of the mixer output and also to reject the frequency components that are produced just outside the 60 MHz bandwidth by the inverse transform operation due to ambiguities from adjacent intervals (Section IV.B.4). Due to their broad bandwidth, the ease with which low-loss LC filters can be constructed at these frequencies, and the moderate shape factor requirement, two LC filters have been constructed for this purpose. Figures 49(a) and (b), respectively, show a seven-pole Butterworth design used for the input and a five-pole Tchebychev filter used on the output. The two filters have a 50 MHz, 3 dB bandwidth corresponding to the maximum frequency range demanded of the adaptable filter with less than 2 dB of insertion loss.

The linear FM (chirp) signals that are generated to perform the chirp transform are provided by exciting the impulse response of the 275 MHz SAW devices with a gated rf pulse at 275 MHz with a nominal width of 10 nsec. (A pulse of width equal to the reciprocal of the 50 MHz bandwidth would attenuate the band edges 4 dB.) The gated rf is generated with two Olektron Schottky diode balanced SPST switches separated by an Avantek unit amplifier (UTO-513). The on-off ratio is improved by this cascade from -35 dB for a single switch to -65 dB. Since the 275 MHz pulse is expanded in the SAW linear FM device (BT = 140, 20.6 dB) from 10 nsec to 1.905 μsec, the cw feedthrough would be only 14 dB below the linear FM signal with a single switch. This spurious level is -44 dB below the chirp by cascading a second switch.

The 10 nsec gating pulse is used for timing inside the TAPS prototype as well as for all test equipment to demonstrate the system. The 1.2 V input pulse, shown in Figure 50(a), is divided to drive each of the two switches. The

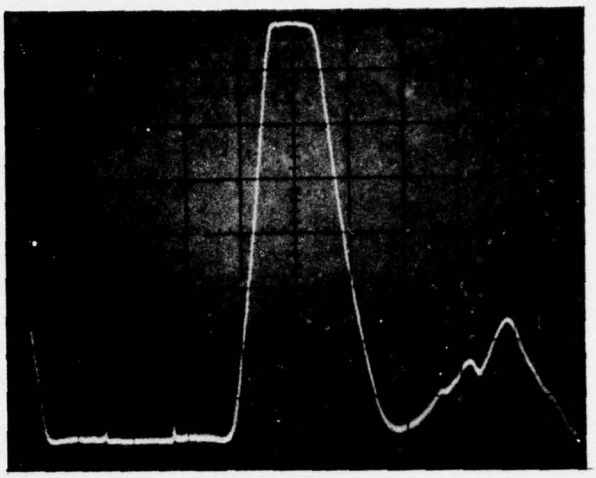

0 dB Ref

10 dB/Div

150 MHz
50 MHz/Div

(a) Seven-Pole Butterworth

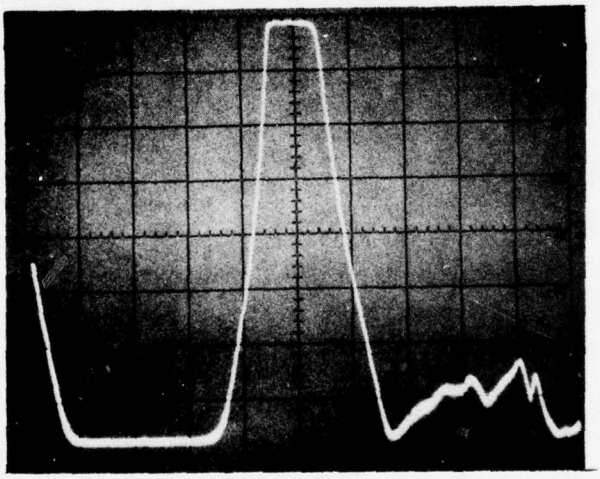

0 dB Ref

10 dB/Div

150 MHz
50 MHz/Div

(b) Five-Pole Tchebychev

Figure 49 Broadband LC Filters for the Input and Output to the Transform Adaptable Processor System

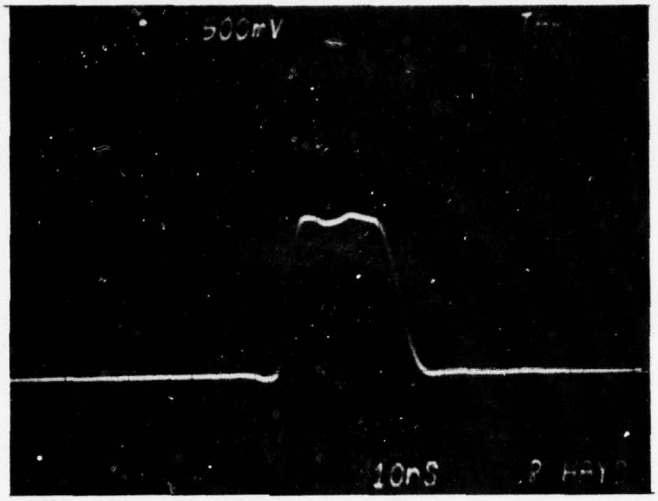

(a) Rf Gating Pulse

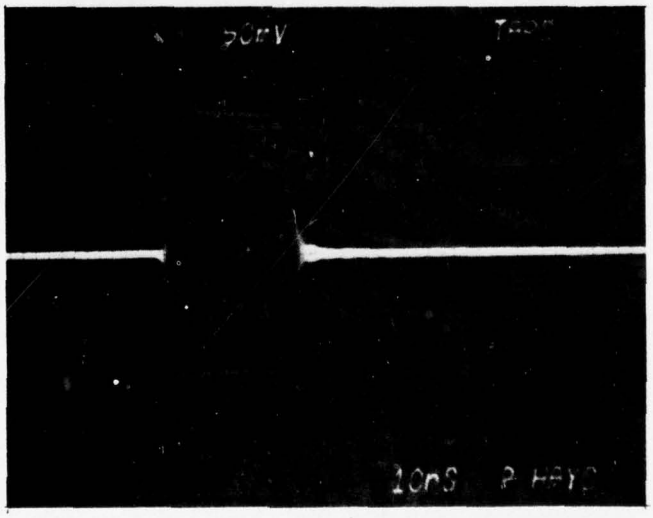

(b) 275 MHz Pulse

Figure 50 275 MHz Pulse Generation for Excitation of SAW Chirp Devices

275 MHz cw signal to be gated has a 0 dBm level to the prototype. The gated rf pulse shown in Figure 50(b) is amplified to +9 dBm and then divided three ways to provide excitation to the input multiplying chirp of the transform and the output multiplying chirp of the inverse transform and an output from TAPS to be used for a test point or for the programmable demonstration of Section V.

The block diagram of Figure 51(a) shows all the components of this system. The 275 MHz SAW chirp filters are excited by the 10 nsec gated rf to produce the 60 MHz bandwidth linear FM signal required for the multiplying operations. Since these components exhibit 36 dB insertion loss and an expansion loss equivalent to the BT product (21 dB), 63 dB gain is provided following the SAW filters to produce a +7 dBm signal at the LO port of the mixers. The pre-multiplying chirp of the first transform is divided to provide the linear FM signal not only to the adaptable filter, but also for an external connection to the reference channel transform of the programmable matched filter bread-board described in Section V.

An amplifier follows the first mixer to raise the maximum signal level back to 0 dBm prior to convolution with the 425 MHz up-chirp SAW filter. [Figure 51(b) is a photograph of this packaged and matched device.] This filter exhibits a loss of 51 dB, but the signal to be transformed experiences compression gain, which can be as large as the BT product of the premultiplying chirp (21 dB). The subsequent amplifier has 36 dB gain to produce a maximum signal level at the switch of +6 dBm. Another amplifier recovers the switching loss and raises the maximum modulated transform signal level to +17 dBm. This signal is the chirp transform of the input signals, and an external connection is provided to observe the transform results or to multiply with a reference transform for the programmable matched filter of Section V. This signal is fed into the input of the inverse chirp transform process through an external cable.

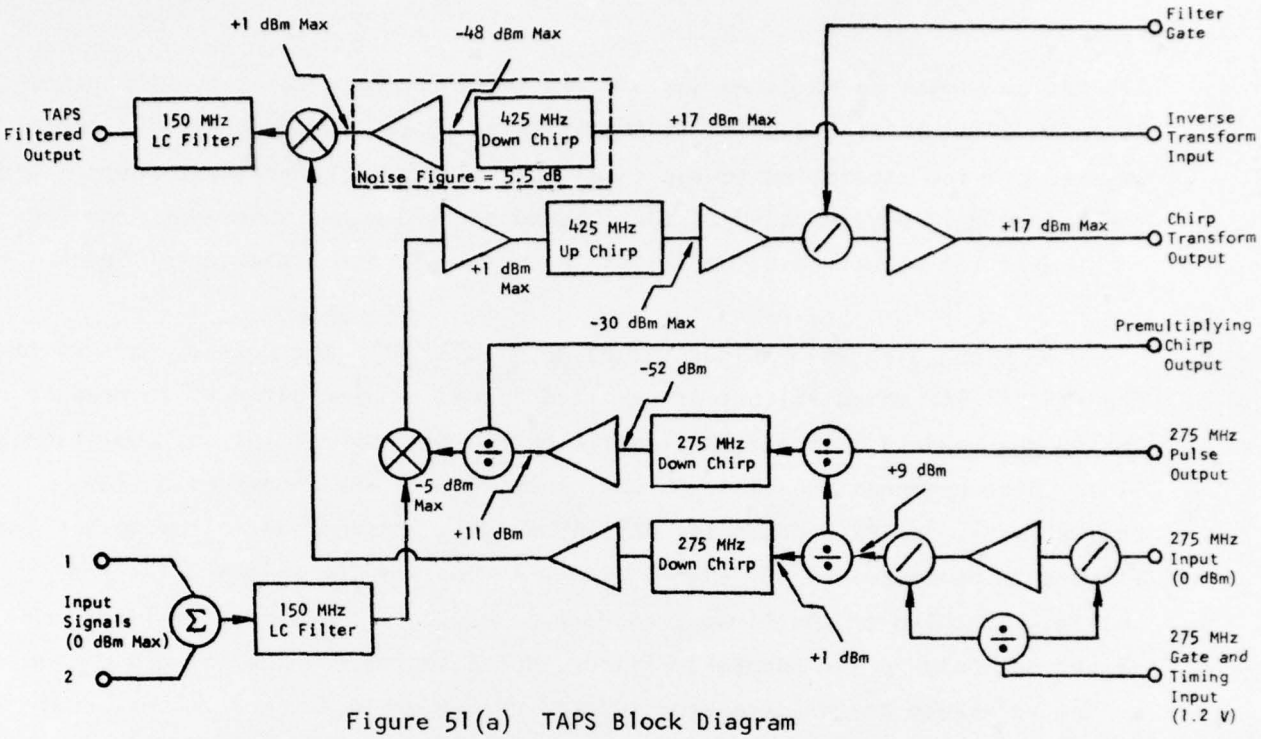

Figure 51(a) TAPS Block Diagram

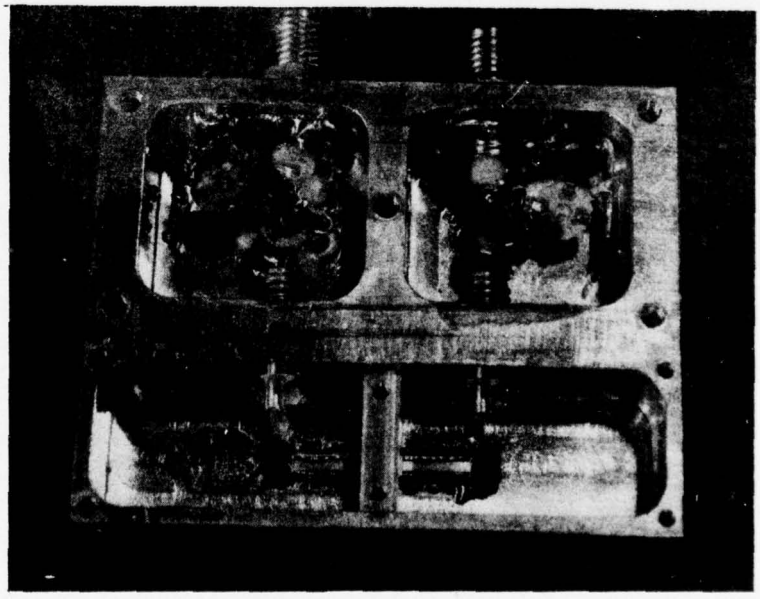

Figure 51(b) Packaged SAW Linear FM Filter

The inverse transform is provided by first convolving the modulated spectrum signal with the 425 MHz SAW down-chirp filter as described in earlier sections. The 44 dB insertion loss, together with the maximum expansion loss of 21 dB, prescribes an amplifier with 53 dB gain to provide 0 dBm maximum signal to the post-multiply mixer. The 275 MHz chirp filter used for the linear FM LO signal at this mixer has additional delay implemented by spacing the transducers farther apart to account for the propagation time of the original input signals through the convolving filters. The mixer output is then filtered by the LC filter described earlier.

The dynamic range of the transform processor is primarily set by the largest loss component and the maximum signal levels at the mixers. A 40 dB dynamic range was desired, and a 100 MHz bandwidth was prescribed in the signal path. The noise level is -94 dBm minus the amplifier noise figure of 5.5 dB, or nominally -88 dBm. The peak signal level after the SAW filter is -48 dBm for a 40 dB margin over the noise floor.

The complete Transform Processor block diagram is shown in Figure 51 with the major loss component and ensuing amplifier identified by dotted lines. The assembled processor shown in Figure 52 is packaged in three levels with the external ports identified in the photographs as discussed. A schematic representation of the layout of the components on each level is shown in Figures 53(a) through (c).

D. Transform Adaptable Processor Prototype Results

The Transform Adaptable Processing System configured for adaptive bandpass or bandstop filtering clearly demonstrates its capability to handle pulsed signal filtering. The results of the prototype included here, along with supporting simulations, compare favorably with the performance of fixed-tuned filters of comparable shape factor and bandwidth. The simulations are required

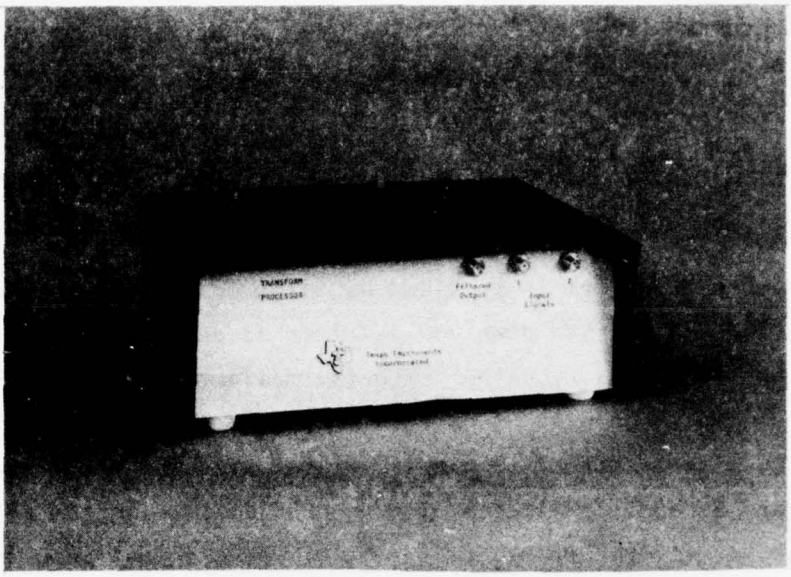

(a)

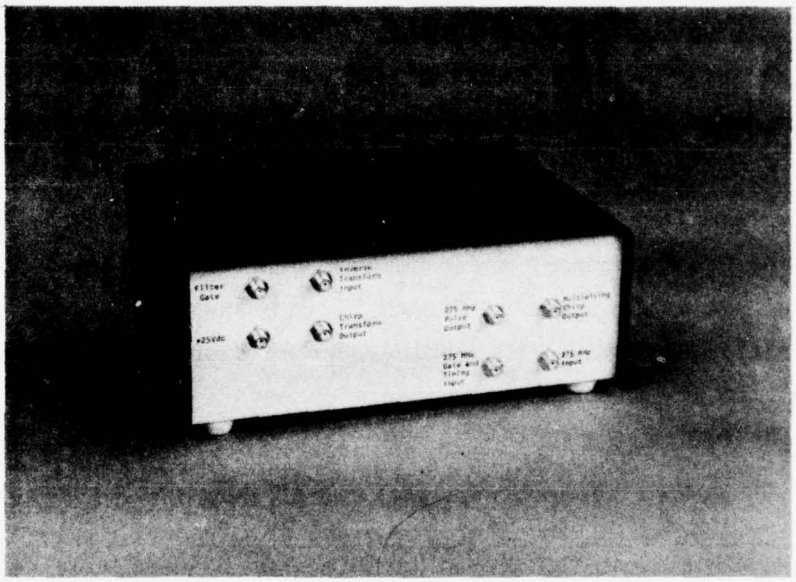

(b)

Figure 52 Transform Adaptable Processing System (TAPS) Prototype. (a) Front view; (b) back view.

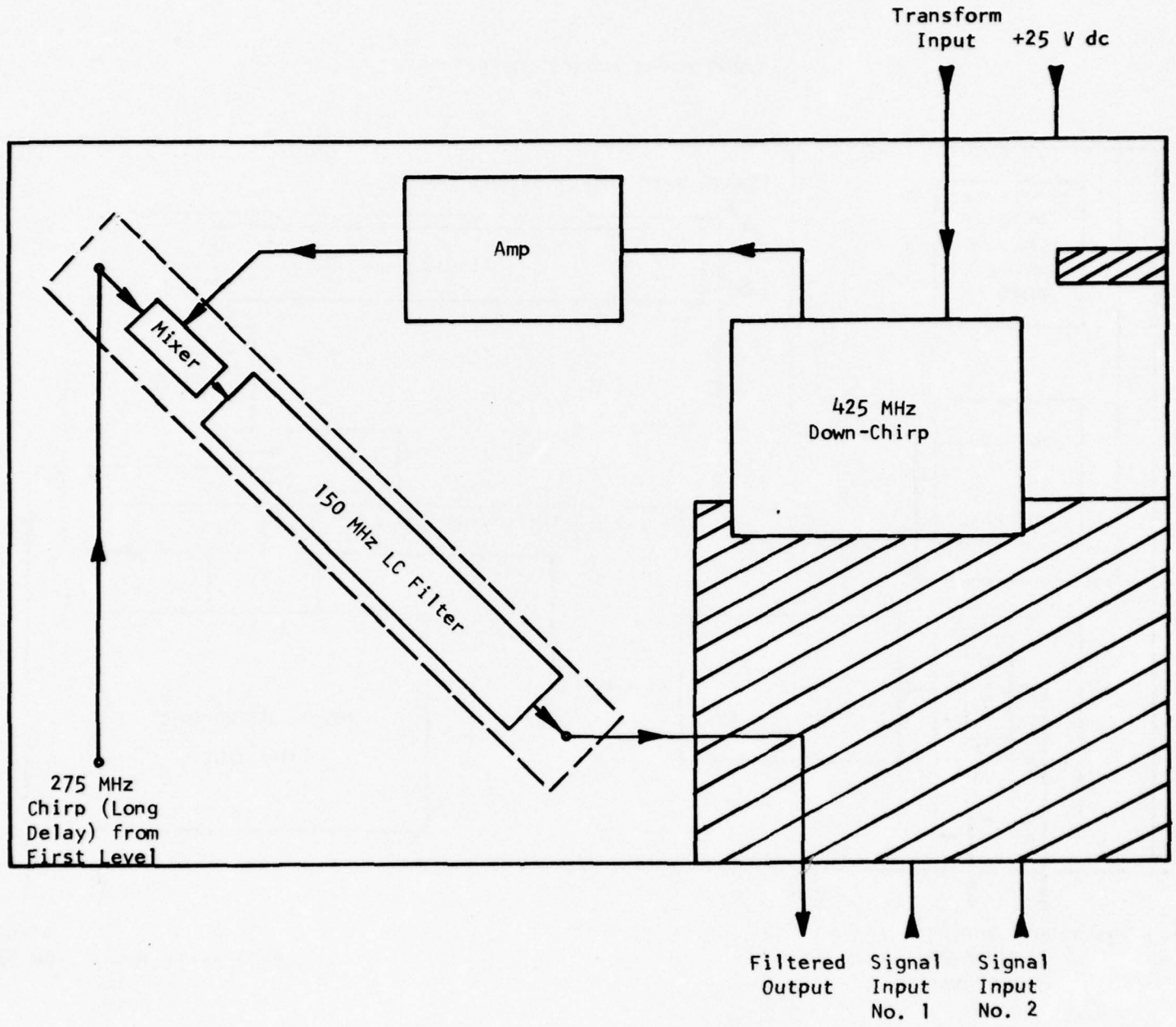

Figure 53(a) Third Board Level

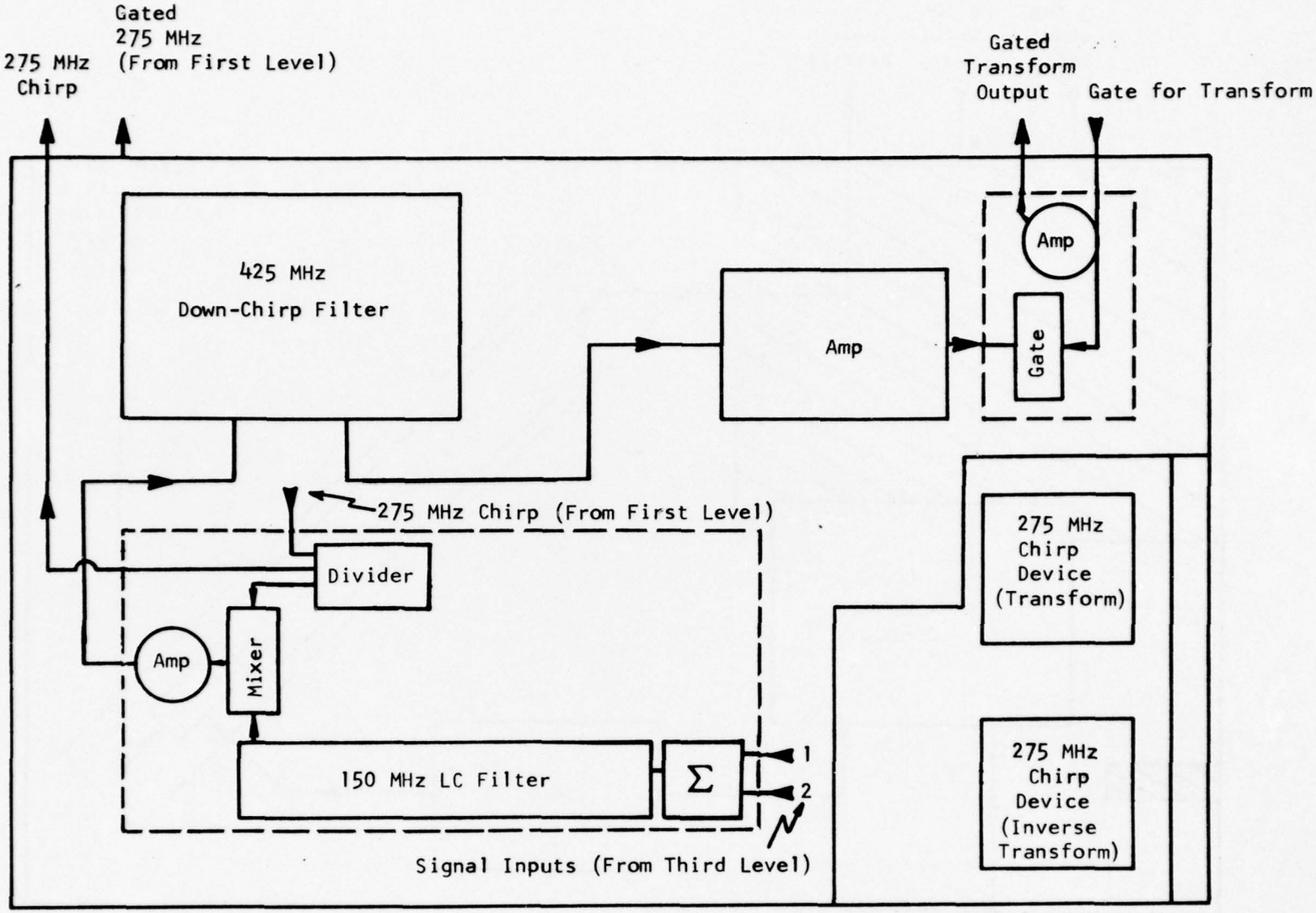

Figure 53(b) Second Board Level

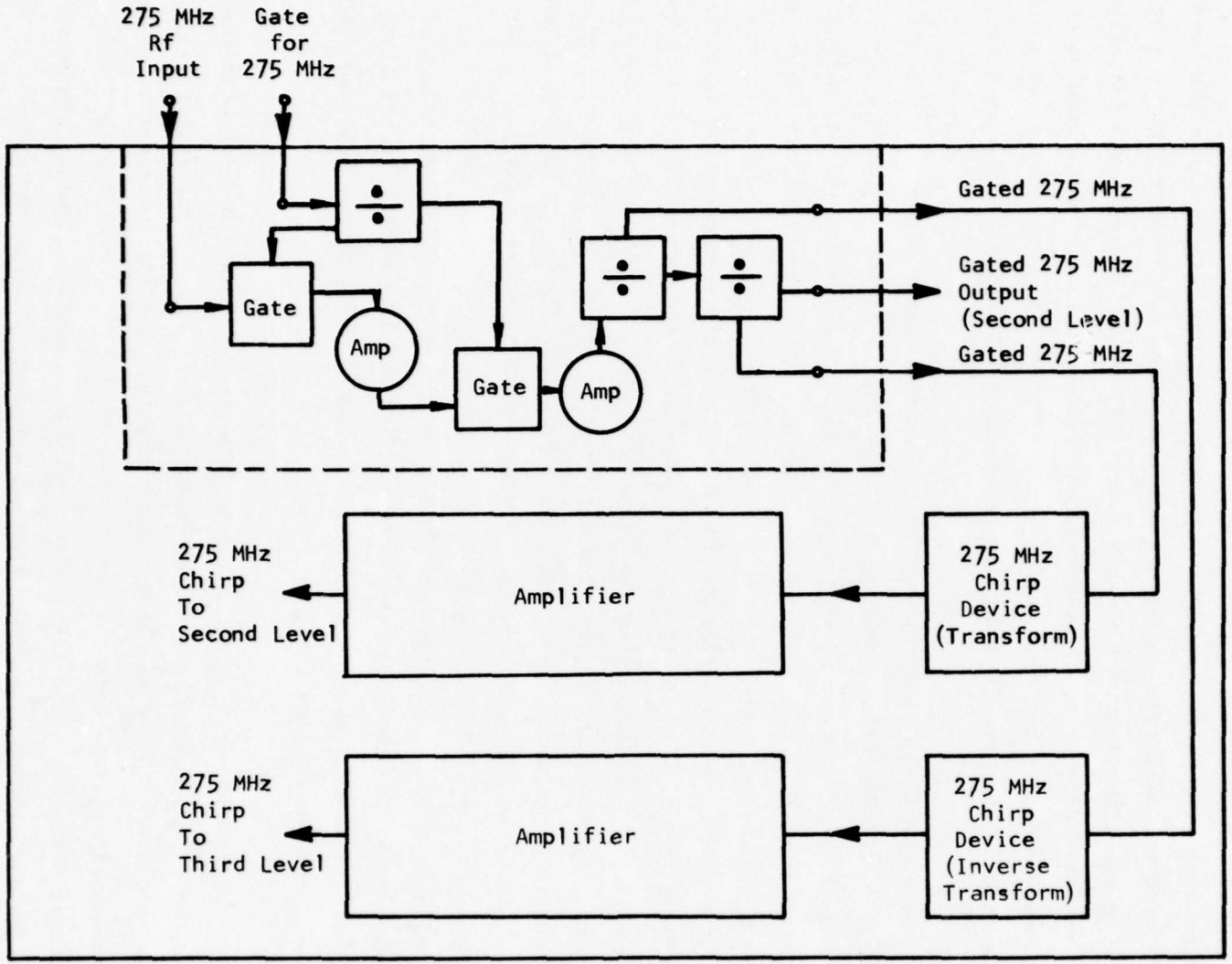

Figure 53(c) First Board Level

to provide a frame of reference for appraising the results since the bandpass and bandstop filtering operations introduce some distortions such as ringing due to band-limiting that are characteristic of any conventional filtering operation. Without specific reference to that fact, erroneous conclusions may be drawn from the introduction of these effects. Two representative simulations are shown in Figures 54 and 55 to demonstrate the validity of this observation.

For the first case (Figure 54), a two-tone input signal is used. The input contains a pulse train of 0.51 μsec pulses at 144 MHz with a period of 1.2 μsec, and a second pulse train of 0.33 μsec pulses at 162 MHz with a period of 1.8 μsec. The true spectrum of this input is shown in Figure 54(b), where the transform of a single pulse at each frequency is sampled by the repetition of the pulse train. Following the chirp transform to obtain the spectrum [Figure 54(c)] of a single 1.2 μsec interval, a modulation function is applied to pass the 0.33 μsec pulses by gating "on" the 162 MHz region of the time trace [Figure 54(d)]. (Rejection of 40 dB is assumed.) The modulation corresponds to a bandwidth of 6.0 MHz with a 2:1 shape factor. Figure 54(g) shows the reconstructed output following the time domain modulation and subsequent inverse transformation. The simulated output clearly demonstrates the fidelity of the adaptable bandpass filtering by TAPS with the narrow 0.33 μsec pulses at 162 MHz passed and the other pulse train at a different frequency rejected along with all other frequencies outside the 6.0 MHz passband. The actual measured results from the prototype confirm this, as shown later.

Of further note, however, is a comparison of these results with those expected from a conventional fixed-tuned filter. A 2:1 shape factor filter with bandwidth of 6.0 MHz at 162 MHz was simulated, and its impulse response was convolved with the two-tone input. Figure 54(h) shows that output under conventional filtering. The TAPS output and the conventional output are remarkably alike and, indeed, the deviations between the two are more than -20 dB down from the output as shown in Figure 54(f). In other words, for pulsed signal filtering, TAPS exhibits performance comparable to that of conventional filtering.

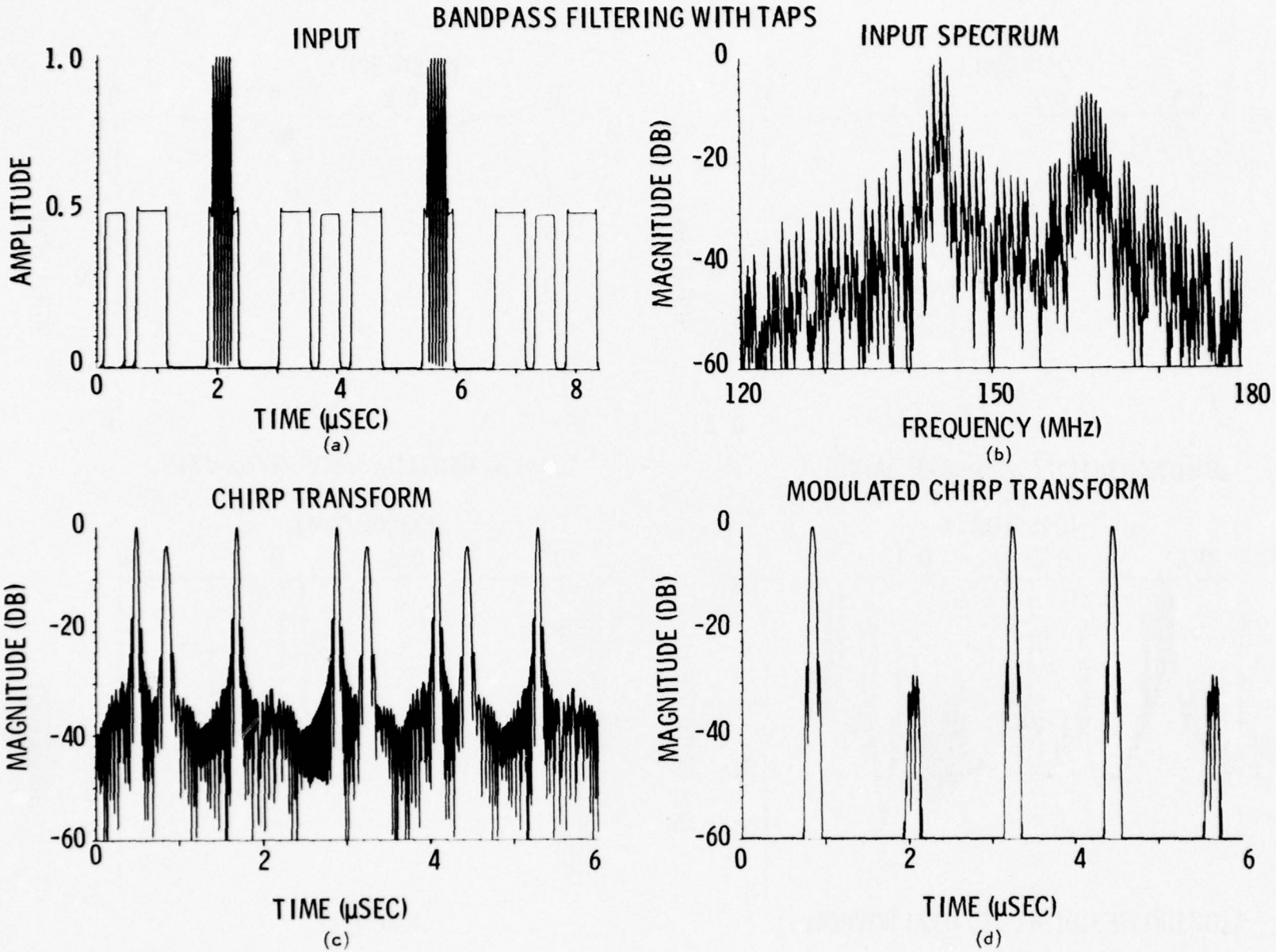

Figure 54 Bandpass Filtering with TAPS

BANDPASS FILTERING WITH TAPS (continued)

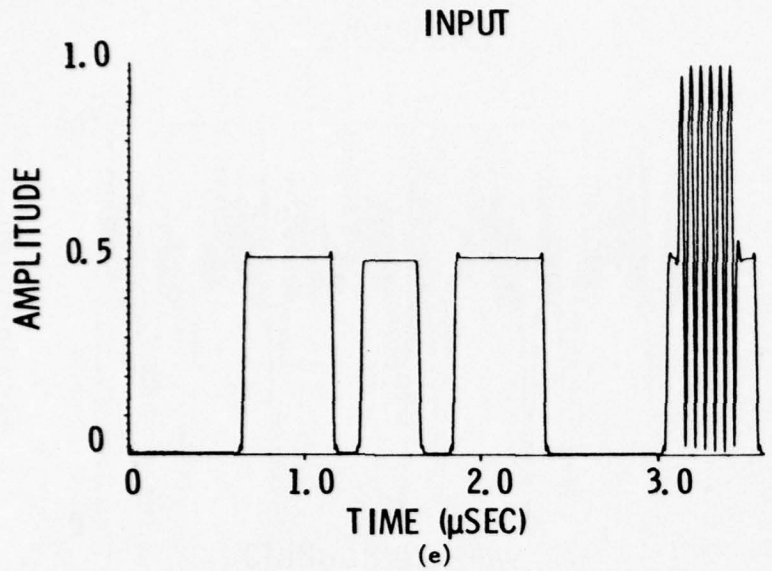

(e)

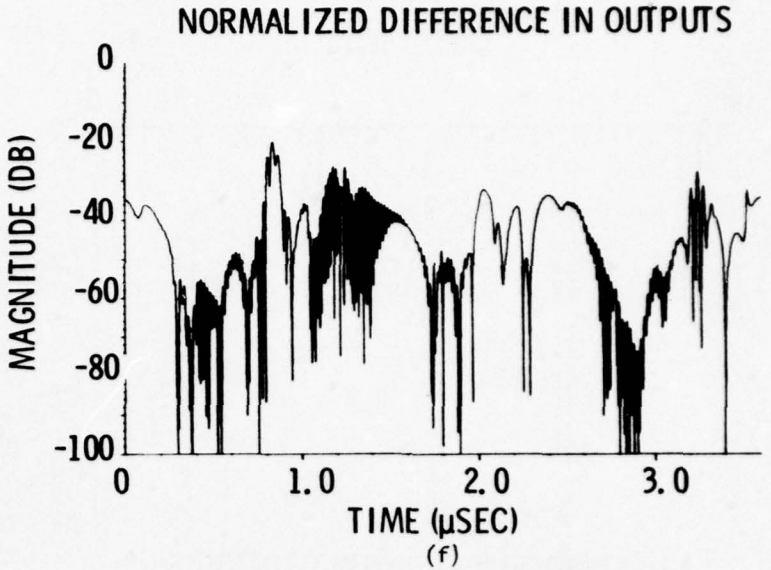

(f)

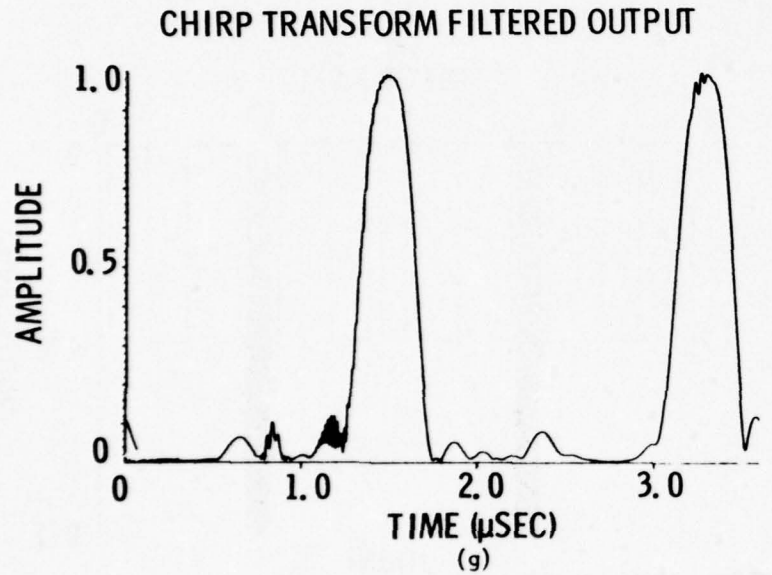

(g)

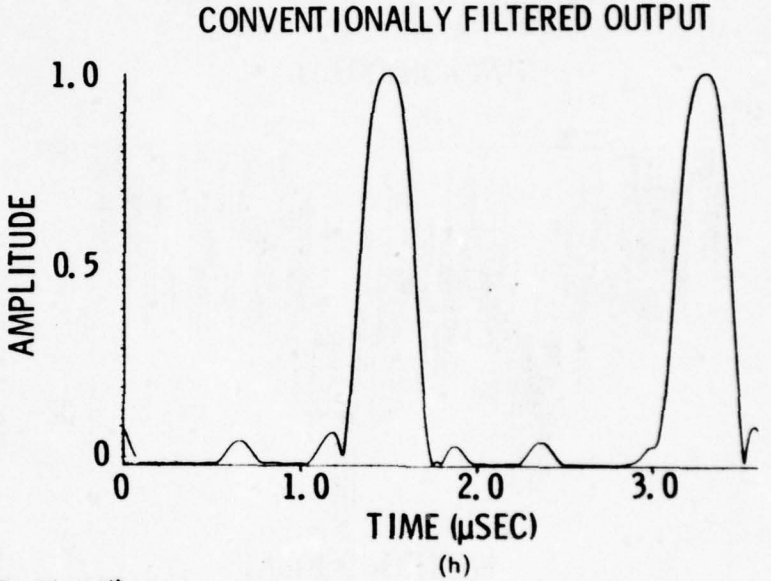

(h)

Figure 54 (Continued)

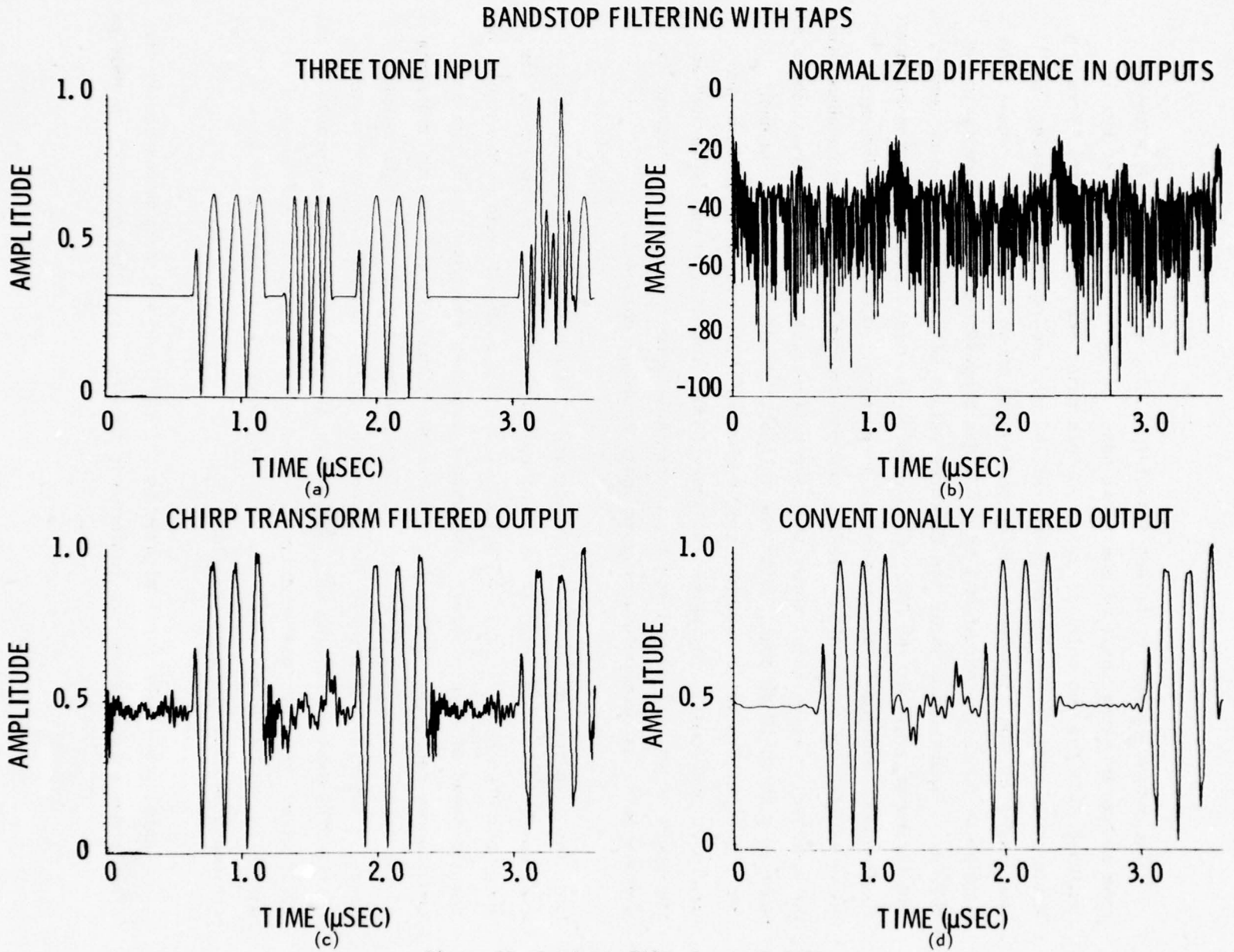

Figure 55 Bandstop Filtering with TAPS

The second example of pulsed signal filtering (Figure 55) adds a third tone to the two-tone input of the first case. A cw frequency at 150 MHz is included with the two pulse trains. In this case, the complementary filtering function is shown. The narrow pulses at 162 MHz are rejected by gating "off" that region of the time domain which represents those frequencies. Again, the modulation function corresponds to a 6.0 MHz bandwidth and 2:1 shape factor at 162 MHz. Figure 55(c) shows the filtered output with the remaining cw term and the pulse train at 144 MHz. Figure 55(d) shows the output of a conventional fixed-tuned bandstop filter of similar parameters. Again, the results are quite similar for both TAPS filtering and conventionally available nonadaptable performance. Figure 55(b) shows that the differences between the two outputs are nominally 20 to 30 dB down. With the introduction of the cw term, however, the principal limitation of the "single channel" TAPS system is exposed, as discussed previously. As shown in Figure 55(b), the distortion is largest at the edges of the 1.2 μsec intervals where TAPS cannot properly reconstruct cw signals as it is presently configured with a single channel.

The true test of the system is not the simulation, but the actual prototype performance. To demonstrate the transform - inverse transform operation, the input chosen was a train of pulses at 165 MHz with 300 nsec widths shown in the top trace of Figure 56(a). The second trace is the chirp transform in continuous, repetitive operation, and the third trace is the inverse transform of the second trace, or the reconstructed waveform out of TAPS. The output waveform demonstrates clearly the successful transform and inverse transform of the TAPS system with the only noticeable distortion due to feedthrough in the first mixer. Further confirmation of these results is shown in Figures 56(b) and 56(c), in which the spectra of the TAPS input and output, respectively, are measured on a spectrum analyzer.

Applying multiple input signals to the TAPS system inputs demonstrates the transform - inverse transform performance for the cases that are used to show

Input

300 nsec Pulses at 165 MHz

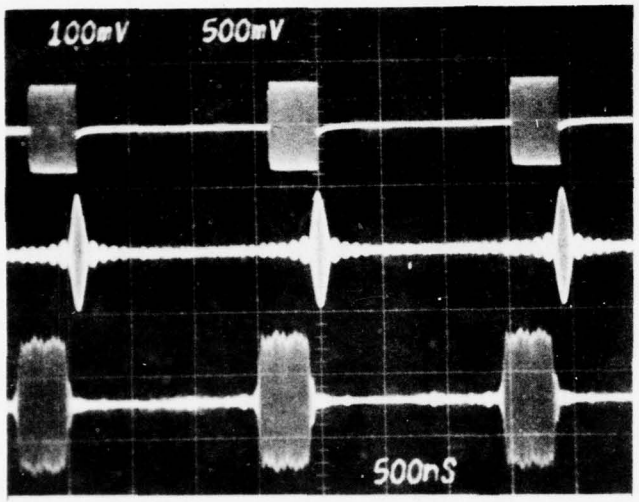

Input

Chirp Transform

TAPS Output

1 μsec/Div

(a)

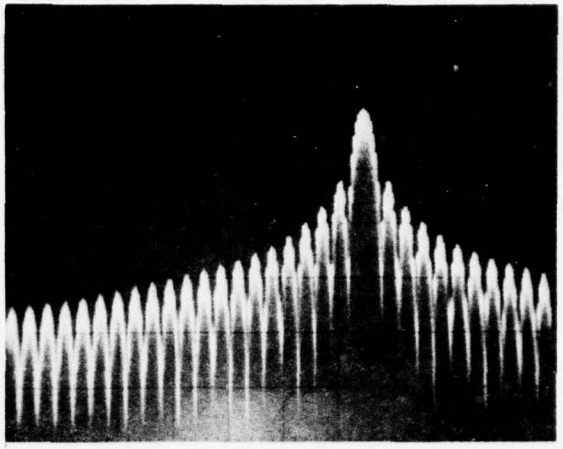

(b) Input Spectrum

150 MHz
10 MHz/Div

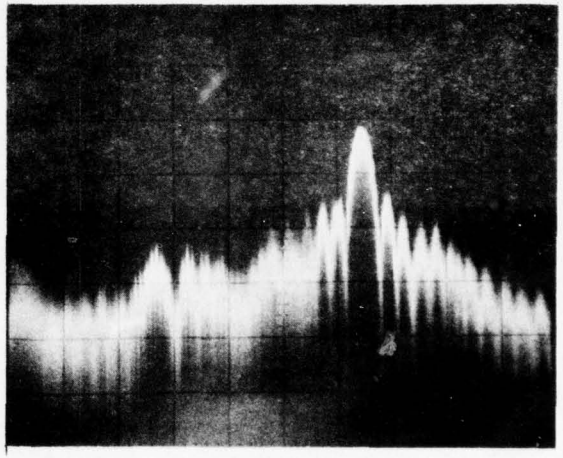

(c) TAPS Output Spectrum

Figure 56 Chirp Transform-Inverse Transform Performance

the filtering capability of the processor. Figure 57(a) shows simultaneous input time signals at 134 MHz and 168 MHz with 800 nsec and 200 nsec pulse widths, respectively. The middle trace is the chirp transform, and the bottom trace is the output, corresponding to a TAPS passband width of 50 MHz. Figures 57(b) and (c) show the pulse spectrum before and after processing through TAPS. Figure 58 demonstrates a third instance of simultaneous signals, which, in this case, are not coincident in time and only occur in alternate transform intervals. These pulses are centered at different frequencies with different widths also (140 MHz and 160 MHz pulses with 0.5 μsec and 0.2 μsec widths, respectively). Comparable performance is achieved over the full range of TAPS parameters.

The actual filtering performance of the prototype system fully demonstrates the validity and realizability of this programmable filtering approach. The results which follow demonstrate the system's operation both in bandpass and bandstop roles. For this demonstration, two sets of pulses are used as before for the input signal: the first pulse train has 0.8 μsec widths at 134 MHz and the second 0.2 μsec widths at 168 MHz. This input signal is shown in the top trace of Figures 59(a) and 60(a). Figure 57(b) shows the spectrum of the two-tone pulsed input signal measured on a spectrum analyzer. The second trace of Figures 59(a) and 60(a) is the now-familiar chirp transform of the input signal repeated every 1.9 μsec with the transform of each successive interval of the input signal. To implement a bandpass filter, the modulation function, or gate, is simply turned off except when the desired frequency components of the transform are present in time. The third trace of Figure 59(a) shows the modulated transform data for the case where the 0.8 μsec pulse train at 134 MHz is passed and all other frequencies are rejected. Since the transform repeats each 1.9 μsec, the gate must also be activated every 1.9 μsec to remove the shorter pulses from every interval of the signal. The final trace of Figure 59(a) is the output of the prototype following the inverse transform of the modulated transform trace. The short pulses are clearly rejected, and the desired longer pulses are correctly passed and reconstructed, completing the demonstration of the bandpass characteristics of the prototype system. Further

INPUT

800 nsec Pulses at 134 MHz and 200 nsec Pulses at 168 MHz

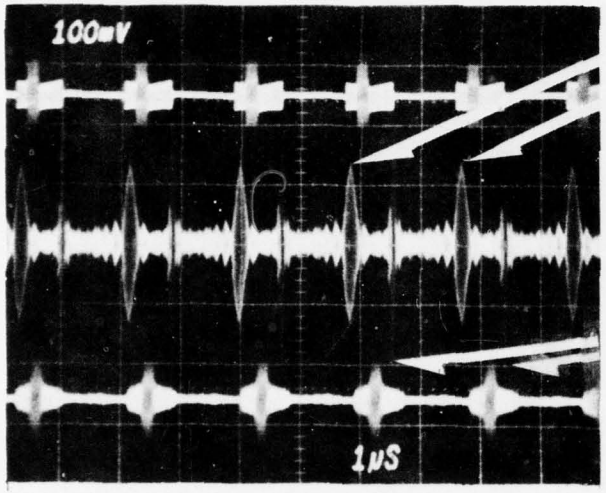

Input

Chirp

TAPS Output

Peak of 200 nsec Pulse Transform

Peak of 800 nsec Pulse Transform

1 μsec/Div

(a)

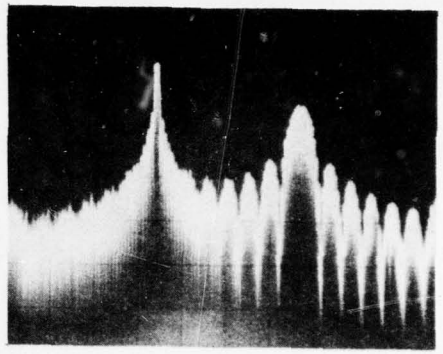

(b) Input Spectrum

150 MHz
10 MHz/Div

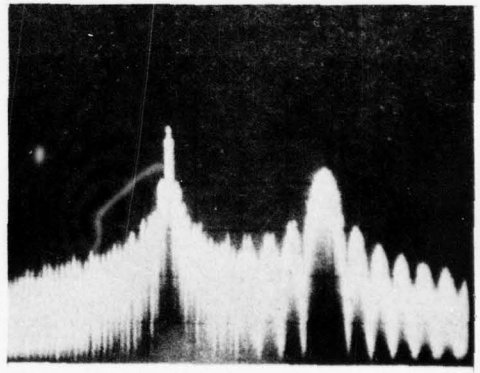

(c) TAPS Output Spectrum

Figure 57 Chirp Transform-Inverse Transform Performance

INPUT

500 nsec Pulses at 140 MHz and 200 nsec Pulses at 160 MHz

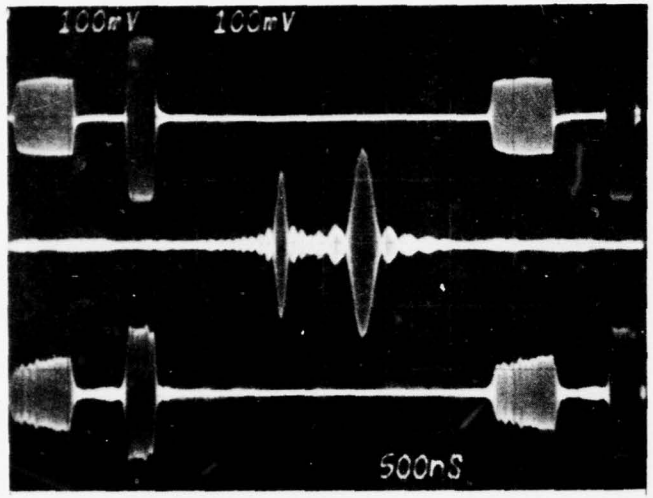

1 μsec/Div

(a)

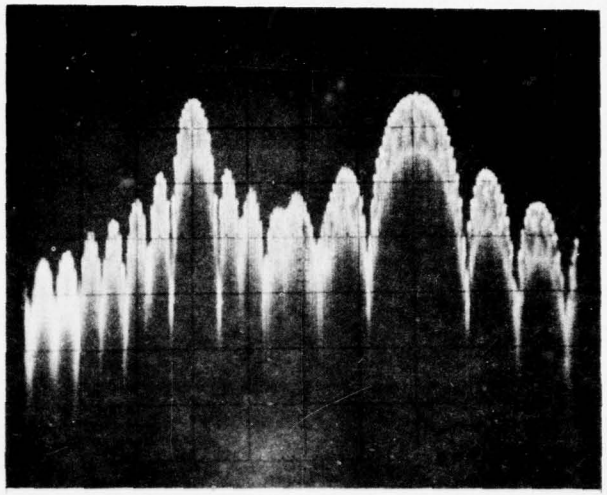

(b) Input Spectrum

150 MHz
5 MHz/Div

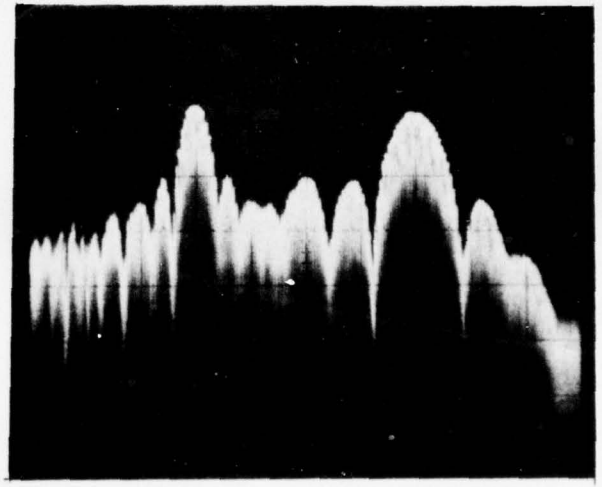

(c) TAPS Output Spectrum

Figure 58 Chirp Transform-Inverse Transform Performance for a Two-Channel System

INPUT

800 nsec Pulses at 134 MHz and 200 nsec Pulses at 168 MHz

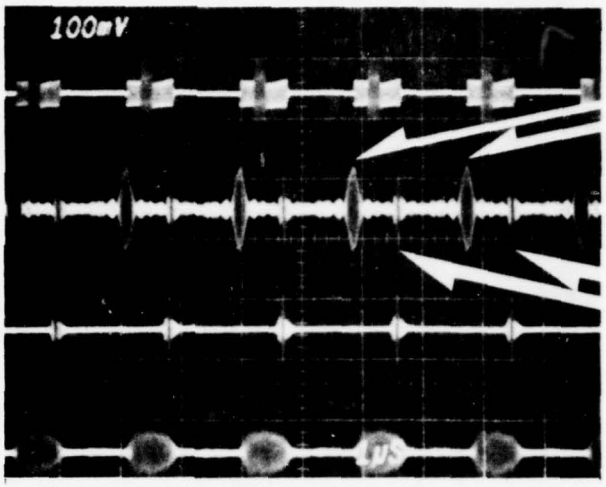

1 μsec/Div

(a)

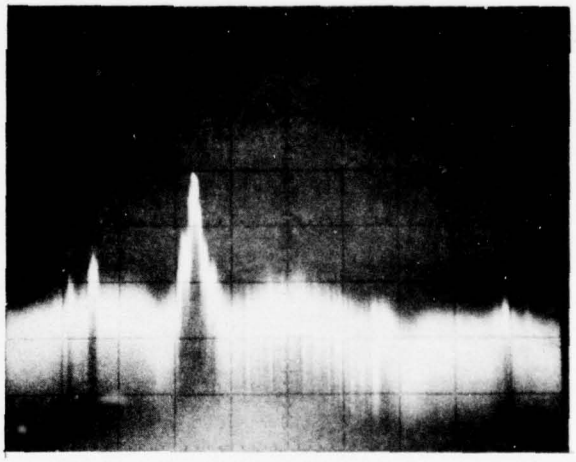

150 MHz
5 MHz/Div

(b) TAPS Filtered Output Spectrum

Figure 59 Response of the TAPS Prototype System Implementing a Bandpass Filter to Pass the 0.8 μsec Pulses at 134 MHz

INPUT

800 nsec Pulses at 134 MHz and 200 nsec Pulses at 168 MHz

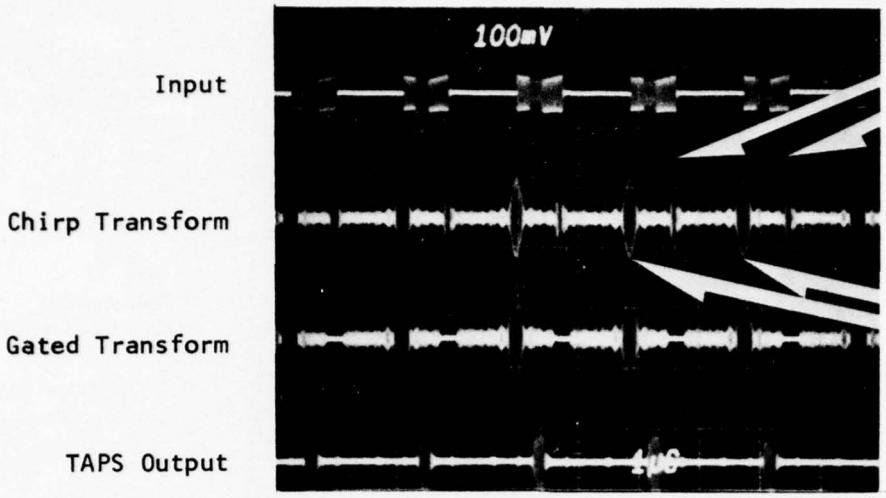

1 μsec/Div

(a)

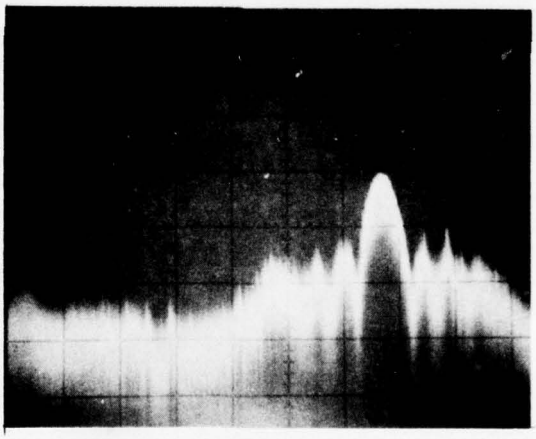

150 MHz
5 MHz/Div

(b) Input Spectrum

Figure 60 Response of the TAPS Prototype System Performing Bandstop Filtering to Reject the 0.8 μsec Pulses at 134 MHz

confirmation that only the longer pulses have been passed is shown in the TAPS output spectrum analyzer photograph of Figure 59(b). Comparison to the input spectrum of Figure 57(b) shows that the frequencies corresponding to the narrower pulses at 168 MHz have been rejected and the output signal possesses the spectral character of the 134 MHz pulses.

Alternatively, one might wish to reject the longer pulses at 134 MHz and pass all other frequencies. This would be implemented by turning off the gate only during the time corresponding to the frequency components of the 134 MHz pulses as shown in the third trace of Figure 60(a). The inverse transform in the last trace shows that only the narrow pulses of the two sets are passed and properly reconstructed by the inverse transform. That more than 40 dB of rejection has been obtained against the offending frequencies is demonstrated by comparison of the spectrum of the output in Figure 60(b) with that of the input in Figure 57(b).

Figures 61 and 62 demonstrate that better spurious behavior can be achieved by employing a two-channel system as described earlier. In continuous operation spurious responses from adjacent transform intervals can be eliminated by alternating between these two channels. TAPS demonstrates the effectiveness of this technique by employing input signal pulse trains that are present only in alternate intervals of the chirp transform, as was the case in Figure 58. Figure 61(a) shows the dual input pulse train, the chirp transform, the bandpass filtered transform, and the reconstructed output time signal. The pulses are 0.5 and 0.2 μsec pulses at 140 and 160 MHz, respectively. They repeat each 3.8 μsec, or twice the chirp transform interval of 1.9 μsec. The filtered spectrum for this bandpass implementation is shown in Figure 61(b) and confirms that the 0.5 μsec pulses at 140 MHz have been passed as desired [see the last trace of Figure 61(a)]. The complementary bandstop operation is demonstrated in Figures 62(a) and (b), where the 140 MHz signal is rejected as desired, reconstructing the 0.2 μsec pulses that lie at 160 MHz, outside the stopband of the adaptable filter.

INPUT

0.5 μsec Pulses at 140 MHz and 0.2 μsec Pulses at 160 MHz

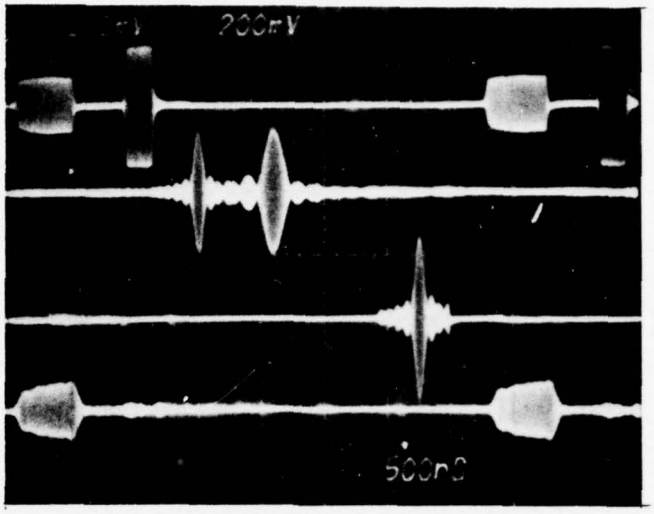

(a)

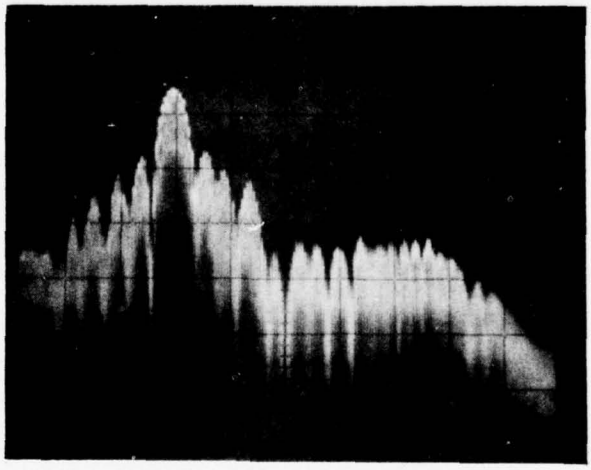

150 MHz
5 MHz/Div

(b) TAPS Filtered Output Spectrum

Figure 61 Bandpass Filtering with TAPS to Pass 140 MHz Signals as in a Two-Channel Transform System

INPUT

0.5 μsec Pulses at 140 MHz and 0.2 μsec Pulses at 160 MHz

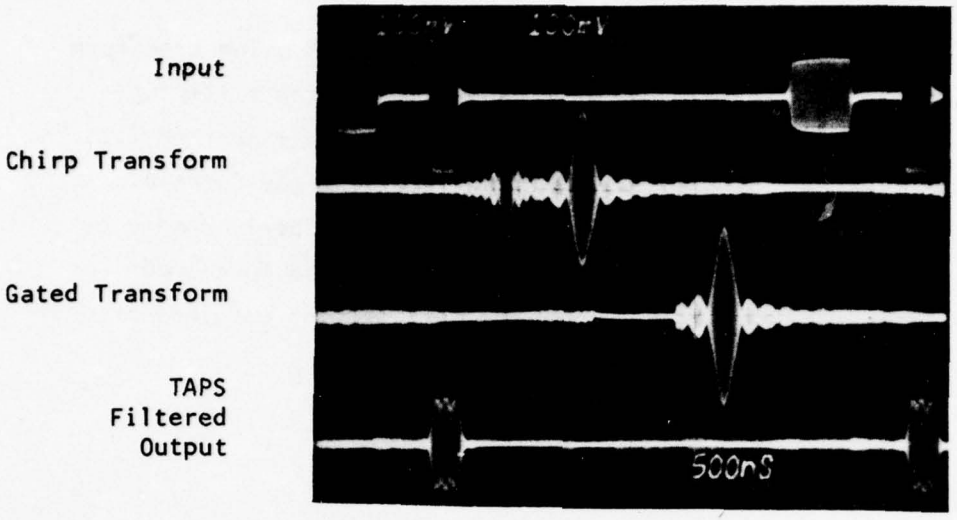

(a)

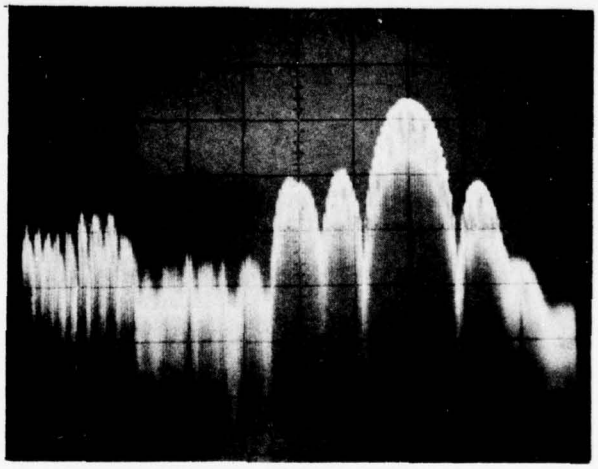

150 MHz
5 MHz/Div

(b) TAPS Filtered Output Spectrum

Figure 62 Bandstop Filtering with TAPS to Reject 140 MHz Signals as in a Two-Channel Transform System

The prototype results demonstrate the effectiveness of using transform processing to provide continuously variable bandpass/bandstop filtering. The desirability of improving the insertion loss of the SAW linear FM filters, employing longer chirp lengths utilizing RAC (Reflective Array Correlator) technology, and configuring two channels in parallel to properly handle cw signals, has been shown as well. Other applications portend more important results for signal processing, however, and the next section examines programmable matched filtering and prewhitening.

SECTION V

TRANSFORM PROGRAMMABLE MATCHED FILTERING AND PREWHITENING

TI's demonstrated ability to perform the accurate transform of signals can be utilized to implement a programmable matched filter with greater versatility than other approaches. The system to perform a general correlation function is shown in Figure 63(a). The need for programmable PSK filters exists in developmental spread spectrum systems and some existing PSK communication systems. The programmable feature is important because the coded waveforms used in these systems are almost never fixed, but vary over a wide range of possible codes, permitting multi-user access. The standard tapped delay line adaptive filter approach can perform this type of filtering, provided the chip rate is an integral submultiple of the reciprocal of the intertap time delay and other technological obstacles can be adequately overcome. However, if the chip rate is arbitrary, the fixed tap spacing can lead to significant filter response degradation in spite of the variable phase and amplitude control theoretically available at each tap. In contrast, the Transform Adaptable Processing System handles all possible chip rates within its bandwidth with equal ease, because the transform technique gives the equivalent of continuously variable tap spacing.

The transform approach to programmable matched filtering is discussed and supported with numerous simulations. A laboratory prototype is described, and its results clearly establish feasibility for matched filtering, programmability, and prewhitening, an important additional advantage for the Transform Adaptable Processing System.

A. Programmable Matched Filter Description

The usual implementation of the matched filter operation takes the form of Figure 63(b). The output of the filter is the convolution of the input signal s(t) with the impulse response of the filter h(t):

$$o(t) = s(t) \ast h(t) \quad .$$

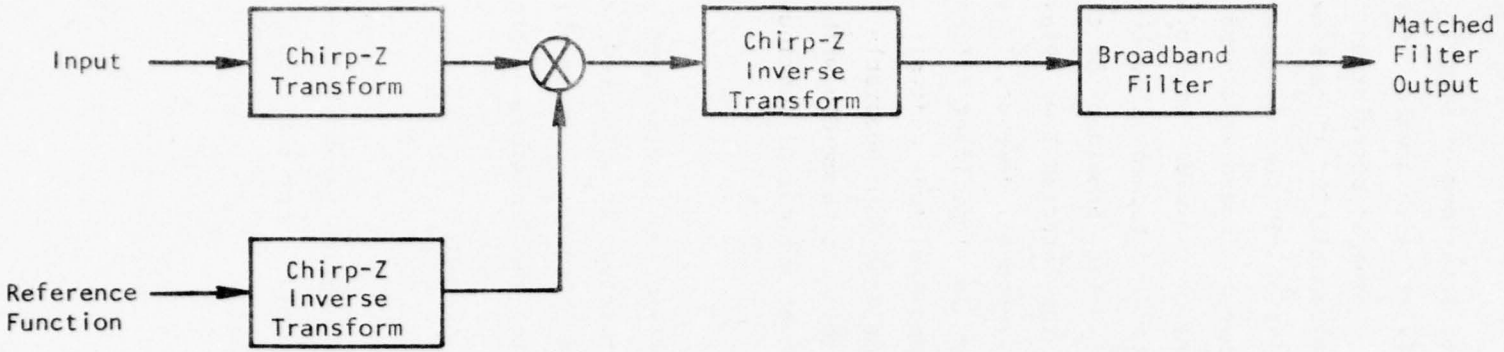

(a)

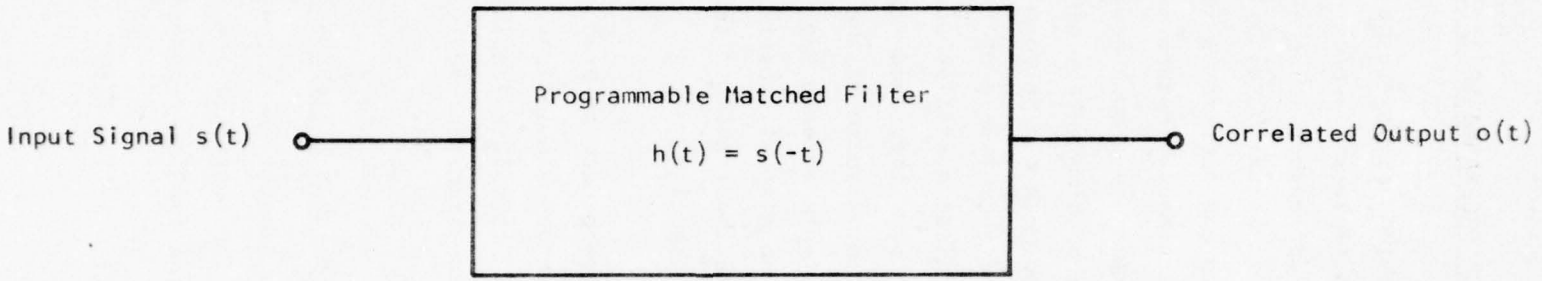

(b)

Figure 63 (a) Transform Programmable Matched Filter to Produce the Correlation of the Input Signal with the Reference Function. (b) Conventional Matched Filter.

When the filter response is the time-reverse of the input signal, the signal is matched and the correlated output exhibits the processing gain of the code. However, the surface wave chirp-z transform [Figure 63(a)] enables this operation to be performed by a simple multiplication in the frequency domain. That is, from transform theory, convolution in the time domain is the equivalent of frequency domain multiplication,

$$O(w) = S(w)\ H(w) \quad .$$

The correlated output is then given by the inverse transform of that product:

$$o(t) = F^{-1}[O(w)] = F^{-1}[S(w)\ H(w)] \quad .$$

The surface wave chirp-z transform provides the real-time transform of the time signals such that with the configuration of Figure 63(a) a more flexible and powerful processing system is now possible. Thus, a variable filter can be made by transforming the input and a reference signal to the frequency domain, mixing the signals to obtain a product, and transforming back to the time domain. If a transformer is used on both the input and the reference, the output is the convolution of the two signals. If the reference signal is the time reverse of the input signal, the output is the desired correlation.

Alternative configurations are possible with accompanying simplifications for specific cases. The implementation shown in Figure 63(a), in contrast to the analog programmable matched filters that utilize nonlinear convolvers, does not require a time-inverted reference to obtain correlation. Had a transform rather than an inverse transform been used on the reference, a time-reversed reference would be needed. If an inverse transform, rather than a transform, is used on the reference channel, the reference spectrum is inverted in time, and the output is the correlation of the input and the reference. This effect is a consequence of the inverse transform of a PSK signal being equivalent to the transform of a time inverted version of that signal. The same result can be

obtained by taking the conjugate of the transform of the reference, but this method requires an extra mixing process. Nonetheless, to most effectively utilize existing hardware, this approach was selected for feasibility demonstration.

Simulations were performed to demonstrate the validity of this approach. The system of Figure 63(a) is simulated by multiplying and convolving the appropriate surface wave chirp device impulse responses. The system simulated provides a bandwidth in excess of 50 MHz with a center frequency of 150 MHz and utilizes 1.2 μsec blocks of data. The 50-chip code whose envelope is shown in Figure 64(a) (a 50-chip section randomly selected from an all-day code) was used as input signal and reference. This is merely an arbitrary example of the type of real signal that might be processed by a programmable matched filter. The output of the transform adaptive processor is shown in Figure 64(d). The correlation is nearly equal to the ideal correlation of Figure 64(b), and the difference is no more than the effects of the finite bandwidth of the system smoothing the sharp peaks of the ideal PSK correlation. In addition, the spectrum of the signal is available at the output of the first transform unit and is plotted in Figure 64(c). A second example included here is the simulation of the familiar Barker code of length 13. Figures 65(a) and 65(b) show the signal spectrum and system correlation achieved through the use of the Transform Adaptable Processing System, exhibiting 13:1 correlation gain, 13:1 peak-to-sidelobe ratio, and the expected correlation waveform.

To further demonstrate the superior flexibility of the transform approach over competing programmable techniques, a linear FM signal was used in exactly the same system. Figure 66(a) shows the magnitude of the spectrum of the linear FM input that is available at the output of the first chirp-z transform unit. The transform processor correlation output is plotted in Figure 66(b). No weighting is included on the reference signal, and the compressed pulse

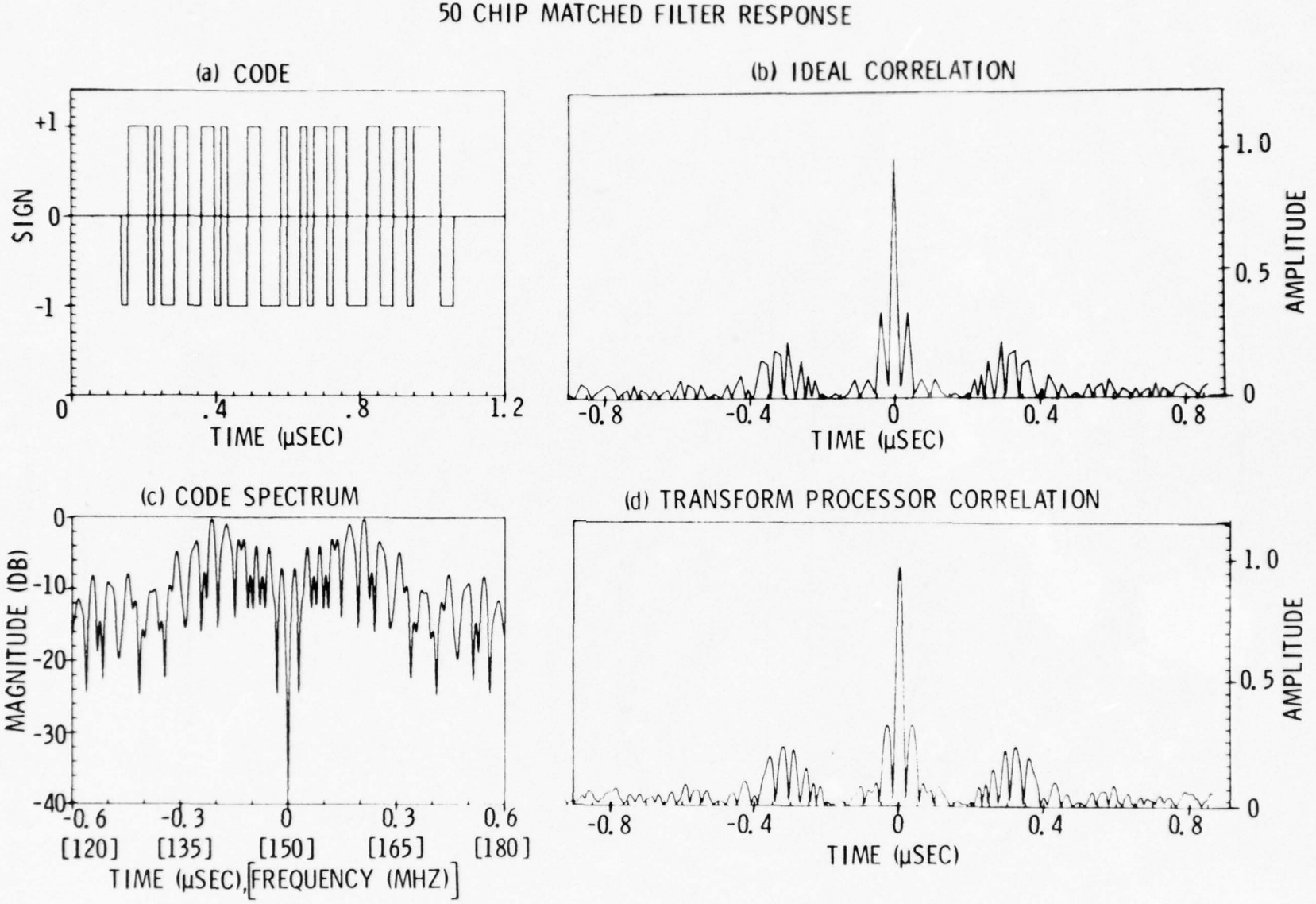

Figure 64 Simulation of the TAPS Programmable Matched Filter for an Arbitrary 50-Chip Sequence from a Longer Code

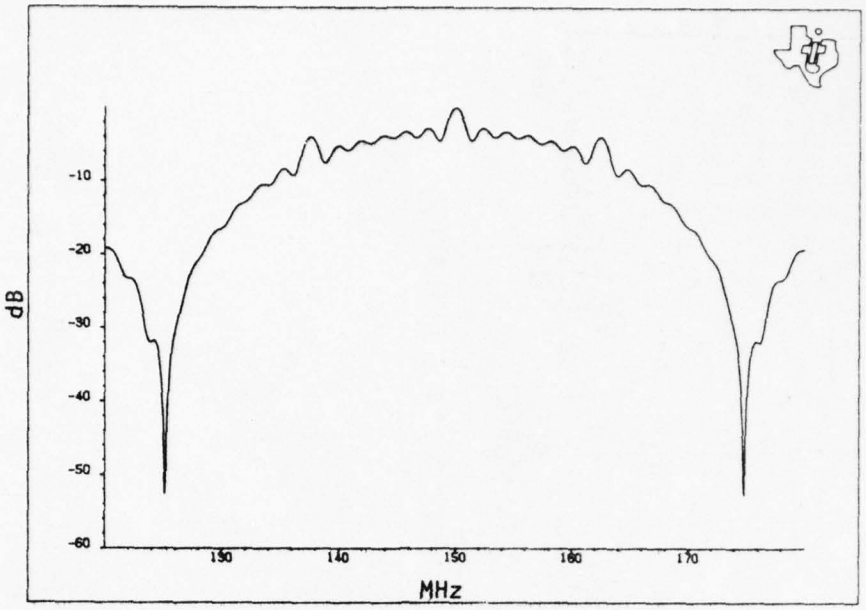

(a) Barker Code Transform

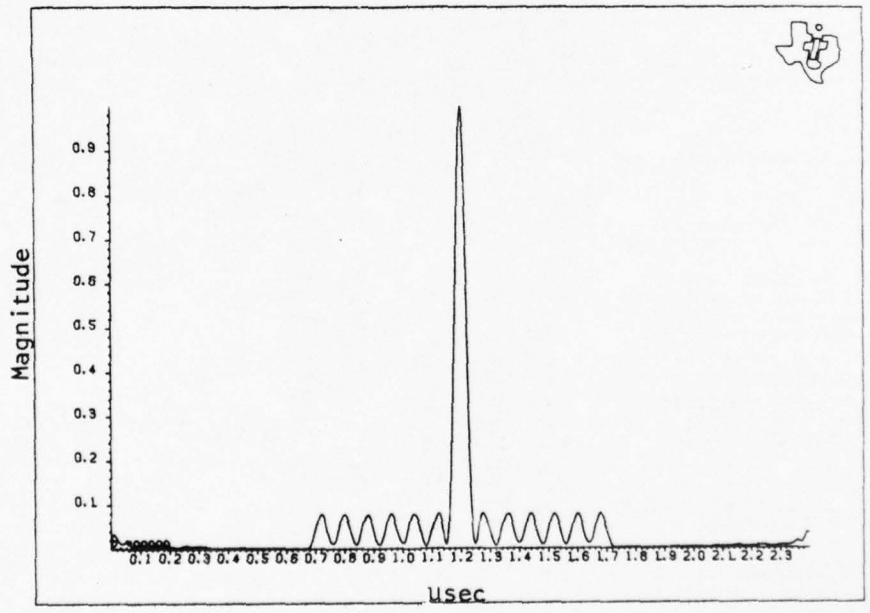

(b) Transform Processor Correlation

Figure 65 Simulation of the Transform Programmable Matched Filter for a Barker Code of Length 13

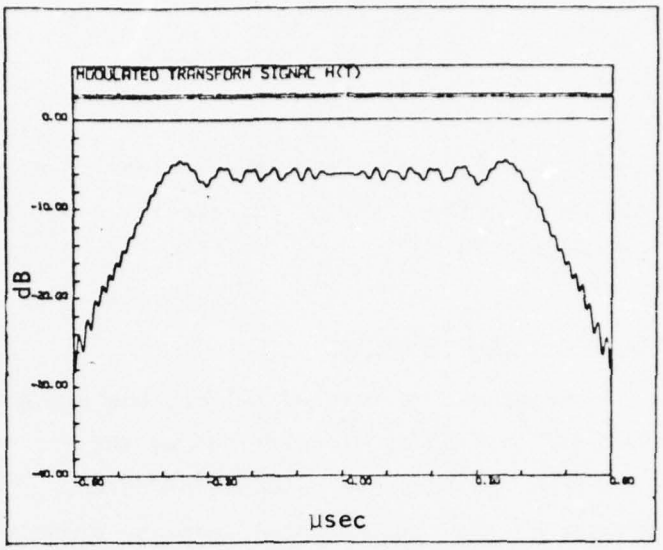

(a) Transform of the Linear FM Input

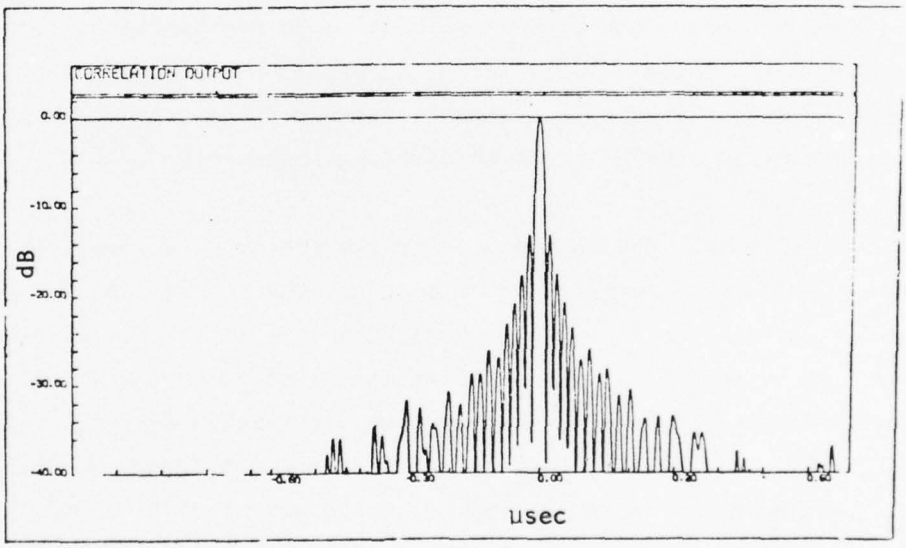

(b) Transform Processor Correlation

Figure 66 Simulation of the Transform Programmable Matched Filter for a Linear FM Waveform

sidelobe level of -13 dB is achieved as expected. Clearly, no other programmable approach can perform the range of correlation available with the Transform Adaptable Processor System.

B. Prototype Programmable Demonstration

To demonstrate the programmable matched filter, the signal transform and the inverse transform in Figure 63(a) are provided by the Transform Adaptable Processing System delivered for adaptive bandpass/bandstop filtering. The reference channel transform, the time-reversal, and the product of the two transforms must be performed with a separate breadboard. Figure 67 diagrams the additional hardware required in conjunction with the Transform Adaptable Processing System noted above to do general correlation. The same components are used as those designed for TAPS. The breadboard configured here can perform matched filtering for signals with up to 30 MHz bandwidth (or chip rate) and 0.96 μsec length. These restrictions do not apply for systems designed specifically for the programmable matched filter, however, but are accepted to establish feasibility with existing components.

The examples shown here to demonstrate the concept are inputs of 13-chip Barker codes and several rectangular rf pulses. The correlation of two rectangles is, of course, a triangle whose base-line is the sum of the lengths of the two rectangles. A succession of rf pulses of different widths is used as the signals and references to the programmable matched filter. Figures 68(a), (b), (c), (d), and (e) show the input in the top trace and the correlated output in the bottom trace for 150 MHz pulse widths of 0.6, 0.5, 0.3, 0.1, and 0.05 μsec, respectively. Similar results are achieved for any frequency between 135 MHz and 165 MHz, as predicted. Figure 68(f) shows the transform of the 500 nsec rf pulses compared to (sin x/x) ideally and the correlated spectrum which is nearly $(\sin x/x)^2$ as required for the triangle's spectrum.

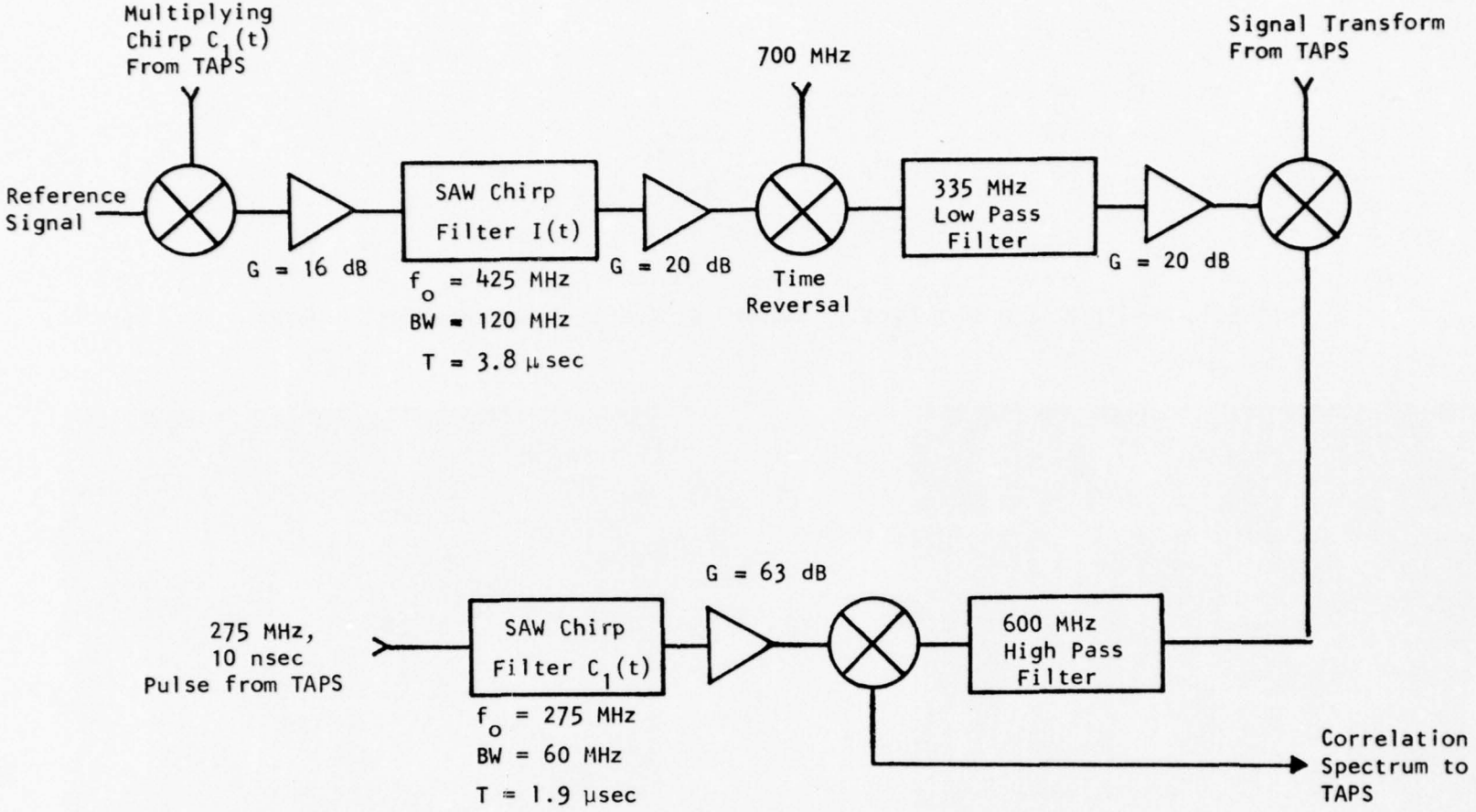

Figure 67 Hardware for Programmable Matched Filter in Addition to the TAPS Adaptive Filter

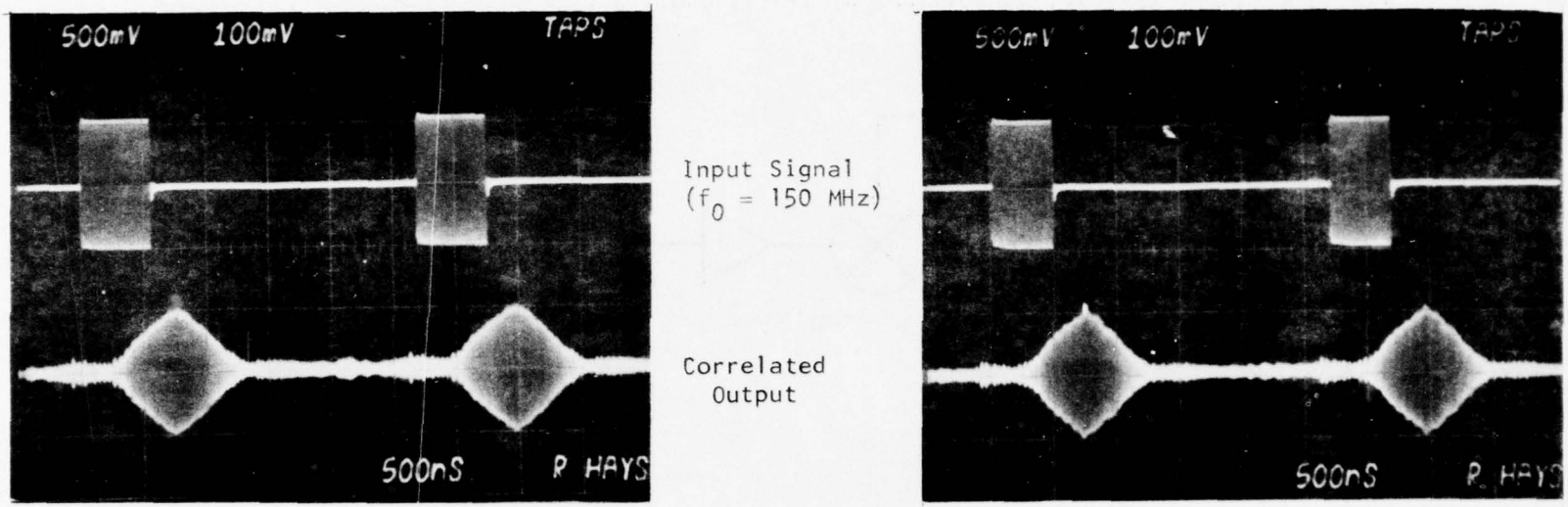

(a) (b)

Figure 68 Correlation of Rectangular RF Pulses for Widths of 0.6, 0.5, 0.3, 0.1, and 0.05 μsec

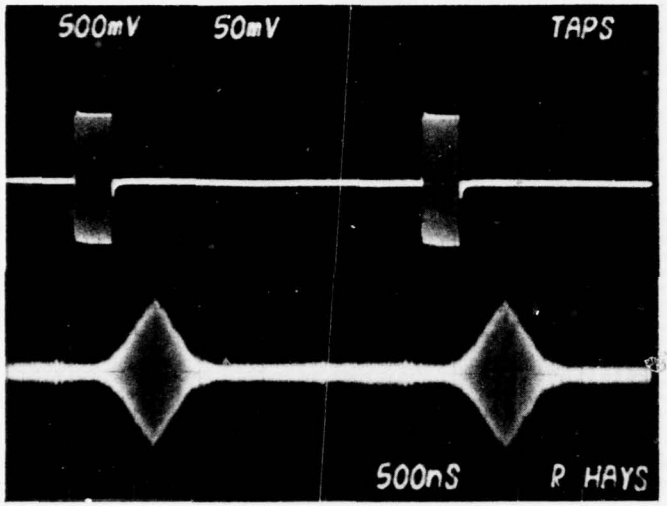

(c)

Input Signal
(f_0 = 150 MH:

Correlated
Output

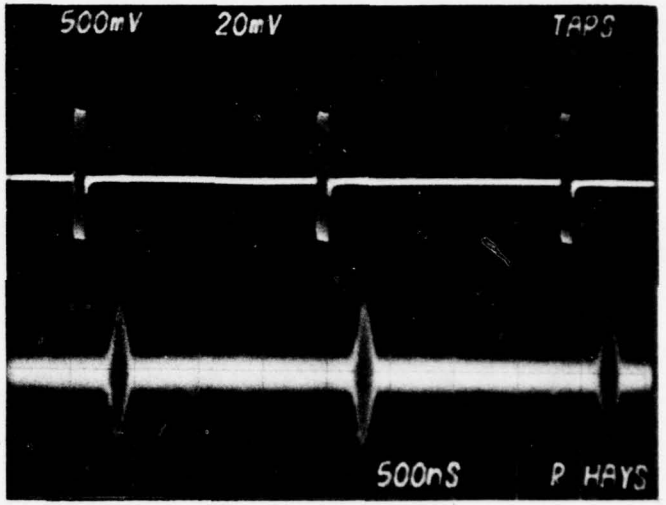

(d)

Figure 68 (continued)

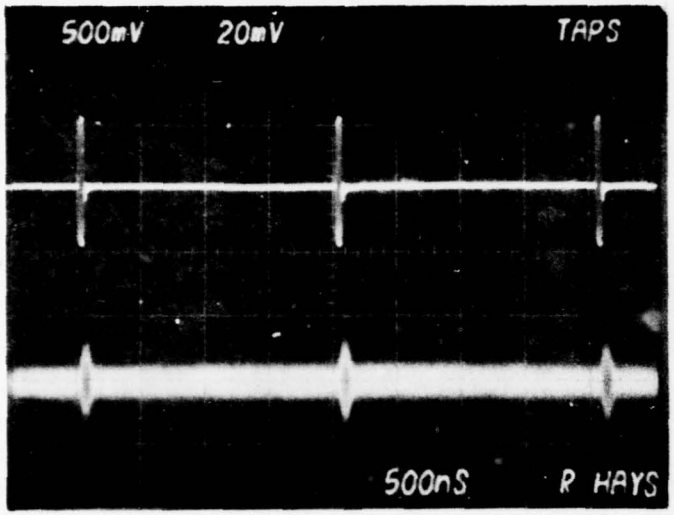

Input Signal
(f_0 = 150 MHz)

Correlated
Output

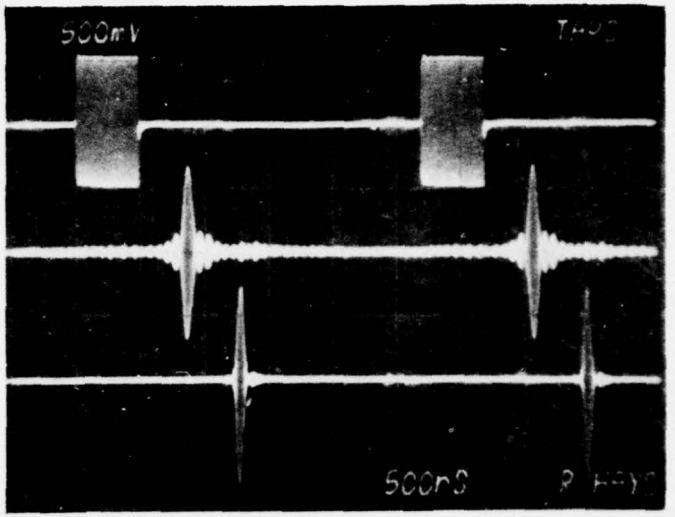

(e)

(f)

Figure 68 (continued)

The Barker codes of length 13 are more representative of coded waveforms required in spread spectrum systems. For this example the bandwidth (or chip rate) and signal time length are reciprocally related, with their product equaling 13. The example codes used have bandwidths of 8 MHz and 26 MHz and corresponding time lengths of 1.63 μsec and 0.5 μsec. Figures 69(a) and (b) show the familiar triangular main-lobe of the PSK codes, while Figure 69(c) shows the code transform. The pulse width varies inversely with the bandwidth, and the correlated null-to-null pulse widths measure 260 nsec and 80 nsec, very near the ideal. The sidelobe level is degraded by 2:1 by spurious responses from adjacent intervals adding constructively at certain times. These results demonstrate the validity of the approach as desired.

C. Prewhitening

The availability of the signal spectrum with the chirp transform approach leads to an important additional advantage for TAPS programmable filters. Narrowband interference is a common problem in spread spectrum systems, and accurate operation often requires taking corrective action, a heretofore difficult task in friendly environments and even less successful under hostile circumstances. A simple clipping operation on the chirp transform often suppresses narrowband interference sufficiently to enable continued system operation.

Two examples of cw interference with PN code input are shown in Figure 70. In 70(a) the spectrum of an input signal consisting of the PN code plus a cw interference source with amplitude equal to that of the code is shown. The frequency of the interference was chosen to correspond to the largest frequency response in the code spectrum. Thus, the examples shown represent a worst case for the effect of cw interference. Comparison of this spectrum with the pure code spectrum in Figure 64(c) shows the distortion introduced in the frequency range from 135 to 145 MHz. The correlation of this input

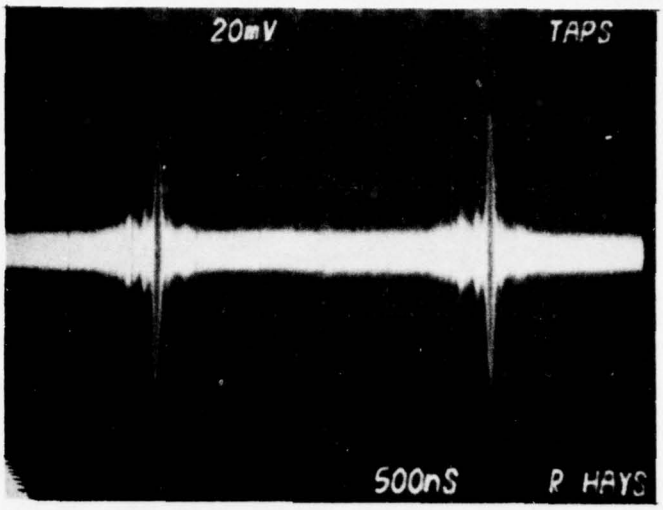

(a) B = 26 MHz, T = 0.5 μsec

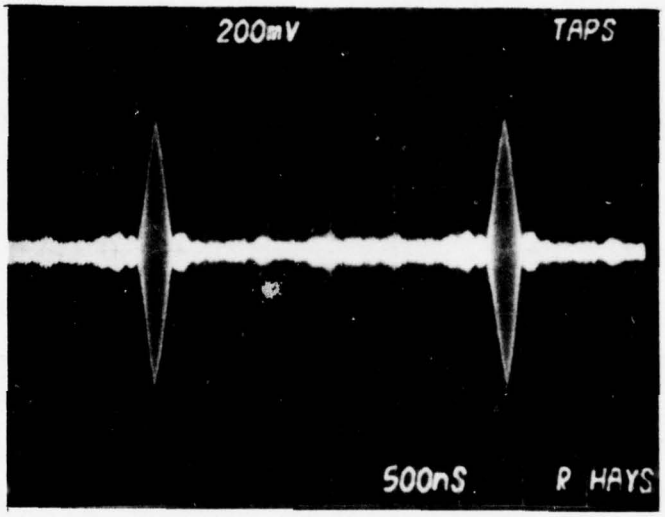

(b) B = 8 MHz, T = 1.63 μsec

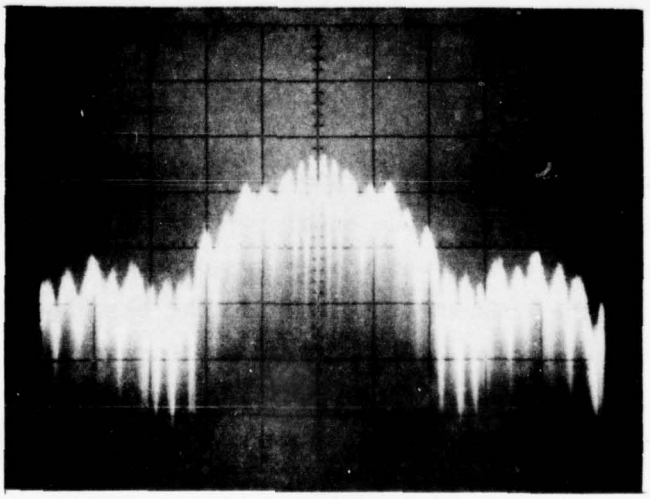

(c) Transform of Code (a)

Figure 69 Correlation of Barker Codes of Length 13

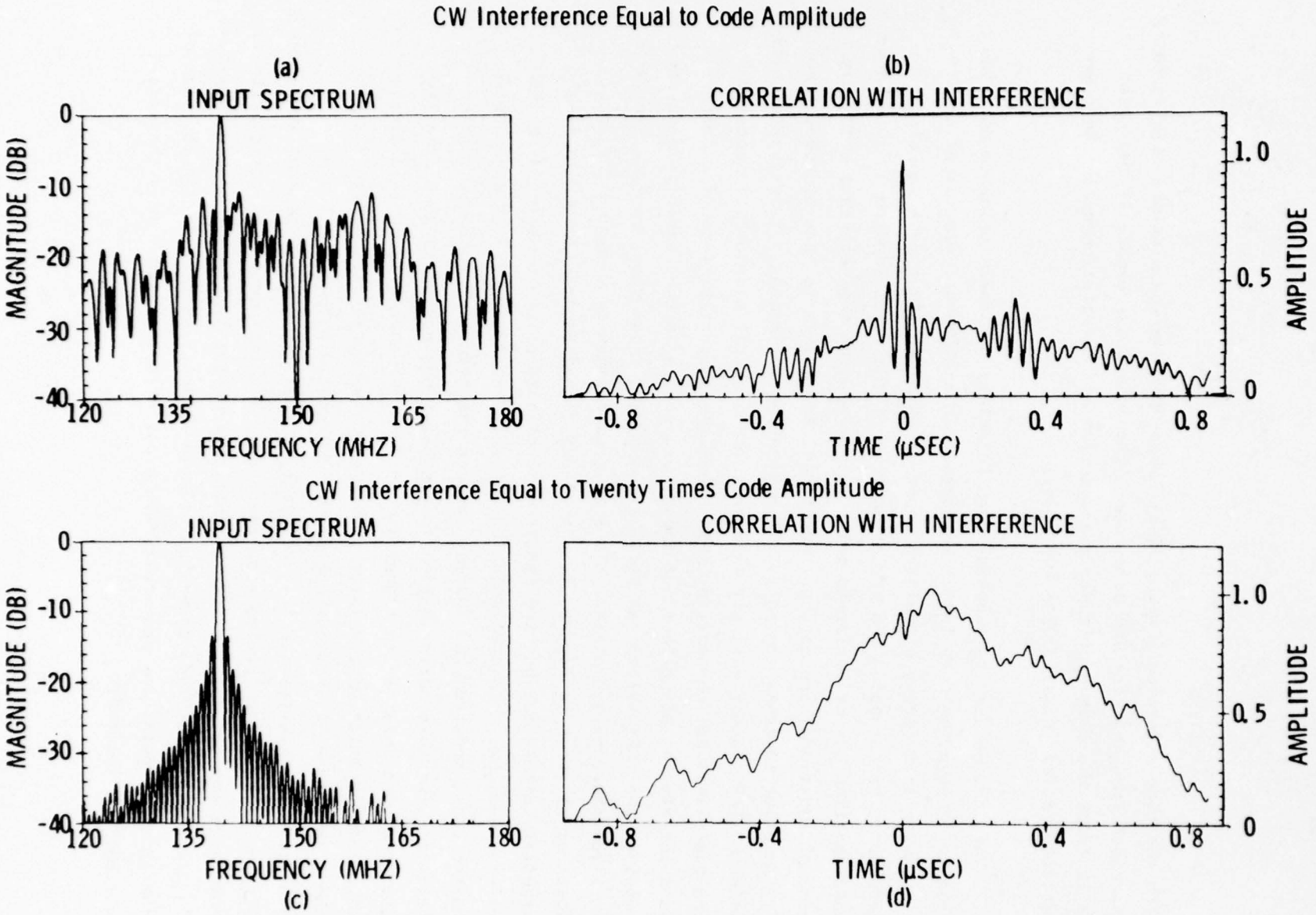

Figure 70 Simulation of the TAPS Programmable Matched Filter with cw Interference Equal to the Code Amplitude and Equal to Twenty Times Code Amplitude

with the code reference [Figure 70(b)] shows the average sidelobe level greatly increased from that for the pure code. When the interference is increased to 20 times the code amplitude, the spectrum and correlation of the code are entirely masked [Figure 70(c) and 70(d)].

TAPS can be used to suppress such interfering signals prior to correlation to improve the correlation response. If the characteristics of the narrowband interfering signal are known in advance, its effect can also be reduced by bandstopping the proper section of the input spectrum. This bandstop function can be performed prior to mixing with the reference with only minimal additional processing. For fixed, known interference sources, a notch filter prior to transforming is the most effective remedy. Bandstopping after entering TAPS cannot entirely eliminate the spectral sidelobes introduced by the time-limiting inherent in TAPS. When the characteristics of a narrowband interfering signal are not known, or hostile jamming exhibits frequency hopping, the TAPS system can still clean up the input spectrum sufficiently to allow the code processing. This is accomplished by clipping the input spectrum as shown in Figure 71. The input signal is transformed as in the standard correlator, but the spectrum is clipped prior to mixing with the reference signal. This clipping effectively removes any large contributions to the input spectrum and thereby reduces the effect of narrowband interference. For this approximation to prewhitening, no knowledge of the frequency of the interfering signal is required. The results of this simple clipping operation on the interference examples considered previously are shown in Figure 72. Comparison of the correlated output for the equal amplitude cw interference [Figures 70(b) and 72(b)] shows a general improvement in peak-to-sidelobe level across the band. The improvement in correlation is much more obvious for the case of interference twenty times the code amplitude. Figures 70(d) and 72(d) show that clipping brings the correlation peak out of the noise. Again, the peak-to-sidelobe ratio is improved across the entire correlation interval.

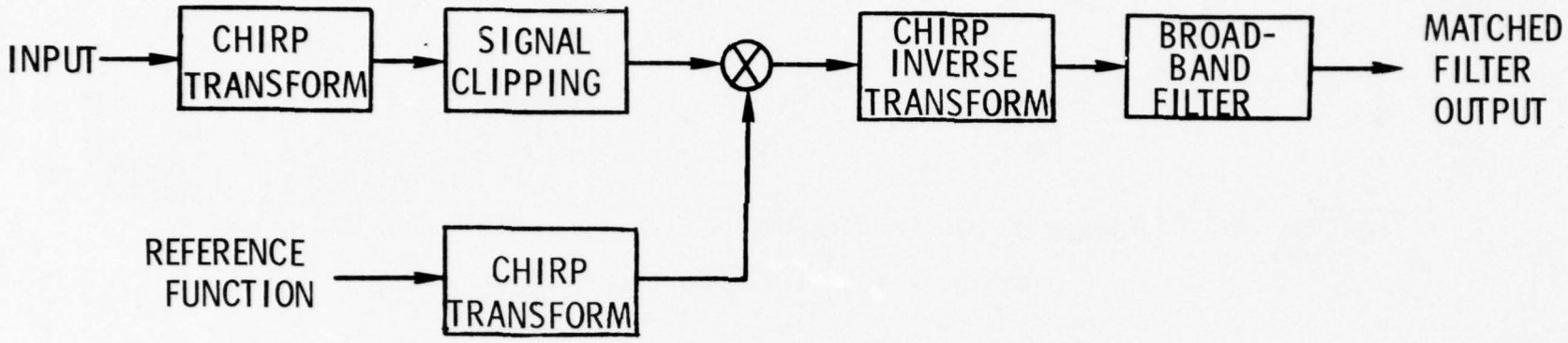

Figure 71 Chirp Transform Programmable Matched Filter with Suppression of Narrowband Interference by Transform Clipping to Approximate Spectral Prewhitening

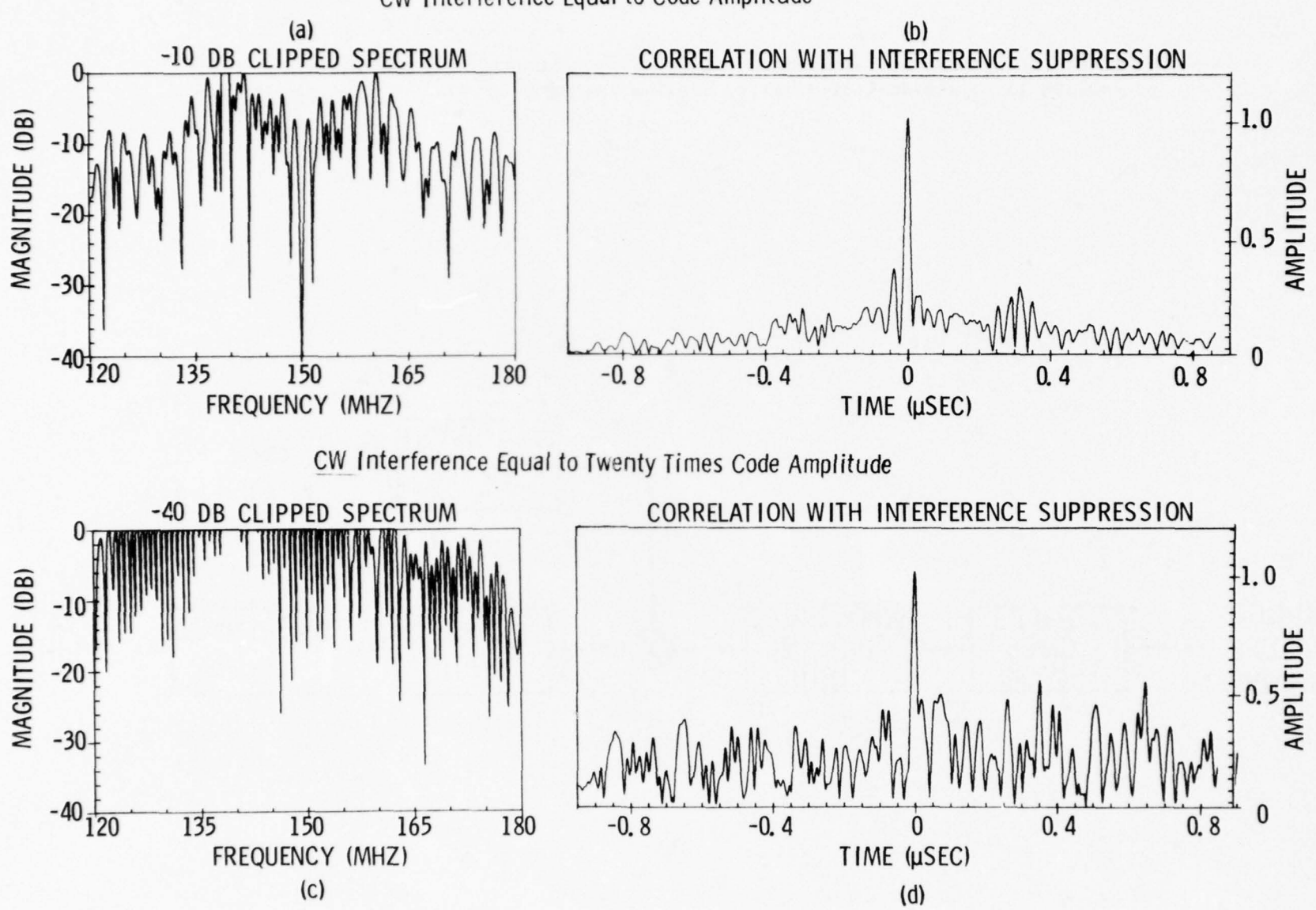

Figure 72 Simulation of the TAPS Programmable Matched Filter With cw Interference Suppressed by Transform Clipping

These two examples demonstrate that even in the worst case of narrowband interference of unknown or varying frequency, incorporating a simple clipping function which approximates prewhitening into the TAPS correlator suppresses the interference in the input spectrum. In other cases, the gating function provided by the adaptable bandpass/bandstop filter effectively removes much of the interference. The latter case is best suited to friendly environments, however, when the jamming signal will not have changed frequency by the time corrective action has been taken. (Introducing additional delays can circumvent this problem.) Other techniques of correction might be implemented after examining the real-time transform of the input signal as noted previously. Clearly, code processing can be significantly improved through the use of transform processing.

Many spread spectrum systems may employ codes that are too long to permit use of the transform programmable matched filter. The prewhitener, fortunately, can be used regardless, with the matched filtering performed by some other method. For this application, the transform configuration is the same as that of the TAPS bandpass/bandstop filter (Figure 73) with the filter modulation function prescribed to gate out the interfering terms or the clipping operation substituted for the gate shown in Figure 73. To demonstrate prewhitening, this configuration was used. The clipping was performed by varying the signal level into a low-power amplifier which saturated on the large narrow spectral components of the interference. Figure 74(a) shows a correlated PSK signal with cw interference whose amplitude is larger than that of the coded signal by the 13 dB correlation gain. Figure 74(b) shows nominally a 6 dB improvement in visibility of the correlation peak with spectral clipping. The range of this demonstration is limited by the saturation technique used, but feasibility is established, and significantly greater improvements are possible with better clipping and AGC. The final prewhitening demonstration is performed using the gating technique in which the small portion of the spectrum containing the narrow-band interfering term is rejected by a switch and the remaining spectral code information is correlated. Figures 75(a) and (b) show the

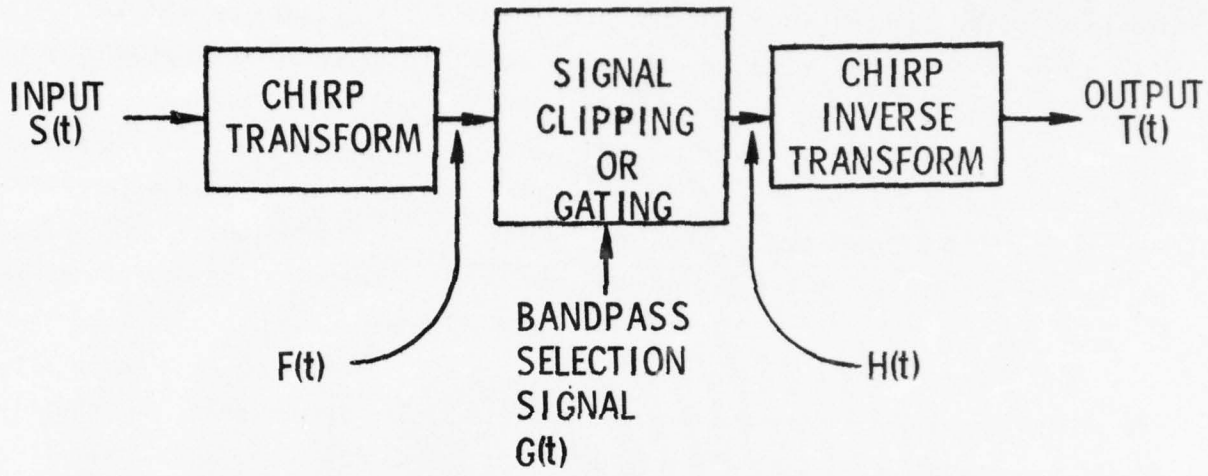

Figure 73 Configuration to Perform Prewhitening (But Not Matched Filtering)

Without Prewhitening

With Prewhitening

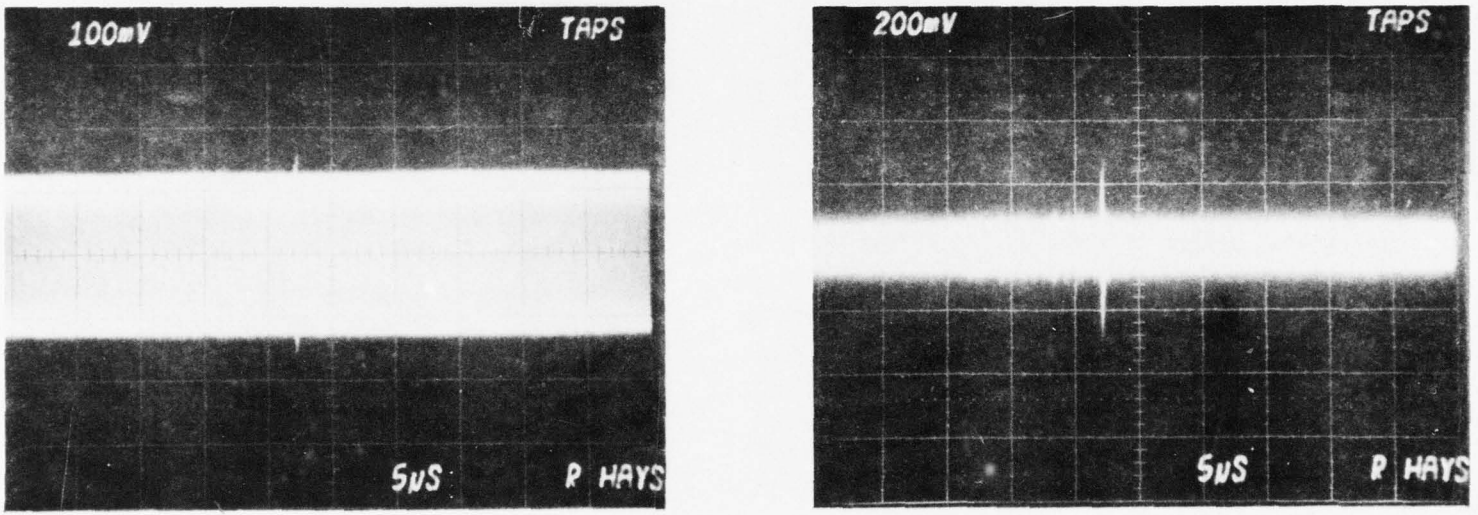

(a)

(b)

Figure 74 Prewhitening by Limiting the Interference Spectral Components at the Transform

Without Prewhitening

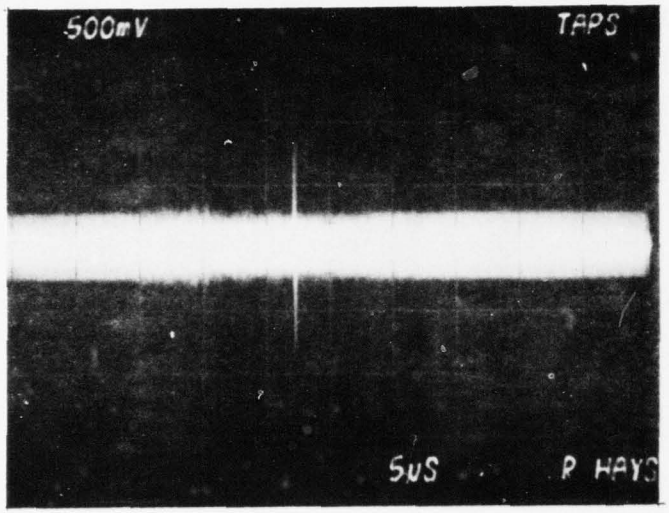

(a)

With Prewhitening

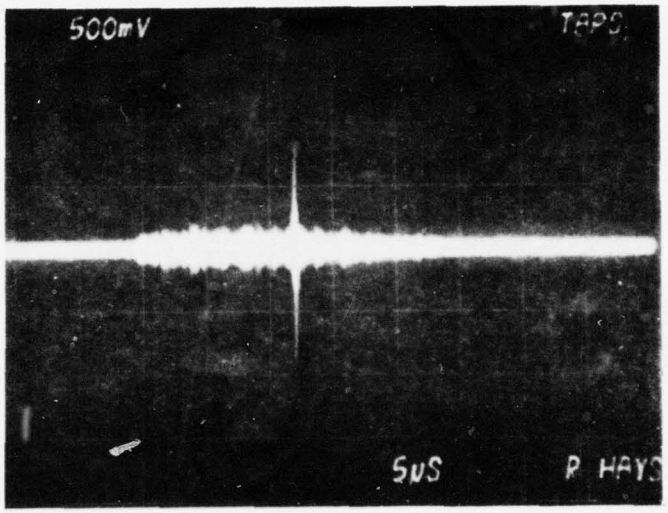

(b)

Figure 75 Prewhitening by Rejecting the Interfering Frequencies at the Transform

correlation without prewhitening and with prewhitening performed by this gating approach. Again, the improvement is more than 6 dB, and transform techniques for prewhitening are convincingly demonstrated.

D. Asynchronous and Continuous Operation

The transform system has been described as processing short rf signal blocks. However, the system very easily processes continuous input signals, since it automatically divides the signal into short time blocks, sequentially processes each signal block separately, and finally sums the processed signal blocks to obtain the desired continuous processed output. Thus, while this technique operates in a radically different manner from the classic programmable Kallmann filter approach, it provides the identical filter function.

For the programmable matched filter this allows asynchronous operation with the restriction that the reference signal cannot exceed the transform time block dimensions (1.9 μsec). However, the input signal S(t) to be correlated can partially span two neighboring time intervals rather than requiring synchronous operation. The reference signal must be repeated for each subsequent time block such that the convolution of the reference signal with each portion of the input signal then occurs in adjacent time blocks. These two convolution output signals overlap one another in time, and they have the property that the sum of these two outputs is exactly the desired asynchronous matched filter correlation response. This is illustrated in Figure 76. The code in the first case falls within only the first time block $s_1(t)$, and the operation is as already described. The correlated output with the reference function is given by:

$$o(t) = s_1(t) * h(t) \quad ,$$

where $s_1(t) = s(t)$. In the second case the signal s(t) is divided into two

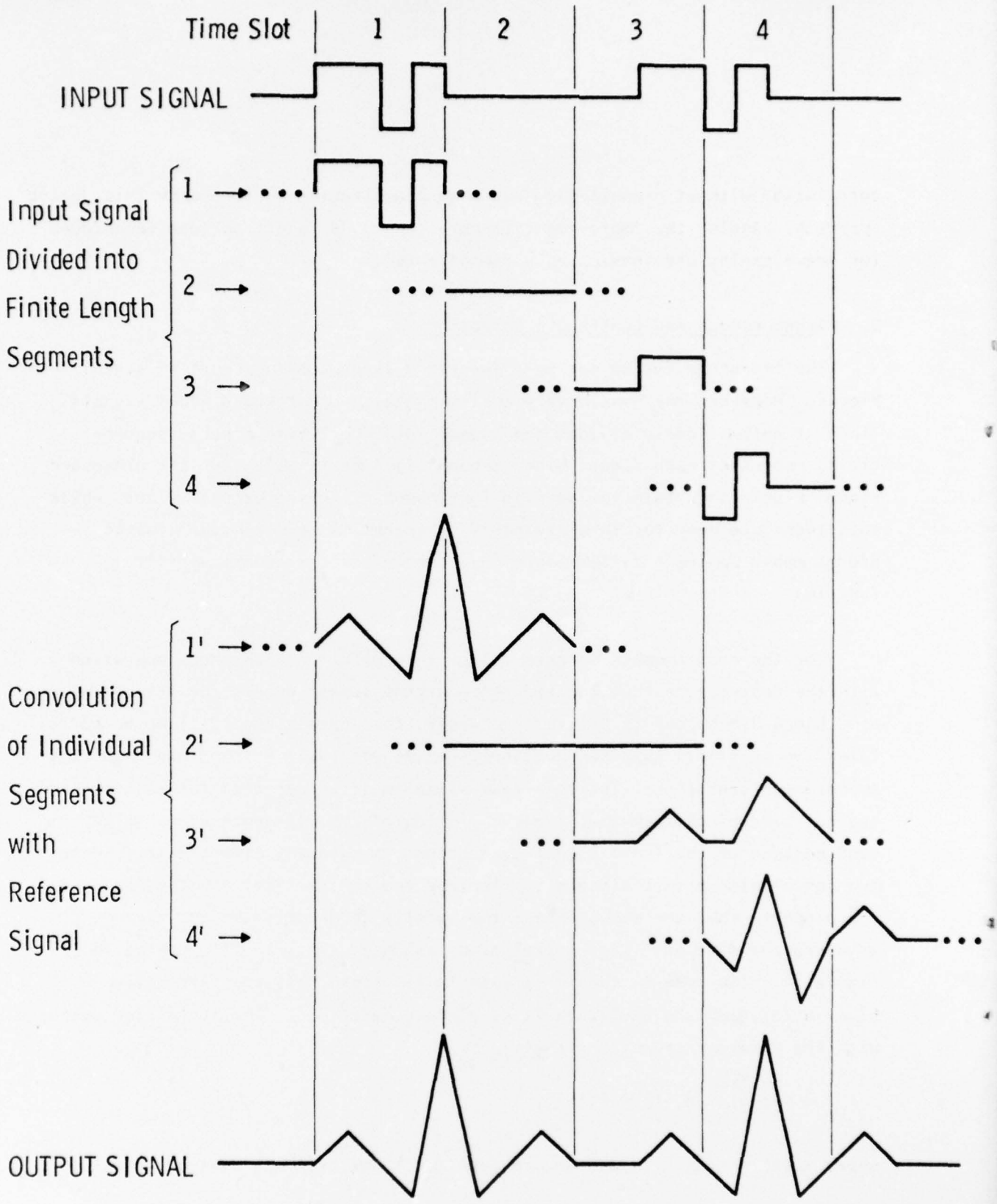

Figure 76 Continuous Signal Processing by Processing Finite Time Length Segments

pieces, or two time intervals:

$$s(t) = s_3(t) + s_4(t) \quad .$$

As already described, $s_3(t)$ is correlated with the reference signal, as is the next time interval, $s_4(t)$. The output of the transform processor is also in sequential time blocks:

$$o_3(t) = s_3(t) \ast h(t)$$

$$o_4(t) = s_4(t) \ast h(t) \quad .$$

The key to achieving continuous operation is, then, no more than summing these signals, since superposition holds and convolution is distributive.

$$o(t) = o_3(t) + o_4(t)$$

$$= s_3(t) \ast h(t) + s_4(t) \ast h(t)$$

$$= [s_3(t) + s_4(t)] \ast h(t)$$

$$o(t) = s(t) \ast h(t) \quad .$$

That this summation takes place can be viewed in terms of the summing by the convolving chirp electrodes of the two signals that are simultaneously within the convolving filter. As shown in Figure 76 and described earlier, the correlation output for the single block of data in interval 3 and the reference is contained accurately in intervals 3 and 4 of the output, since the correlation must be twice as long as the convolving intervals. Similarly, interval 4 is correlated to the reference and is contained in intervals 4 and 5 of the output. The time interval they have in common must be summed to produce the correct correlation, as shown in the arithmetic discussion, and

since this can never exceed two intervals, or $2\Delta T$, then the summing will occur within the convolving chirp, which is $3\Delta T$ long. A second possibility is to operate two parallel channels for the inverse transform and simply sum the two alternating outputs in a resistive or some other network.

This type of operation makes timing errors more critical to performance than does operation of the transform adaptable bandpass/bandstop filter. In the matched filter case, small errors in the timing of successive intervals can cause the correlation for successive intervals to add sufficiently out-of-phase to seriously degrade signal-to-noise improvement and peak-to-sidelobe levels. This represents an area of needed development to ensure that timing accuracies sufficient to maintain correlator performance are achieved. A similar problem exists for the case of prewhitening without matched filtering, as just described. In this instance, also, the successive intervals must experience similar phase shifts to avoid performance degradations. On the other hand, these problems are obviously not insurmountable, as demonstrated by the following results. The input signal is a 128 length PSK waveform with 10 MHz bandwidth and 12.8 μsec length (Figure 77). This requires seven transform intervals of 1.9 μsec each to pass the code through the transform, prewhitening, and inverse transform. The code is correlated in a surface wave matched filter. Figure 77(a) shows the correlated output without the intervening transform processor. Figure 77(b) shows the equivalent correlated output for the case in which the code is transformed and inverse-transformed piecewise in seven successive transform time blocks prior to the correlation. The compressed pulses are similar in each case with a 3 dB pulse width of nominally 80 nsec and compressed pulse sidelobes of 23 dB over the entire convolution of 25.6 μsec. The feasibility of prewhitening for long codes is established with this demonstration of correlation for long codes and the earlier prewhitening results.

Matched filter output

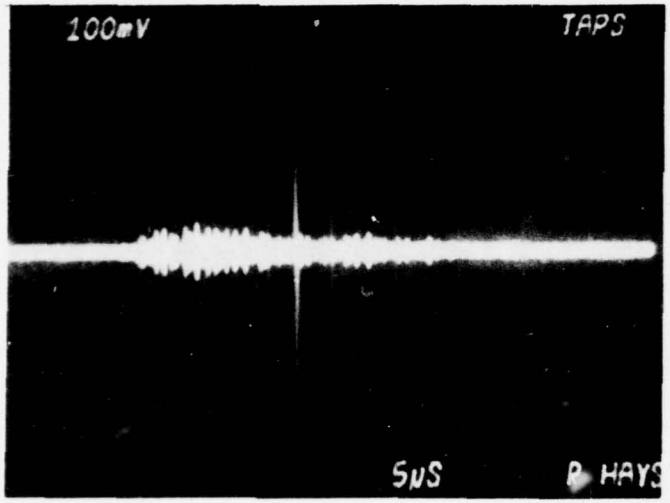

(a)

Matched filter output
after transform-inverse
transform operation

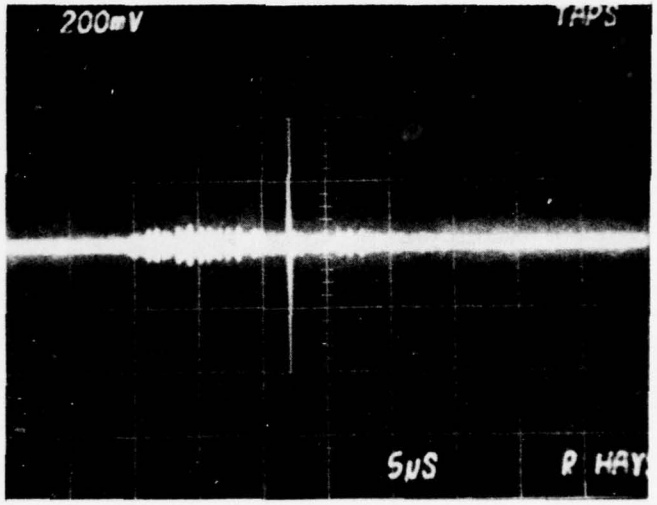

(b)

CODE

T = 12.8 μsec
B = 10 MHz
N = 128

Figure 77 Correlation After Transform Processing Required for Prewhitening Long Codes

E. Summary and Comments on Needed Development

There are numerous possible configurations for the transform programmable matched filter and prewhitener. The choice of whether to inverse-transform the reference signal or follow a transform with a mixer for time reversal is but one of the choices to be made. Others include whether to accept reference data at rf as is the case for the received signal or to input the reference at baseband via digital storage techniques. Figure 78 shows one possible programmable filter using SWD chirp transforms. The figure is divided into the four primary functions of the programmable matched filter: the signal transform, the reference transform, the frequency multiplication, and the inverse transform. The convolving chirp in the inverse transform for programmable matched filtering must be three times the time length of the block processing time interval in order to inverse-transform the correlated signal, which is twice the length of the reference. The selection of the best system architecture depends on the specific application, the spurious behavior of the mixers and amplifiers, control of timing errors, and other design considerations.

Among the several important areas of needed development for these programmable PSK filters are timing errors, spurious responses, and the accuracy of linear FM surface wave filters for large BT systems. The timing errors manifest themselves most particularly for continuous, or asynchronous, operation where variations in the timing of pulses to excite the multiplying chirp devices can interfere with the addition of successive time intervals to produce good correlation results as discussed previously. These can partially be alleviated by implementing the necessary delays in the surface wave chirp filters, but temperature effects and other sources of error may require difficult compensation and control techniques. Spurious responses due to harmonics and undesired products in the mixers must be considered to configure the system. The time intervals on either side of

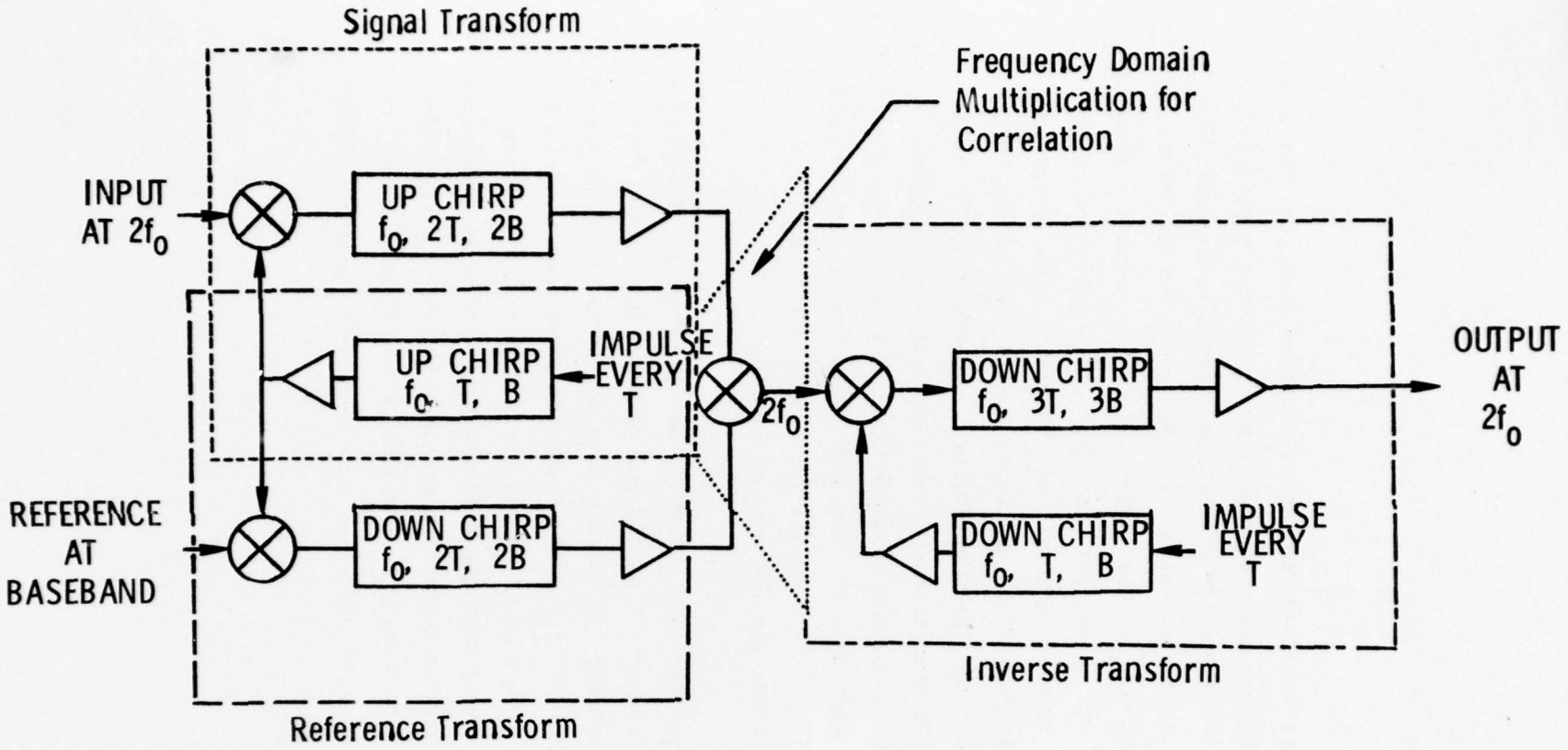

Figure 78 Chirp Transform Programmable Matched Filter Prototype

the desired time block that accurately represents the transform contains sidelobes of other chirp convolutions and multiplications. These are obviously within the succeeding time intervals, as distortion in continuous operation and appropriate design must secure suitable sidelobe levels for satisfactory operation. Implementation of surface wave chirp filters is currently capable of delivering between 30 dB and 40 dB spurious levels, and achieving better than that depends on more accurate and expensive synthesis. The insertion loss of the SAW components is one of the principal limitations of the transform processor, although even with low-power mixers, dynamic range in excess of 40 dB can be achieved. The mixers themselves represent a troublesome component in the role of providing multiplication of two time signals that vary in amplitude as do PSK code spectra. Nevertheless, realization of good results for a programmable PSK filter is relatively straightforward, but study and refinements are appropriate for most system uses.

In summary, with state-of-the-art components and the promise of significant technological spin-offs, a more flexible and powerful processing system can be configured for programmable PSK filters than would otherwise be available. The programmable matched filter with prewhitening has been described and feasibility established with simulations and prototype results. Even systems that require codes longer than those that can be easily attained with SAW components can benefit from the transform approach to prewhitening and correlation of long codes after transform - inverse transform processing has been demonstrated, despite the time segmentation of the code by the transform operation.

SECTION VI
CONCLUSIONS

An acoustic adaptive transversal filter based on a novel transform processing technique has been developed and demonstrated. This approach has capabilities far beyond those of previous SAW programmable filters; simultaneously, it circumvents many serious fabrication difficulties associated with various conventional tapped delay line methods of achieving variable response. Not only does the prototype developed under this contract perform continuously tuned, programmable filtering for adaptable bandpass/bandstop applications, but it also enables the performance of many important new signal processing functions such as prewhitening for spread spectrum systems.

In addition to the fabricational simplicity, there are several other important advantages of the Transform Adaptable Processing System. First, this approach uses standard SAW technology and thus automatically benefits from SAW technology advances. The competing techniques use specialized technologies that have limited use elsewhere. Second, in addition to adaptive filtering, TAPS can provide the frequency spectrum of the input signal. This spectral information is needed in many systems applications of an adaptive filter. For example, when an adaptive filter is used to cancel unwanted interference in a wideband communications system due to friendly or jamming transmitters, the frequency spectrum of the interfering signals may first need to be measured so that the proper programming information for the adaptive filter can be calculated. The TAPS system provides this spectrum information with no additional hardware, whereas additional hardware and processing time would be needed to obtain this vital information with a programmable Kallmann filter. Thus, TAPS not only provides all the filter functions of a classic adaptive filter, but it also has the additional capability of providing the spectral information needed in many systems that use adaptive filters. For some cases, simple, effective, antijam measures can be implemented by only adding a clipper after the transform to the frequency domain; no additional complexity for characterizing the interfering signal in frequency, etc., is necessary.

The use of SAW linear FM filters, mixers, and amplifiers to perform the chirp transform has been demonstrated. This is the basic building block of the transform processing approach to variable response filters. The transform of numerous signals in the 120 to 180 MHz band has been accurately performed along with its mathematical and heuristic description. The experimental model delivers this accurate spectral information in real-time and has led to the investigation of other signal processing applications such as in radar Doppler processing in conjunction with time compression and in EW systems.

The principal objective of this contract was met with the demonstration and delivery of the Transform Adaptable Processing System (TAPS) for continuously variable bandpass/bandstop filtering. This is achieved by simply modulating the time signal after the transform to pass or remove the desired frequency components and then inverse-transforming the modulated signal to produce the filtered time domain signal. Experimental results and numerous simulations have established design objectives and confirmed the effective filtering performance of the TAPS prototype for pulsed rf signals. The requirement for a two-channel parallel processor for cw filtering has been shown. The TAPS system can implement bandpass or bandstop filter bandwidths of nominally 1 MHz to 50 MHz between 120 and 180 MHz in virtually any combination of responses.

This accessibility of the input signal spectrum in real-time and the ease with which it can be modified to produce a variety of programmable filter responses led to the demonstration of other signal processing functions such as programmable matched filtering and prewhitening. This approach offers much greater versatility than other programmable approaches, since it can process a larger class of signals encompassing both PSK and FM signals within the same system. Of more importance, however, is the facility to suppress narrowband interference, a common problem in spread-spectrum system processing. This is achieved with simple clipping or adaptable filtering of the spectrum

made available by the chirp transform approach. The feasibility of employing transform techniques in these applications has been established through both simulations and completed breadboard results with the TAPS system.

The insertion loss of the SAW components is one of the principal limitations of the transform processor, although even with low-power mixers, dynamic range in excess of 40 dB was achieved. Among other important areas of needed development to improve TAPS are timing errors, spurious responses, and the accuracy of linear FM surface wave filters for large BT systems. The timing errors manifest themselves most particularly for continuous, or asynchronous, operation in programmable matched filtering or prewhitening, where variations in the timing of pulses to excite the multiplying chirp devices can interfere with the addition of successive time intervals to produce good correlation results. These can be alleviated by implementing the necessary delays in the surface wave chirp filters. Temperature effects and other sources of error may be corrected with lock-loop techniques for compensation and control. Spurious responses due to harmonics and undesired products in the mixers may be avoided in configuring the system, but the time intervals on either side of the desired time block that accurately represents the transform contains sidelobes of other chirp convolutions and multiplications. These are obviously within the succeeding time intervals, as distortion in continuous operation and appropriate design must secure suitable sidelobe levels for satisfactory operation. Implementation of surface wave chirp filters is currently capable of delivering between 30 dB and 40 dB spurious levels, and achieving better than that depends on more accurate and expensive synthesis. The mixers also represent a troublesome component in the role of providing multiplication of two time signals that vary in amplitude as do PSK code spectra. This problem also has been resolved, and realization of good results for programmable filters is relatively straightforward, requiring refinements appropriate to specific system uses.

The availability of spectral information in real-time clearly permits many important new signal processing applications. Although understanding the basic operating principles of the Transform Adaptable Processing System is more complex than is the case for a conventional programmable filter, its physical implementation is considerably simpler, since it consists of a small number of SAW chirp filters, mixers and amplifiers, and a timing generator. The capability of providing accurate transform information in real-time has been demonstrated, and prototype results for continuously variable bandpass/bandstop filtering, versatile programmable matched filtering, and prewhitening for suppression of narrowband interference evidence the power of the transform processing approach to many signal processing problems. This report has described this approach in detail and demonstrated its feasibility with extensive experimental results of the prototype Transform Adaptable Processing System.

REFERENCES

1. R. M. Hays, W. R. Shreve, D. T. Bell, Jr., L. T. Claiborne, and C. S. Hartmann, "Surface-Wave Transform Adaptable Processor System," Proceedings of the 1975 IEEE Ultrasonics Symposium, p. 363 (1975).

2. R. M. Hays, "SAW Transform Signal Processing," 1976 MTT-S International Microwave Symposium Digest, 292 (1976).

3. C. S. Hartmann and R. M. Hays, "Review of System Applications of Chirp-Z Transform Devices," 1976 Ultrasonics Symposium, Session G-1 (1976).

4. H. E. Kallmann, "Transversal Filters," Proc. IRE 28, 302 (1940).

5. R. M. Hays and C. S. Hartmann, "Surface Acoustic Wave Devices for Communications," Proc. IEEE 64, 652 (1976).

6. L. T. Claiborne, C. S. Hartmann, R. M. Hays, and R. C. Rosenfeld, "VHF/UHF Bandpass Filters using SAW Device Technology," Microwave Journal, 35 (May 1974).

7. H. M. Gerard, W. R. Smith, W. R. Jones, and J. B. Harrington, "The Design and Application of Highly Dispersive Acoustic Surface-Wave Filters," IEEE Trans. Microwave Theory Tech. MTT-21, 176 (1973).

8. J. D. Maines and E. G. S. Paige, "Surface-Acoustic-Wave Components, Devices and Applications," IEE Reviews 120, 1078 (1973).

9. D. T. Bell, Jr., J. D. Holmes, and R. V. Ridings, "Application of Acoustic Surface-Wave Technology to Spread Spectrum Communications," IEEE Trans. Microwave Theory Tech. MTT-21, 263 (1973).

10. L. A. Coldren and H. J. Shaw, "Surface-Wave Long Delay Lines," Proc. IEEE 64, 598 (1976).

11. H. G. Vollers and L. T. Claiborne, "RF Oscillator Control Utilizing Surface-Wave Delay Lines," Proceedings of the 29th Annual Frequency Control Symposium, 256 (1974).

12. R. M. Hays, Jr., "Switchable Multichannel Surface-Wave Devices," Final Tech. Report, ECOM Contract DAAB07-73-C-0094, December 1974.

13. R. M. Hays, R. C. Rosenfeld, and C. S. Hartmann, "Selectable Bandpass Filters - Multichannel Surface Wave Devices," Proceedings of the 1973 Ultrasonics Symposium, 456 (1973).

14. R. M. Hays, "A Surface-Wave Selectable Bandpass Filter System with 150 Addressable Channels," presented at the 1974 IEEE Ultrasonics Symposium, Paper 04 (1974).

15. E. J. Staples and L. T. Claiborne, " A Review of Device Technology for Programmable Surface-Wave Filters," IEEE Trans. Microwave Theory Tech. MTT-21, 195 (1973).

16. J. D. Maines, G. L. Moule, C. O. Newton, and E. G. S. Paige, "A Novel SAW Variable Frequency Filter," Proceedings of the 1975 Ultrasonics Symposium, 355 (1975).

17. G. R. Nudd and O. W. Otto, "Chirp Signal Processing Using Acoustic Surface Wave Filters," Proceedings of the 1975 Ultrasonics Symposium, 350 (1975).

18. T. M. Reeder and T. W. Grudkowski, "Real Time Fourier Transform Experiments Using a 32 Tap Diode Convolver Module," Proceedings of the 1975 Ultrasonics Symposium, 336 (1975).

19. W. E. Morrow, J. Max, J. Petriceks, and D. Karp, "A Real Time Fourier Transformer," MIT Lincoln Labs., Report No. 36G-4 (1963).

20. J. M. Alsup, "Surface Acoustic Wave CZT Processors," Proceedings of the 1974 Ultrasonics Symposium, 378 (1974).

21. J. M. Alsup, R. W. Means, and H. J. Whitehouse, "Real Time Discrete Fourier Transforms Using Surface Acoustic Wave Devices," International Specialist Seminar on Component Performance and Systems Applications of Surface Acoustic Wave Devices, IEE Conference Publication No. 109, 278 (1973).

22. M. Luukkala and G. S. Kino, "Convolution and Time Inversion Using Parametric Interactions of Acoustic Surface Waves," Appl. Phys. Lett. 18, 393 (1971).

23. J. H. Cafarella, W. B. Brown, E. Stern, and J. A. Alusow, "Acoustoelectric Convolvers for Programmable Matched Filtering in Spread-Spectrum Systems," Proc. IEEE 64, 756 (1976).

24. W. R. Shreve and G. S. Kino, "Strip Coupled Acoustic Convolvers," Proceedings of the 1973 Ultrasonics Symposium, 145 (1973).

25. J. H. Cafarella, "Surface Acoustoelectric Correlator with Surface State Memory," Proceedings of the 1974 Ultrasonics Symposium, 216 (1974).

26. K. Ingebrigtsen, "The Schottky Diode Acoustoelectric Memory and Correlator, a Novel Programmable Signal Processor," Proc. IEEE 64, 764 (1976).

27. W. D. Squire, H. J. Whitehouse, and J. A. Alsup, "Linear Signal Processing and Ultrasonic Transversal Filters," IEEE Trans. Microwave Theory Tech. MTT-17, 1020 (1969).

28. B. J. Hunsinger and A. R. Franck, "Programmable Surface-Wave Tapped Delay Line," IEEE Trans. Sonics Ultrason. SU-18, 152 (1971).

29. W. C. Fifer, R. LaRosa, and J. F. Crush, "Switchable Acoustic Matched Filter," RADC Report TR-72-72, April (1972).

30. G. D. O'Clock, D. A. Gandolfo, and R. A. Sunshine, "16-Bit Switchable Acoustic Surface-Wave Sequence Generator/Correlator," Proc. IEEE (Lett.), p. 732 (June 1972).

31. L. T. Claiborne, E. J. Staples, J. L. Harris, and J. P. Mize, "MOSFET Ultrasonic Surface-Wave Detectors for Programmable Matched Filters," Appl. Phys. Lett. 19, 58 (1971).

32. P. J. Hagon, F. B. Micheletti, R. N. Seymour, and C. Y. Wrigley, "A Programmable Surface Acoustic Wave Matched Filter for Phase Coded Spread Spectrum Wave Forms," IEEE Trans. Microwave Theory Tech. MTT-21, 303 (1973).

33. P. J. Hagon, "Programmable Analogue Matched Filters," Conference on Component Performance and Systems Applications of Surface Acoustic Wave Devices, IEE Conference Publication No. 109, 25 (1973).

34. R. W. Means, D. D. Buss, and H. J. Whitehouse, "Real Time Discrete Fourier Transforms Using Charge Transfer Devices," *Proceedings of the CCD Applications* Conference, p. 95 (1973).